



DEPARTMENT OF ENERGY TECHNOLOGY
AALBORG UNIVERSITY

Vestas

WIND. IT MEANS THE WORLD TO US. | vestas.com



*While the future for renewable energy in
Denmark is really cheerful,
the energy industry knew there would be
a few clouds along the way*

Designing of a Meter Model for Flicker and Harmonics Measurement

Designing of a Meter Model for Flicker and Harmonics Measurement

Project Report

Group No.924

Noman Khan and Usman Frooq

Aalborg University
Department of Energy Technology

Copyright © Aalborg University 2018

This project focused on power quality challenges flicker and harmonics measurement. Aim of the project to design flicker and harmonics measurement model according to the IEC standard. The present study and analysis specially provide the benefits of the industry of WT manufacturers concerned with power quality and power production.



Department of Energy Technology
Aalborg University
<http://www.et.aau.dk>

AALBORG UNIVERSITY

STUDENT REPORT

Title:

Designing of a Meter Model for Flicker and Harmonics Measurement.

Theme:

Wind power systems, assessment of harmonics and flicker measurement.

Project Period:

9-10th Semester 2016

Project Group:

PED-EPS

Participant(s):

Noman Khan and Usman Farooq

Supervisor(s):

Xiongfei Wang

Pooya Davari

Lars Helle (Vestas-Danmark)

Copies: 1

Page Numbers: 130

Date of Completion:

September 2, 2018

Abstract:

The wind energy is becoming the mainstream source of the power sector. The installation of the grid-connected wind farm is increasing because of their contribution to the green energy. The power quality is the challenge of the wind energy. Moreover, the critical issue in the measurement of power quality effects such as severity of flicker and harmonic. Therefore, the IEC standards define the measurement procedure for flicker and harmonic. The effects of voltage fluctuations associated with the flicker and the signal distortions are known as harmonics. The measurement of flicker and harmonic to the wind turbine is dealt with in this dissertation. The thesis consists of two parts. The first part described the flicker measurement model and the second part define the harmonics measurement model. The results demonstrated through simulation according to the upgraded version of IEC measurement and assessment standard.

The content of this report is freely available, but publication (with reference) may only be pursued due to agreement with the author.



Department of Energy Technology
Aalborg Universitet
<http://www.et.aau.dk>

AALBORG UNIVERSITET

STUDENTERRAPPORT

Titel:

Designing of a Meter Model for Flicker and Harmonics Measurement.

Tema:

Wind power systeme.

Projektperiode:

9-10th semester, 2017

Projektgruppe:

PED-EPS

Deltager(e):

Nøman Khan and Usman Farooq

Vejleder(e):

Xiongfei Wang
Pooya Davari
Lars Helle (Vestas-Danmark)

Oplagstal: 1**Sidetal: 130****Afleveringsdato:**

2. september 2018

Abstract:

Vindenergi er blevet hovedkilden indenfor strømforsyningssektoren. Oprettelse af grid-forbundne vindparker er stadig stigende på grund af deres bidrag til grøn energi. Kvaliteten på strømmen er en udfordring for vindenergisektoren, Endvidere, er det kritiske punkt måling af strømkvaliteten, såsom omfanget af flicker og harmonisk forvrængning. Derfor, fastsætter IEC standarden måleprocedureerne for flicker og harmonisk forvrængning. Effekterne på spændingsvariationer associeret med flicker og signal forvrængning er kendt som harmonisk forvrængning. Målingen af flicker og harmoinisk forvrængning i vindturbiner er emnet for denne afhandling. Afhandlingen falder i to dele. Den første del beskriver flicker målemetoden og den anden del definerer målemetoden for harmonisk forvrængning. Resultaterne demonstreres ved hjælp af simulering gennem den opgraderede IEC måle- og vurderingsstandard.

Rapportens indhold er frit tilgængeligt, men offentliggørelse (med kildeangivelse) må kun ske efter aftale med forfatterne.

Acknowledgments

In our capacity, as the writer of the thesis project, first of all I would like to express my sincere appreciation to the project team for their valuable contributions and enormous efforts in their project. In particular, we would like to thank supervisors from Aalborg University (AAU) Pooya Davari and Xiongfei Wang.

Special thanks also to Lars Helle (Vestas Wind systems) for his continuous support and record our special thanks to the Vestas Wind System A/S for making documents available to us free of charge and sanctioning the permission to use some of the material therein.

Our grateful thanks go to the Prof. Frede Blaabjerg from the Institute of Energy Technology (AAU), for his help and encouragement he has given in these twelve months.

Last but not least, our special thanks to all academic and administrative staff in the Institute of Energy Technology at Aalborg University. Without their tremendous help on the scientific as well as organizational field.

Finally, the authors wishes to take this opportunity to express their gratitude to Pooya Davari, Xiongfei Wang and Lars Helle for valuable suggestions to make this thesis successful and excellent supports since 2017.

Contents

1	Introduction	1
1.1	Project Objectives	3
1.2	Content of Thesis (Part 01)	3
1.3	Content of Thesis (Part 02)	4
2	State of the Art	6
2.1	Survey of Flicker measurement	6
3	System Modeling	11
3.1	Model of the Flicker Measurement	11
	Implementation of Fictitious Grid	14
	Techniques for estimation of $u_o(t)$	16
	Implementation of IEC Flicker meter	17
4	Framework of IEC Measurement	20
4.1	IEC Framework of Flicker Measurement	21
	Continuous Operations	22
	Switching Operations	23
5	Measurement Procedure for Flicker	24
6	Simulation Model Design and Execution	26
6.1	Simulation Model for Flicker Measurement	26
6.2	List of Annexes	29
6.3	Simulation Work flow for operational decision	29
7	Measurement and Assessment	31
	1. Test to validate the results of flicker measurement and assessment.	31
	2. Performance test of the Fictitious grid.	35
	3. Results of Accuracy Verification for IEC flicker meter	39
8	Conclusion and Future Work	44
8.1	Scientific Contribution	46

Todo list

Introduction

1 Introduction

WIND energy is sustainable and fastest rising energy source in the world [1]. Moreover, the development of renewable energy sources has a positive impact on the environment [2]. The increasing scale of the installed capacity of the wind farms as well as increase the penetration level in the power systems. Several power quality challenges are affecting the performance of wind energy [3]. As per the literature survey, the power quality challenges do not only the cause of voltage fluctuation as other factors also play an important rule i.e. distortion in the voltage and current, transient, harmonics and flicker. Moreover, the grid-connected wind turbine creates critical challenges to the industry such as harmonics and flicker measurements [4], [5], as shown in Fig. 1.

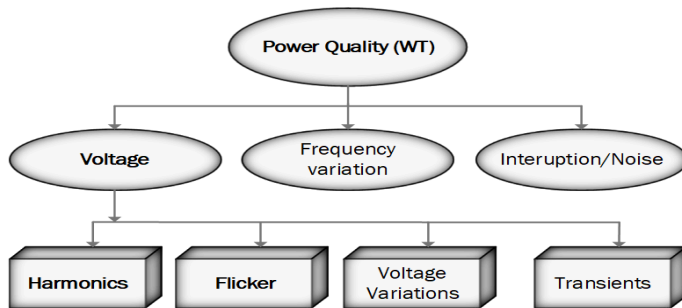


Figure. 1: IEC series of Power quality challenges in wind turbine))

The flicker produces by grid-connected wind turbine, the mainly cause of rapid changes in wind speed, variable load connected to the grid and the voltage control devices which can lead to voltage fluctuations at the

IEC Standard	Description
61000-3-6	It explains the instrument type to be used for harmonic measurement such as voltage and current transducer.
61000-4-7	It defines the characteristic about the harmonic measurement tool.
61400-21	It explain the measurement procedure from the grid-connected wind turbine.
61400-4-15	It explains the procedure of flicker measurement by flicker meter.
61400-21-1	It defines the validation of measurement of harmonics and flicker, during continuous and switching operations.

Table 1: Description of IEC Standard for flicker and harmonics measurement

point-of-common-coupling (PCC). In addition, the power electronic equipment is the potential source of harmonics emission. The generated harmonics and flicker will cause great threat to the sustainability and stability of the overall wind energy systems.

Currently, the wind industries are facing the challenges rather not only related to the pollution of harmonic and flicker but also the problems in the measurement and assessment of flicker and harmonics. Therefore, International Electro-technical Commission (IEC) is working to specifies the procedures for the measurement and assessment of power quality disturbances such as flicker and harmonics emission by grid-connected wind turbine (WT) [6]. The manufacturer of the wind turbine and IEC maintenance team have been taken actions for the standardization of flicker and harmonics measurement [7], [6], and currently working on the validation of measurement procedure. The IEC standard described the four primary objectives, namely aligning the dynamic simulation model with the upcoming standards of wind energy generation, designing the robust measurement procedure standard, specify the consistency in the results and enhancing the accuracy in the results during continuous and switching operation. There are currently published IEC standard for the measurement of harmonics an flicker, described in the table.1.

The project will focus on measurement procedure of harmonic and flicker. There are two main goals of the research project *"how to design the robust model of flicker and harmonics measurement, and validate the measurement procedure by comparing the results with the desired requirement of the IEC standard"*.

This project thesis will achieve the goals of the flicker measurement and assessment by employing upgraded standard IEC-61400-21-1. First, the simulation model will be designed according to the standard IEC 61400-21, and the simulation results validated by the possible desired values in the

IEC standard. Second, verified that the designed simulation model follows the procedure of the standard IEC-61400-21-1, and then analysis the simulation results. Finally, examine the overall assessment results, to find the performance to the components of flicker measurement model. Thus, the project outcomes will be beneficial for the IEC committee, renewable energy systems, and wind turbine industries.

1.1 Project Objectives

There are following milestones/objectives would be investigate in the project.

- To provide a concise review for the flicker and harmonics measurement and assessment according to the IEC-standard.
- To design and demonstrate the flicker and harmonics measurement model by using upgraded IEC standards.
- Investigate the impact on the accuracy of flicker and harmonics measurement and assessment system.
- Based on the simulation results, to validate the simulation results of the design measurement model and compare all the measurement values (flicker and harmonics) with the desired requirement of the IEC standards.

1.2 Content of Thesis (Part 01)

The chapters of the project reports present the following content:

Chapter 2: State of the Art

This chapter elaborates the cutting-edge coherence about the impact of flicker in the power quality of grid-connected wind turbine. Further, investigating the highest level of model general development with respect to measurement device.

Chapter 3: Systems Modeling

Gives an over view of the system modeling for measurement of flicker. This chapter explains the basic parameter of flicker measurement model.

Chapter 4: Framework of IEC Measurement

Detail procedure of flicker measurement according to standard. It describes the measurement of flicker during continuous and switching operation of the grid connected wind turbine.

Chapter 5: Simulation Model Design and Execution

Demonstrate the simulation model build for the flicker. The procedure is

according to the IEC standard 64100-21-1. A digital Matlab tool was used to developed simulation framework for the implementation of the flicker measurement and assessment procedure.

Chapter 6: Measurement and Assessment

This chapter presents the simulation results, a correlative analysis of the flicker measurement and assessment concerning continuous and switching operations. All the obtained simulation results analysis with the IEC standard.

Chapter 7: Conclusion and Future work

Draws the conclusion and finding from the thesis and gives some suggestion on the future work.

1.3 Content of Thesis (Part 02)

The chapters of the project reports present the following content:

Chapter 2: State of the Art

An overview about the harmonic issues, definition and characteristic about the tool to measure the harmonic levels.

Chapter 3: Harmonics measurement Model

Developed the harmonic model according to the standard 61000-4-7, explain the important of resampling, grouping and frequency detection to reduce the spectral leakage and improve the model performance. The model is developed in Graphic user interface (GUI) in MATLAB .

Chapter 4: Harmonics Measurement of the Wind turbine

It gives an overview of the measurement procedure of the harmonic from the grid connected wind turbine at the point of common coupling (PCC). Also elaborate about the equipment use at each step of measurement.

Chapter 5: Simulation of the harmonics model

Show the result obtain from different method to measure the harmonic levels and compare the result for the development of the harmonic model.

Chapter 6: Simulation of the harmonics model

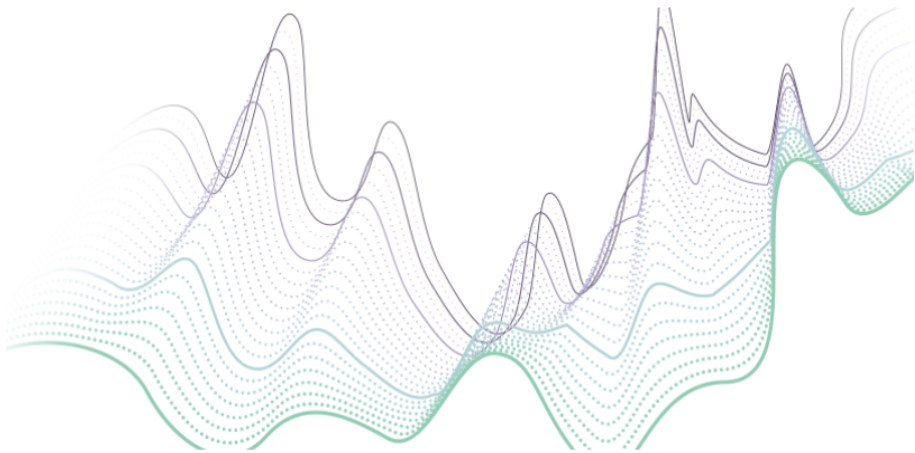
Give an overview about the validation of the developed model through prevailing angle, probability density function and standard deviation.

Chapter 7: Conclusion and Future work

Give the conclusion about the project and purpose some suggestion for the future work.

Part 1

Model of the Flicker Measurement and Assessment



State of the Art

2 State of the Art

There are many challenges comes under the umbrella of the power quality of wind turbines, two of them are critical such as flicker and harmonics. The flicker and harmonics measurement of wind turbines is dealt in this dissertation. This chapter elaborates the cutting edge coherence about the impact of flicker and harmonics measurement in the power quality of grid-connected wind turbine. Further, investigating the highest level of model general development with respect to measurement device. Moreover, the scientific contribution to the IEC standards development reached at any particular time as a result of the standard methodologies employed at the time.

The state of the art work is subdivided into two parts. In the first part, this chapter focuses on the critical review of the flicker phenomena with standardized measurement process of grid-connected wind turbine, and next part, the chapter addressed main survey of the harmonics assessment and measurement as per specified standard.

2.1 Survey of Flicker measurement

This section, briefly described the literature survey in the area of flicker phenomena with flicker measurement and assessment process. The flicker estimated by the voltage fluctuation, and in case of a grid-connected wind turbine, the flicker values depend upon the harmonics in the signals. In the traditional way of measurement, the voltage fluctuation quantified by light-lamp. In this context, the human eye and brain play an essential role to detect the variation in the luminance of the light bulb. In the early 80's, fluctuations are estimated by weighted of two cascade filters. One filter directly corresponds to the response of light-bulb and the other filter detect

Table 2: Specification of Lamps

Light Source	Principle of specification of the lamps operation
Incandescent Lamp	Light source by an incandescent lamp is made of fiber material by using tungsten. It increases body temperature and its molecules emit energy in the form of visible radiation. The luminous efficient of 60W is estimated at about 12Lm/W luminous intensity.
CFL	CFLs are also known as discharge light source. CFLs have two main component, 1) a gas-filled 2) tube with an electronic circuit which used to control the voltage operation. CFLs operate at the frequency (20-50 kHz) and luminous efficiency depends on the frequency. It is 5times higher than for incandescent lamps.
LED lamp	This is solid-state lamps that use light-emitting diodes as a light source. The luminous efficiency of LED lamps influenced by the individual unit and it can be reached approximate 140Lm/W with

the reaction of the human eye and brain in the luminance of the light-bulb [8]. The historical references covered in the history of voltage flicker by Walker [9].

Critical Review on light-lamp and human eye-brain for Flicker measurement: In the last decade, many devices have been developed to measure and assess the flicker level [10]. Most of them were produces in Denmark, France, Germany, and Japan. The detection range of these devices is up to 0.5 – 33Hz which is approximately equal to the detection and perception range of human eye-brain 0.5 – 30Hz [11]. The various types of electric lamps have been used to display the flicker [8]. These lamps have their self-characteristics and operations (i.e., temperature, radiation and luminescent), as described in the Table.2. Therefore, light sources have always been a debatable issue in the industrial and academic research [12].

Nowadays, there are different methods used to evaluate the effects of voltage fluctuation, the voltage fluctuation usually estimated by employing lamps. According to the recent literature survey, advanced technological bulbs like CFLs and LED demonstrated their sensitivity concerning light flicker to inter-harmonics [13]. However, practical results are showing that Light flicker to inter-harmonics frequency (lower and higher) impact on the system frequency not even running operation also in the absence of harmonics [13] [14]. In short, the results of the experiment indicated that CFLs and LED performance quite similar to incandescent lamps for light flicker [8]. The experimental results proved that incandescent lamps for inter-harmonic are below *2nd – order* harmonics [14]. Moreover, analysis results indicated that CFLs and LED are also sensitive in the presence of inter-harmonics [14] concerning to *3rd – order* and *5th – order* harmonics where flicker is not detect in the incandescent lamps.

Brief Review on Flicker meter: The history of growth (flicker measurement process) is now reshaping the flicker devices with the name of flicker meter [12]. The flicker meter is the synchronized system that measures the obnoxiousness of the flicker caused by voltage changes [10]. In [15], the flicker problem related to low frequency inter harmonics

highlighted and down-up sampling in the discrete-time sample domain solution is also proposed to address the flicker-detection problem associated with interharmonics. In [16], authors focused on improving the response of high-frequency interharmonics in the power supply voltage in which standard demodulator is removed and change with new demodulation. In both [15] and [16] demodulator block is changed by new block. In [17], analysed frequency higher than 85HZ by designing an improved filter, using the border graph of gain factor of various lamps. Most of the flicker meter source is the incandescent lamp, and they show error while measuring non-incandescent lamp. A new block added to the IEC standard flicker meter to perform accurate result [18]. In [5] and [19], measure flicker directly from the lamp radiant flux. The experiment results shown by [15] [18], these results are not fulfilled the desired requirement, and 19,20Hz do not pay attention to nonlinear attenuation introduce by nonlinear DC circuit. Finally [5] [19], assessed the flicker of the different lamp at various voltage fluctuation but due to non-availability of laboratory test results, it is hard to validate the results. In short, the above mention papers discuss the recently updated methods, research problems, and techniques which were implemented by improving the efficiency of flicker meter. No doubt, the flicker meter is and essential part of the flicker measurement of grid-connected wind turbine. This project focuses on the performance of flicker meter into two ways. First, to demonstrated updated framework of the model which is divided into two parts: 1) to evaluate the flicker measurement parameters P_{inst} , and P_{st} by the simulation model, 2) to verify the accuracy and precision flicker measurement results by comparing simulation results with the desired applicable values of IEC flicker meter. The deviation between obtained simulation results and desired values of the IEC standard demonstrates the performance of the flicker meter.

Review of the Flicker measurement and Grid-connected wind turbine:

Flicker measurement of grid-connected wind turbine is the intensive topic of several investigations (L. M. Craig et al., 1996 [20]; Sørensen et al., 1996 [21]; Z. Saad-Saoud and N. Jenkins, 1999 [22]).

The *flicker* detected through the fluctuation in light, and the light fluctured caused of fluctuations in the fundamental voltage. The grid-connected wind turbine may affect the performance of overall wind energy systems concerning voltage quality. Flicker is defined as the change of voltage in a frequency range up to approximate 35Hz, and the most sensitive frequency is 8.8Hz. In the last century, many authors confirmed that the injection of power from wind turbine is main cause of comprise the voltage quality, and considered as a risky (energy loss) source of energy production due to noise and reactive interference from grid [2] [23] [24]. In 1990, the flicker was recognized as a critical challenge and included in the list of International Electrotechnical Commission (IEC) standard IEC60868 with the amendment over time. The IEC standard set the rules and flicker measurement

procedures for the grid in the IEC 61400-21 standard [25]. The first edition of this standard was officially published in 2001 and was the product of the research project "European Wind Turbine Testing procedure Development" supported by European Union [26]. In the current scenarios, the flicker measurement process of the grid-connected wind turbine consists of two different modes of operation: continuous and switching operations by employing fictitious grid [25].

Review, status and outline of the Standard Series IEC 61400-21: The IEC standard IEC 61400-21 series composed by parts and exists for 15-years. Now, IEC series is well established and accepted by the industry. However, the measuring systems interoperability challenges of the IEC series still need attention, and some other problems have added due to the growth of emerging technology which used in the newly developed wind turbine. The development process of the IEC, the outcomes delivered the upgraded standard series: "Measurement and assessment of electrical characteristics". These series subdivide into parts, i.e., Part-I: wind turbines and Part II: wind power plants. The IEC series and phases of standards development can be seen in the framework of IEC-committee draft (CD) as shown in Fig.2.

The primary purpose of the IEC 61400-21 standard is purely related to the measurement test, and to examine the flicker and harmonics characteristics of wind power systems. This standard defines the testing and verification of measurement procedure for the various parts of the electrical capabilities, and assess the power quality level of the wind turbine [25]. However, the manufacturer demands the validate results and desired values of the flicker regarding flicker coefficient C_{ψ_k} , instantaneous flicker P_{inst} , voltage change factors, short flicker P_{st} and the characteristics of flicker measurement in the presence of harmonics during multiple operations of wind turbine [25]. Therefore, the upgraded version recently introduced from IEC known as IEC 61400-21-1-ED1 standard (2017-06-02) [6]. Thus, the project is performing some of the leading tests and validate the results according to the desired values of IEC 61400-21-1-ED1 standard.

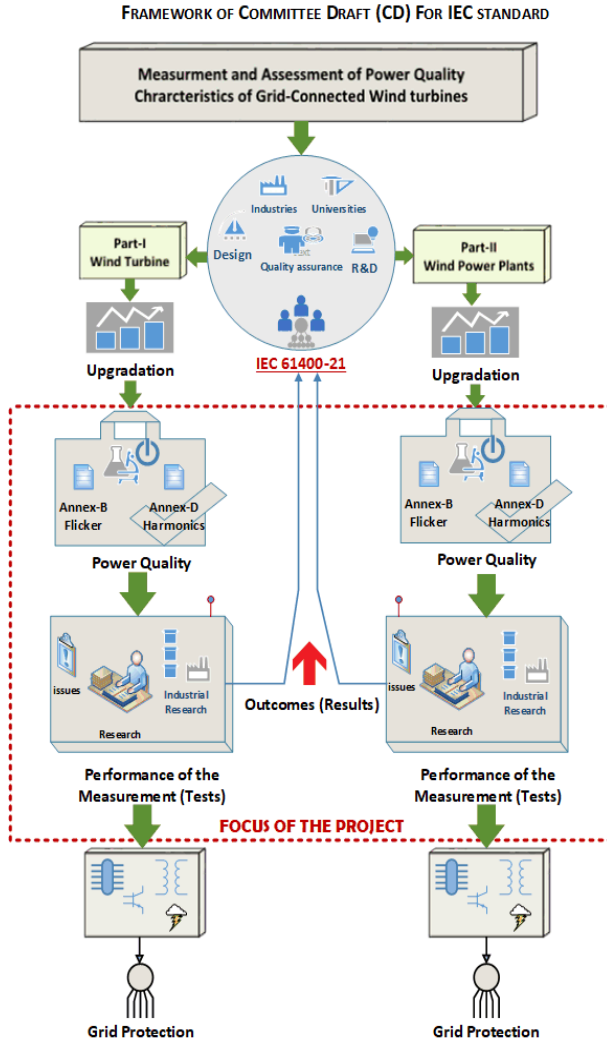


Figure. 2: Framework of IEC Series (CD IEC 61400-4-21-1-2017)

System Modeling

3 System Modeling

The chapter elaborated the system modeling for measurement of flicker and harmonics. Furthermore, the system modeling is defining the development process of the measurement system. The main goal of the project to designed measurement model of the flicker and harmonics. In this section, the system model presenting a different view or perspective of that power quality measurement system in terms of flicker and harmonics. The system modeling helps the analyst to understand the functionality for the measurement and assessment of the flicker and harmonics.

3.1 Model of the Flicker Measurement

The flicker is a conventional way of quantifying voltage fluctuation, and the measurement model is designed to estimates the variation in the voltage duration in amplitude and magnitude. The flicker measurement and assessment procedure designed according to the standard IEC-61400-21-1 [25]. The standard IEC 61400-21-1 defined the measurement procedure of architecture model for voltage fluctuation into three prospective, as follows.

1. The measurement quantities to be determined for the characterizing the electrical parameters characteristics of the grid-connected wind turbine.
2. The measurement and assessment procedure used for quantifying the electrical characteristics.
3. Procedures for assessing compliance according to the requirements such as appropriate accuracy estimation of the power quality including environmental factors of the deployment site of the wind turbine.

The flicker emission specifies that flicker caused by the effects of grid-connected wind turbines [4]. The focused IEC-61400-21-1 standard is measurement and assessment testing of wind turbines and differentiated by characterizing two situations: continuous operation and switching operations [27]. The rest of the other parameters and all the tests are related to the wind power plants covered by IEC 61400-21-2. However, the project focused on the IEC-61400-21-1 standard related to the grid-connected wind turbine. The main goal of the project to design the flicker measurement model according to the IEC-61400-21-1 standard.

The designed model for the flicker measurement that is assessing the electrical characteristics is valid for wind turbines. The verification of flicker measurement performed by conducting tests of analyzing the effects of the accuracy in the values of the measurement. Furthermore, the estimated values should take during stable and unstable grid frequency, and during testing, WT should be connected with the grid. The grid produces the voltage fluctuation cause of the non-linear load which is the leading cause of voltage fluctuation in the grid-connected WT systems. The effects of both grid and WT summing at the point of PCC, which is also known as a point of interest for measurement. Thus, the interaction between a grid and WT represents by a fictitious grid of *Block – 1*, as shown Fig.3.

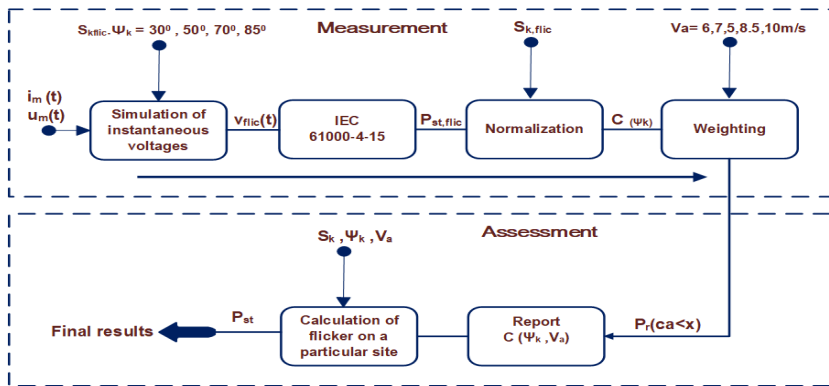


Figure. 3: Measurement and assessment procedures for flicker during continuous operation of the wind turbines according with the IEC 61400-21-1

The normal operation of the turbine excluding start-up and shutdown time of the transaction known as continuous operation of the WT and the measurement model with continuous operation see in Fig.3. Flicker produces during continuous operation cause of the power fluctuation due to variation in wind speed in the wind turbine.

The processes that excluded from normal operation is called switching operations. There are various types of switching operational characteristics such as a) Wind turbine start-up at cut-in wind speed, b) Wind turbine start-up at rated wind speed or higher wind speed, and c) The switching

between generators or a generator with multiple winding. The switching operations determine by flicker step factor and voltage change factor. Further, parameter describes by numbers of switching (N_{10m} and N_{120m}) based on manufacturers information. Where the step factor Kf_{ψ_k} and the voltage change factor Ku_{ψ_k} depending on the control system of the wind turbine. The maximum number of the switching operation within a 2hours period and minimum within a 10min period. The diagram of the flicker measurement procedure shown in Fig.4.

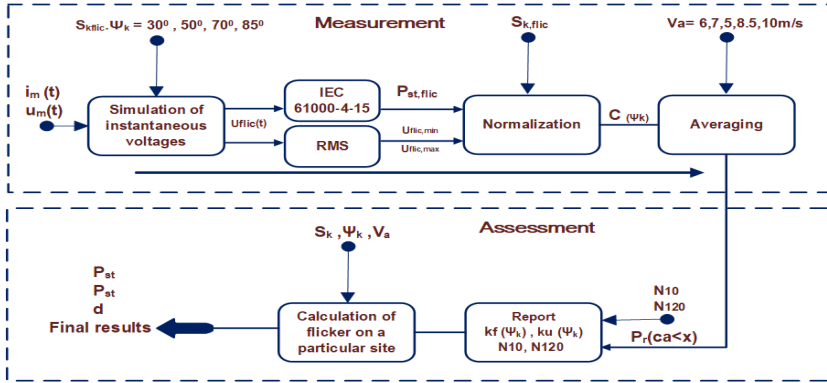


Figure. 4: Measurement and assessment procedures for flicker during switching operations of the WT in accordance with IEC 61400-21-1

As per the standard of IEC-61400-21-1, the flicker measurement procedure consists of the first four blocks, and assessment executed in the last two blocks. The assessment blocks recall the overall evaluated parameters including continuous and switching operations.

In the estimation of the preliminary stage concerns the power quality for standardization of wind turbines. This estimation based on power signal and flicker evaluation which demonstrated in the previous IEC standards of power quality. In this context, the IEC working group of the technical committee have been examined the results and compared the method through the current i_s and voltage signals u_s . Finally, IEC 61400-21-1 introduced that flicker evaluation depends on the current i_{mt} and voltage u_{mt} time-series measured at the PCC terminals nearby wind turbine. However, found that the flicker is not caused only by the wind turbine itself [4]. In short, the voltage fluctuations also ingress from of the grid side at the point of common interest or PCC terminal where flicker is measured [28]. Thus, the voltage fluctuations imposed on the wind turbine, and voltage fluctuation depends on the grid conditions [29]. Therefore, the measurement model developed in the upgraded standard IEC 61400-21-1 allowed independent measurement of the voltage fluctuations. This model is known as a fictitious grid that enables analysis of voltage fluctuations caused exclusively by the wind turbine. According to the standard IEC

61400-21-1, the assessment procedure estimates the flicker emission, voltage changes, flicker step factor, flicker coefficient, and voltage change factors during continuous and switching operations.

The fictitious-grid estimates the voltage fluctuation from an input and precise esitimated voltage fluctuations hand over to the flicker meter. The flicker severity measured by flicker Meter (FM) and the measuring procedure of FM defines in the IEC-61000-4-15 standard [30].

Implementation of Fictitious Grid

The initial stage of the voltage and current processing procedure determines the fictitious voltage $U_{fic(t)}$ and characterizes the causes of the voltage fluctuations which leads to the PCC [31]. The standardized fictitious-grid as shown in Fig.5.

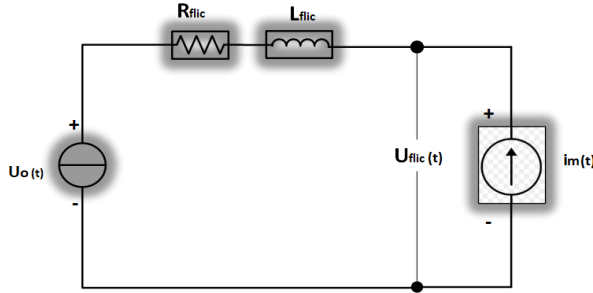


Figure. 5: Fictitious grid use for flicker assessment in Grid-connected WT

The fictitious grid performed by an ideal voltage source (phase-to-neutral) integrated with instantaneous value $u_{o(t)}$ and impedance of the grid represented by two electrical components such as R_{flic} in series with an inductor L_{flic} . Moreover, the WT described instantaneous values of the line current source $i_m(t)$ also represented by the current generator of the WT. The output of the fictitious grid is simulated voltage integrated with the instantaneous values $U_{fic(t)}$, as follows [32].

$$U_{fic(t)} = u_{o(t)} + R_{flic} \times i_m(t) + L_{flic} \times \frac{di_m(t)}{dt} \quad (1)$$

In equation number: 1, the critical signal is ideal voltage source $u_{o(t)}$, which requires assurance for sufficient performance of the ideal voltage source. Therefore, the voltage source $u_{o(t)}$ must fulfill the two conditions. First, the ideal voltage source validated the $u_{o(t)}$ is without fluctuation, its mean flicker should be zero. Second, the electrical angle of the $u_{o(t)}$ should be the same as the fundamental component of the input voltage mean the phase angle must be correct, and in between $U_{fic(t)}$ and current source $i_m(t)$

provides that $|U_{fic(t)} - u_{o(t)}| \ll |u_{o(t)}|$. Thus, $u_{o(t)}$ is same as the fundamental voltage U_{fic} . Therefore, the execution properties of the $u_{o(t)}$ represented [25] as follows:

$$u_{o(t)} = \sqrt{\frac{2}{3}} \times U_n \times \sin(\alpha(t)) \quad (2)$$

Where U_n is the r.m.s values of the nominal voltage in the grid-connected WT, and the electrical angle ($\alpha(t)$) of the pure fundamental component, the ($\alpha(t)$) can be define as follows:

$$\alpha(t) = 2\pi \times \int_t^0 f_{dt} + \alpha(o) \quad (3)$$

where the $f(t)$ varying frequency over the time; t is the starting time-series, and $\alpha(o)$ is the angle at time $t = 0$. Furthermore, R_{flic} and L_{flic} should be selected to drive the appropriate network impedance phase angle ψk determine in the equation below:

$$\tan(\psi k) = \frac{2\pi \times f_g \times L_{flic}}{R_{flic}} = \frac{X_{flic}}{R_{flic}} \quad (4)$$

where f_g is the nominal grid frequency (50 or 60 Hz) and three-phase short-circuit apparent power of the fictitious grid is define by equation as follows:

$$S_{k,fic} = \frac{U_n^2}{\sqrt{R_{flic}^2 + X_{flic}^2}} \quad (5)$$

The flicker meter standard IEC 61000-4-15 is determined the measurement procedure of the flicker severity P_{st} and instantaneous flicker P_{inst} . The measurement of P_{st} and P_{inst} , the flicker meter used the short-circuit ratio $\frac{S_{k,fic}}{S_n}$ (SCR) between the range of 20 and 50. The calculation examines the accuracy of flicker meter parameters, i.e., P_{st} should be better than 5%, this appropriate ratio defined by IEC 61400-21-1. The literature survey indicated that the procedure in IEC 61000-4-15 does not efficiently estimate the minimum voltage fluctuations, mean very low accuracy [11]. However, the maximum voltage fluctuations can be measured accurately by tuning (decreasing) the short-circuit ratio. In case of SCR become too small, it means root mean square (RMS) values of U_o relatively change because of absolute voltage change are normalized to the different mean value. Therefore IEC 61400 recommended their specific parameters for measurement [11].

Table 3: Wind turbine analytical characteristics for testing

Parameters	Description	Values
U_n	Nominal voltage	690 V
S_n	Rated power	600 KVA
f_o	Fundamental frequency	50 Hz
$s_{k, fic}$	Ratio between power parameters	20-to-50
psi_k	Network impedance angle	30-to-95 degree

Techniques for estimation of $u_o(t)$

The voltage u_o is composed of the fundamental component of the wind turbine voltage terminals $u_{m(t)}$, representing the power network and calculate by the above equation 2. In the estimation of u_o requires two mode of operations [6], as follows:

- i The instantaneous phase of the fundamental components of $u_{m(t)}$ should be calculated by fictitious grid.
- ii In the overall calculation, multiple adjustment requires such as adjustment of the amplitude of u_o with the agreement of the nominal voltage of the wind turbine U_n .

However, the $\alpha_{m(t)}$ is difficult part to calculate, this is the phase of the fundamental component of the existing voltage $u_{m(t)}$. To solve the problem normally used two techniques, 1) Transform (STFT) and 2) Zero Crossing Detection (ZCD). All of these techniques have own characteristics and accuracy. In current scenarios, the inter-harmonics considered as a component of the disturbance in the terms which produce measurement errors in the calculation of u_o .

The $u_{m(t)}$ presented in the equation 8. A minimum error in the estimation of the phase of the fundamental component of $u_{m(t)}$ can produces small changes in the $u_{fic(t)}$ equation in 20, which directly impact with the significant changes in the measurement accuracy of the P_{st} values [32].

$$u_{m(t)} = \sqrt{2(U_n)}[\cos(\omega t + \alpha_{m(t)}) + A_i(\omega_i(t))] \quad (6)$$

$$u_{fic(t)} = \sqrt{\frac{2}{3}(U_n)}\cos(\omega t + \alpha_{(o)}) \quad (7)$$

These parameters of the wind turbine affect the fictitious grid and also disturbed the waveform of the testing signals. Therefore, all the tests performed using the wind turbine characteristics as shown in Table.6.

Implementation of IEC Flicker meter

The device for measuring flicker severity P_{st} known as flicker meter (FM) [7]. This section is explaining the working principle of the flicker meter. Furthermore, FM defined in the recently submitted research work [33]. The procedure of measurement procedure according to the standard IEC-61000-4-15 as shown in Fig.6.

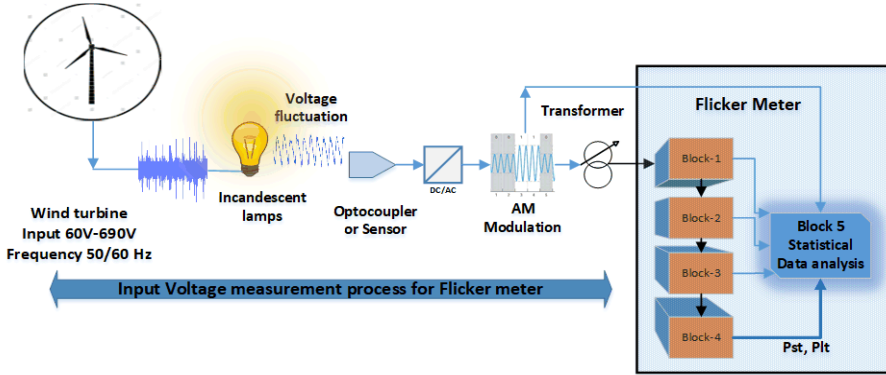


Figure. 6: Measurement procedure of the Flicker meter (IEC 61000-4-15)

The flicker meter standard IEC-61000-4-15 defines voltage fluctuation processing procedure with the four quantifies steps: 1) the voltage change factors presented in percent, 2) the modulated frequency of the voltage change, 3) characteristics of the physical light-source, 4) the procedure of the human brain recognition of the voltage fluctuation [25]. Thus, the flicker measurement procedure through flicker meter is an efficient way of observing voltage fluctuation [7]. This paper does not precisely focus the dynamics of flicker meter. However, flicker meter plays a critical role in the verification tests of the flicker measurement. Therefore, it is essential to presents verification results of the flicker measurement without the fictitious grid. In the practical scenario, the flicker meter ingress the input (voltage fluctuation) from the fictitious grid see in Fig. 4.

The measurement procedure of flicker meter verified by an incandescent lamp with voltage fluctuation [34]. The fundamental phenomenon of flicker measurement design based on the physiological and psychological involved in the measurement of perception [35]. A digital flicker meter presents similar results as the analog flicker meter [30]. However, digital flicker meter is considered as standard flicker for measurement due to its exceptional facilities such as ensures that obtained results following the recommended IEC measurement procedure.

The operational architecture of IEC flicker meter described by the block diagram see in Fig.7. The initial mandatory task is performed by block 1

and blocks 2, 3 and 4, while the final outputs accomplished by block 5. The overall working operation divided into two parts, each block performing one of either both tasks as follows [12] [34].

1. The simulation response of the lamp-eye-brain diagram as per IEC-standard.
2. The results presentation by on-line statistical analysis of the signal.

Block-1: Input voltage adapter The voltage adapting circuit receives the modulated signal from the input such as *AM* modulation. The primary functions of this block-1 to scaling the input voltage, maintain the r.m.s level and keep the voltage fluctuation with the fundamental signal. The internal voltage level does not compromise the functioning of the rest of the instruments [34]. Thus, the level of internal voltage of adapted circuit according to the operation of the flicker meter. The verification test of flicker measurement procedure described in detail [7].

In short, the modulation signals created with rectangular modulation and its amplitude average 1 with 50Hz frequency and 8.8Hz voltage change. A change in the phase relationship directly affected the results of P_{inst} and P_{st} values for the rectangular modulation tests. Moreover, the testing results representing the change of time function in $\Delta u/u$ amplitude modulation approximately equal to the change in the *R.M.S* $\Delta U/U$. This block keeps the level *R.M.S* of modulated voltage and delivers to the input of the block-2. The transformer does not modify the modulating relative fluctuation. Therefore, the half cycle *R.M.S* values are processed by a first order low-pass (Butterworth filter) filter with a time constant of 27.3s. However, the procedure was changed with time, and replace with the new estimations idea for RMS values processing, aim to acquire better accuracy in the estimation (without error or noise) of RMS waveform. Currently, the implementation of rectangular modulation by using zero crossing detection methods for the accurate measurement of RMS values [27]. Thus, the flicker meter output depends on the depth of modulation rate of change which is the fundamental signal applied to the input of adaptive circuit at block-1.

Block-2: Squaring Multiplier The main purpose of this block is to recover the voltage change fluctuation by squaring the output of the block-1 see Fig.7. The squaring the input voltage scaled to the reference level. The testing detail available [7] according to the IEC-61000-4-15 on the basis of simulating the behavior of a lamp. The multiplier integrated with the Butterworth filter in block-3 and this block operated as a demodulation.

Block-3: Weighting filters The block 3 is consists of a cascade of two filters. These filter circuit are first low-pass filter and high pass filter (first order, 3dB at 0.05Hz). The first order low-pass filter eliminates the tipple

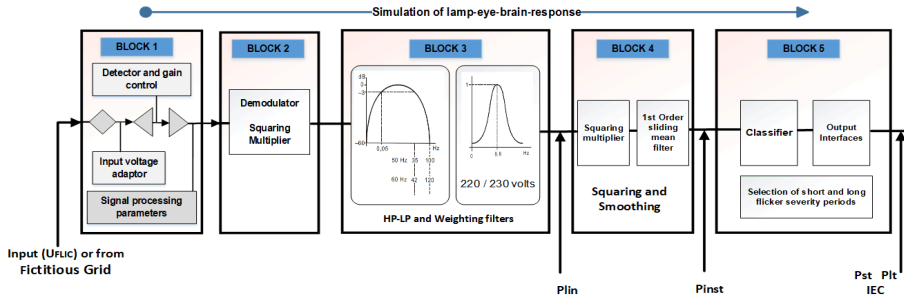


Figure. 7: Operational diagram of the IEC Flicker meter

components of the double mains frequency output. The high pass filter (HPF) can be used to eliminate the d.c. voltage component include the mains effect of HPF with the 0.05Hz known as corner frequency. The second filter is a weighting filter and used to simulates the response of the human visual systems of the voltage change or fluctuation. The correct correct weighting of non-sinusoidal and arbitrary voltage fluctuations is obtained by appropriate choice of the response function for blocks 3 and 4. Normally, the perceptibility threshold found at each frequency by 50% of the persons tested. Similarly, the overall performance of the model has checked with periodic rectangular signals test with transient signals [7] [36].

Block-4: Squaring and smoothing This block is composed of a squaring multiplier and a first order low-pass filter. The block execution on the basis of the human flicker perception such as by the eye and brain mutual combination. The voltage fluctuations applied to the reference flicker objective by simulated combine non-linear response of blocks 2, 3 and 4. The output of this block represents the instantaneous flicker sensation P_{inst} and estimates the flicker severity P_{st} in the systems.

Block-5: On-line statistical analysis This block performs an on-line analysis of the flicker level, the block acquired all the concern parameters which is required to assess the overall flicker severity level. In this context, thus the block executed the direct calculation of the significant evaluation parameters [36]. The statistical analysis method define the 15 classes in the flicker severity P_{st} calculation for a performance test [7]. This block used the cumulative probability function so as to obtained the significant statistical values such as mean, standard deviation, flicker level being exceeded for a given percentage of time or vice-verse. Thus, the flicker level assigned according to the percentage of time. +

Framework of IEC Measurement

4 Framework of IEC Measurement

In general, the measurement and assessment through IEC measurement framework based on the conceptional structure. The conceptual framework intended to serve as an assistant for the building of flicker measurement systems that expands the composition into the useful power quality measurement system.

The chapter focused on the framework of flicker measurement. The outcome of study and analysis of the flicker measurement framework is beneficial for IEC measurement organization and wind turbine manufacturer towards the development of appropriate measurement systems. The power quality monitoring management and wind turbine manufacturers can use to make sound decisions and improve overall performance. The input-output measurement framework as shown in Fig.8 is yet another means of presenting a snapshot of an IEC standard measurement's performance.

The core operational framework process is performing the inputs to outputs of flicker measurement. At this stage, the simulated results justify with the IEC standard. All the results verified by scaling the desired range of IEC standard. For example, the P_{st} desired values of IEC standard is 2 with the tolerances level ± 5 . If the outputs results come under the tolerance range, so it means the high accuracy and if the output values with the deviation considered as the high level of perception [33]. This project also focused on verifying the outcomes through available desired values of the IEC measurement framework. The IEC measurement framework procedure is mainly addressed on the next section.

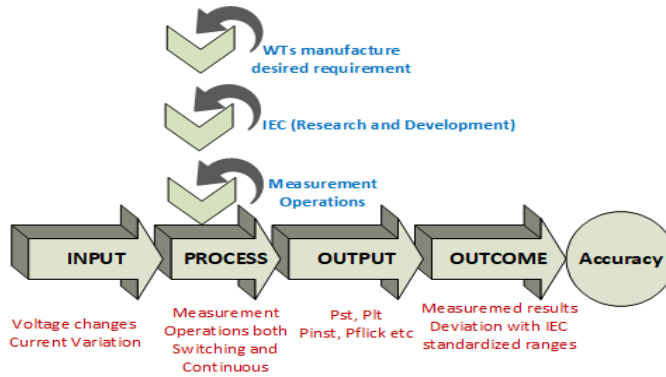


Figure. 8: Input-Output Measurement (Flicker and Harmonics) Framework

4.1 IEC Framework of Flicker Measurement

The grid-connected wind turbine is carrying various voltage fluctuation, the cause of variable grid loads. The voltage fluctuation is estimated at the nearest PCC of the wind turbine. Moreover, all the power quality tests are conducting at the PCC because the point (PCC) carrying the power quality characteristics of both wind turbine and grid. Thus, the voltage fluctuation imposed on the wind turbine depending on the characteristics of the grid. The measurement process of flicker follows the standard IEC 61400-21-1. The standard specified as a measurement framework that uses current and voltage time-series measurement. The voltage-time series waveform and its voltage fluctuations simulated through a fictitious grid 3.1.

The energy produces through a wind turbine, the production engaged with perturbation voltage signal because of the variation in wind speed and load variation on the grid. The further cause of the voltage fluctuations are the abnormal operations such as yaw errors, wind shears. Thus, voltage fluctuation considered the most significant cause of flicker and impact of flicker is the cause of declining the power quality [10].

In the standard (IEC 61400-21-1, 2016), the rules, definition, procedures for the measurement and assessment of characteristics of the grid-connected wind turbine. Concerning the measurement of the flicker emission, the standard considered the two operational modes for practice: 1) continuous operation, and 2) switching operation. The flicker emission measured during continuous operations and the effects of voltage changes measured during switching operations. The continuous and switching operations are establishing the measurement framework, to evaluate the independent characteristics of the grid-connected wind turbine.

Continuous Operations

The detail about the procedure of flicker measurement and assessment during continuous operation is shown in Fig.3. The continuous operation of wind turbine produces the flicker emission (99th or 95th percentile) coefficient ψ_k . The C_{ψ_k, V_a} is (95th percentile) for the grid-connected network impedance phase angles ($\psi_k = 30, 50, 70$ and 85) at different wind speed distribution ranges $V_a = 6, 7, 5, 8.5, 10 m/s$. The range of wind speed according to the Rayleigh distribution [37], the probability distribution fits the annual wind speed distribution as follows:

$$F_v = 1 - \exp\left(-\frac{\pi}{4} \left(\frac{v}{v_a}\right)^2\right)$$

The wind turbine flicker coefficient is measured during continuous operation as follows:

$$C_{\psi_k, V_a} = P_{lt} \times \frac{S_k}{S_n} \quad (8)$$

The flicker coefficient is C_{ψ_k, V_a} , where the flicker coefficient depends on the grid impedance angle ψ_k and wind speed V_a and S_k is the short circuit apparent power of the grid. The rated apparent power of the WTs is S_n , and P_{lt} indicates the long flicker emission. Normally, the low wind speed produces the low flicker coefficient [25] [4].

The flicker coefficient for each set of time 10 – minute measure voltage and current time series can be determine by the procedure for the given in steps 1 to 3 below.

1. The three instantaneous line currents and the three instantaneous voltages should be measured at the PCC of the wind turbine.
2. Measurements shall be 10 – minutes time-series of instantaneous voltage and current measurements. The recommended tests at least twenty-one time series (seven tests and three phases) are collected for each 10% power bin.
3. The wind speed should be measure according to the standard [7], and operations such as start-up and shut-down of the wind turbine are excluded.

The voltage flicker is measured at the wind turbine terminal by employing flicker meter specified in the standard IEC 61000-4-15. However, the flicker coefficient c_{ψ_k} is used to measured the voltage and current time-series and the procedures as follows:

1. The measured time-series is combined with equations of flicker coefficient c_{ψ_k} to give voltage time-series of $u_{fic}(t)$.
2. The voltage time series of $u_{fic}(t)$ is provided the input to the flicker algorithm in compliance with IEC 61000-4-15 to give one flicker

emission values $P_{st,flic}$ on the fictitious grid for every 10 – minute time-series.

3. The flicker coefficient c_{ψ_k} determined the values of flicker emissions.

In this project all the tests based on the phase-to-phase voltages according to the equation.

Switching Operations

The characteristic shall be stated for the switching operations where significant voltage variations.i.e. start-up at cut-in wind speed in wind turbine, ii) wind turbine start-up lead at rated wind speed, iii) the unfavorable situation of switching between generator where wind turbines connected with one or more generator (multiple winding).

The switching operations within a 10 – minute period N_{10} and 2-hours period N_{120} stated executed by modern wind turbine system settings. The flicker step factor is a standardized measurement procedure of the flicker emission with respect to a single switching operation of a wind turbine as follows: —

$$K_f(\psi_k) = (1/30) \times \frac{S_k}{S_n} \times P_{st,flic} \times T_p^{0.31} \quad (9)$$

where $K_f(\psi_k)$ is the flicker step factor of the wind turbine in terms of a single switching operation, and $T_p^{0.31}$ is the duration of the voltage variation which is due to the switching operation, P_{st} is the flicker emission from the wind turbine, S_n is the rated apparent power of the wind turbine and S_k known as short-circuit apparent power of the grid. The flicker step factor considered the network impedance phase angle angle (30,50,70 and 85). The Variable-speed wind turbines to yield expected low flicker step factors. The fixed-speed wind turbines may generate the range from average (pitch controlled) to high (stall controlled). Due to a single switching operation of a wind turbine, the voltage change factor $K_u(\psi_k)$ is a regularized measurement procedure of the voltage change factor as follows: —

$$K_u(\psi_k) = \sqrt{3} \times \frac{U_{flic,max} - U_{flic,min}}{U_n} \times \frac{S_k}{S_n} \quad (10)$$

Where $K_u(\psi_k)$ is the voltage change factor of the wind turbine according to the specified switching operation of the switching U_{min} and U_{max} are the minimum and maximum voltage (R.M.S phase-to-neutral). In other words, $U_{flic,min}$ is the minimum one period R.M.S value of the voltage, and $U_{flic,max}$ is the maximum one period R.M.S value of the voltage on the fictitious grid during the switching operation. U_n is the nominal phase-to-phase voltage, S_n is the rated apparent power of the wind turbine, and the S_k is the short-circuit apparent power of the grid. The flicker step factor and voltage change factor should be evaluated as the average results of the around 15 values.

5 Measurement Procedure for Flicker

The comprehensive measurement procedure for flicker during continuous as depicted in Fig.3. The switching operation included voltage changes, as well as the flicker of the wind turbine, is shown in Fig4. The measurement procedure of the flicker during continuous and switching operation according to the standard IEC-61400-21-1 [6], are as follows:

- The voltage and current time-series values, $u_{m(t)}$ and $i_{m(t)}$, are measured at the PCC. The switching operation is considering the specify switching events as described in Fig.4.
- each set of the measured time-series ingress values use as an input to simulate the voltage fluctuations, $u_{fic(t)}$ through a fictitious grid with four different networks impedance phase angle ψ_k and appropriate short-circuit apparent power Sk_{fic} .
- The simulated instantaneous voltage flicker used as input the IEC 61000-4-15 to generate the flicker emission value Pst_{fic} . In the switching operation, the R.M.S estimation also executed to identify the maximum and minimum one-period R.M.S value of $U_{fic(max)}$ and $U_{fic(min)}$.
- In continuous operation, each value of Pst_{fic} emission have normalized to a flicker coefficient $c\psi_k$, and independently selects the short-circuit apparent power Sk_{fic} . For the switching operation, each Pst_{fic} values is normalized to a flicker step factor $kf\psi_k$ and voltage change factor $ku\psi_k$.
- The impedance phase angle ψ_k measurement procedure evaluated flicker coefficients, $c(\psi_k)$, within the active power bins $0, 10, 20, \dots, 100\%$ of P_n . In the switching operation measured the average flicker step factors and voltage change factor by each impedance phase angle ψ_k .
- In the continuous operation, each power bin is calculated flicker coefficients by accumulated distribution functions $Pr(c < x)$. This function represents the obtained distribution of flicker coefficients where the wind turbine operation operated in the corresponding interval of the percentage of P_n . In the switching operation, averaged flicker step factors and voltage change factors are estimate within a $10min$ and $N120min$.
- the flicker coefficient is reported at each accumulated distribution within $c(\psi_k, 95\%)$.

Measurement and simulation are estimated the voltage change factor $k_u(\psi_k)$, and flicker step factor $k_f(\psi_k)$ for each type of switching operation as described above 4.1.

To determine the voltage change factor $k_u(\psi_k)$ and the flicker step factor $k_f(\psi_k)$, it is necessary to prepare the following measurement patterns.

- i Three instantaneous line currents and as well phase-to-neutral voltages shall be measured from the wind turbine terminal.
- ii The measurement shall be taken within the allocated period, and ensure that the transient of the switching has less and limited as much as possible and try to avoid the power fluctuations due to turbulence.
- iii In order to ensure the measured results are within the average or normal condition, so it is necessary to repeat each case at least five times.
- iv Wind speed measurement should be according to the measurement procedure. The average wind speed during the switching operation shall be around a range of $\pm 2m/s$ of the required wind speed.

The measurement used the following formulation for the voltage change factor $k_u(\psi_k)$ and the flicker step factor $k_f(\psi_k)$.

- i The time series of the measurement is combined with the given time-series of $u_{fic}(t)$.
- ii The simulation voltage time-series $u_{fic}(t)$ shall be input of the flicker meter (IEC 61000-4-15 standard). To give one flicker emission values $P_{st,fluc}$ on the fictitious grid as per each time-series of $u_{fic}(t)$. Thus, the results will be obtained by 15 values of $P_{st,fluc}$ for each within five tests and three phases.
- iii The flicker step factor $k_f(\psi_k)$ can be calculated according to the equation 20.
- iv The voltage change factor $k_u(\psi_k)$ can also be calculated as per above given equation 10.
- v Both the flicker step factor $k_f(\psi_k)$ and voltage change factor $k_u(\psi_k)$ shall be determine the values at the average level and considered the average results of the 15 values.

Simulation Model Design and Execution

6 Simulation Model Design and Execution

The conceptual models already discussed in the above chapter 4.1. The input data of the overall specification for simulation, to obtained from the static and dynamic knowledge about the physical system (grid-connected wind turbine). The simulation model is a tightly coupled with three main cycling process 1) simulation model design, 2) model execution (flicker measurement), and 3) analysis execution, as shown in Fig.9.

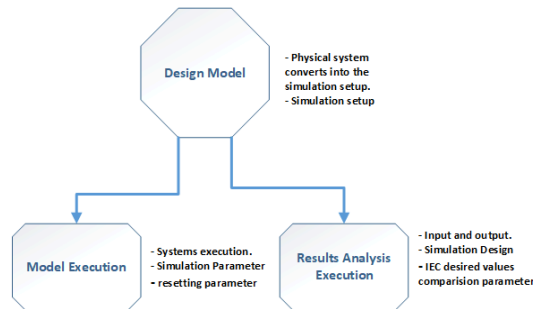


Figure. 9: Design of Simulation model

6.1 Simulation Model for Flicker Measurement

The simulation model designed according to the measurement and assessment procedure of standard IEC-61400-21-1. In the general scenario, the simulation setup established for the specific part of the research interest. In this situation, the simulation is performed to obtain the specific part of the measurement results.

Table 4: Overview of the Simulation Framework

Simulation framework		
Simulation setup	Description	Measurements
Flicker measurement (Start)	To generate a set of measured flicker values according to the IEC 61400-21-1.	To governor simulation framework and function.
Scaling function	To estimate the mathematical operation like maximum and minimum. Defined window range with a reduction range etc	The output of this function grid frequency, mean, maximum and minimum and time.
Analysis function	Measured the capacity of power in the generated three-phase signals (voltages and currents).	Measured the positive sequence values like active and reactive power and nominal frequency from the grid.
A function of fictitious grid IEC 61400-21-1.	Input as a simulated three-phase input voltage and current.	The output of fluctuated voltage
Function of Flicker meter IEC 61000-4-15	Input as simulated fluctuated voltage with flicker.	Flicker severity (Pst, Plt)
Measurement Function (switching operation)	The input of the impedance phase angle or the short-circuit ratio.	Flicker coefficient, flicker coefficient average etc
Function final calculation (continuous operation)	Measurement of the final flicker values during a continuous operation	To govern all the measured values for final calculation.

The overall model verification test required the complete simulation setup to measurement entirely flicker emission in the grid-connected wind turbine. This model produces the simulation into two scenarios 1) flicker measurement and assessment procedure should interlink with end-to-end analysis, 2) the simulation setup validated by the various testing and obtained results should be according to the IEC standards. Therefore, the designed simulation setup is ensured the measurement and assessment procedure through verification testing of each interlink components and produces the final results of an overall grid-connected wind turbine.

A digital Matlab tool was used to developed simulation framework for the implementation of the flicker measurement and assessment procedure. The implemented measurement model has used the WT voltage and current time series signals as an input. Moreover, the reported input parameters such as voltage fluctuations, the modulation depth, R.M.S values and instantaneous flicker considered in the final calculations. The working principle of simulation is based on the four Matlab functions excluding fictitious grid and flicker meter. All the functions interlinked with a simulation platform, where the input signal is process to obtained the overall flicker calculation. The fictitious grid is process the voltage fluctuations, the method defined by the IEC 61400-21-1 standard. The fictitious grid estimated the voltage fluctuation (voltage changes) and flicker meters used the vottage fluctuation as an input, to calculate the P_{st} , defined in the IEC 61000-4-15 [7]. All the simulation function required input data to

process the signals for fictitious grid, described in the following Fig.10.

<i>Input parameter abbreviation</i>	<i>Description</i>	<i>Default value</i>
Simulation module .mdl inputs:		
<i>I1,2,3_NS</i>	Three phase currents of the measured data	[A]
<i>U1,2,3_NS</i>	Three phase measured voltage	[V]
Input for calculation according to the norm:		
<i>Sn</i>	Apparent power in kW	1700 [kW]
<i>Fn</i>	Nominal Frequency	50 [Hz]
<i>Un</i>	Nominal Ph-to-Ph Voltage	400 [V]
<i>n</i>	The rate between Sfic/Sn	20 [pu]
<i>Sk</i>	Short circuit apparent power in MW	105 [MW] in
<i>N10</i>	Number of switching operation within 10 min	2 [switch]
<i>N120</i>	Number of switching operation within 2 hours	24 [switch]
<i>F_Sample</i>	Sampling Time used in recording the measured data	0.00025 [S]
<i>Alpha</i>	Impedance phase angle (psyk) in degree	30°, 45°,70°,90°
Differentiable user input Parameter:		
<i>endval1</i>	Number of times a different phase angle is calculated	4 [times]
<i>Kp</i>	Proportional Gain factor of the PLL (used in Simulink)	50
<i>Ki</i>	Integral Gain factor of the PLL (Used in Simulink)	1400
<i>Simulation_dynamic_cut_time</i>	Is the time to be excluded from the simulation results	0.06 [s]
<i>i</i>	Selector: i = 1 continuous operation and i = 2 Switching operation	2
<i>endval</i>	Number of times of the same row data and is different between i = 1 (then it is given using the Matlab governing .m file) or i = 2 (in this case it is determined by the user in FAMOS- Cut.seq file after seeing the graphic of the Row data)	i = 1 (endval = 3) i = 2 (endval = 0)
Internally calculated inputs (by Matlab):		
<i>Sk,fic</i>	Fictitious Short circuits apparent power grid	n*Sn = 34000 [kW]
<i>Fs</i>	Sampling Frequency	1/F_Sample=4000[Hz]
<i>x_l_(endval)</i>	Graphical input using FAMOS cursors (Only active for i = 2 Switching operation mode)	Defined by the user
<i>x_r_(endval)</i>	Graphical input using FAMOS cursors (Only active for i = 2 Switching operation mode)	Defined by the user
<i>Simulation_Time = Tp</i>	Is the difference between x_r - x_l	Defined by the user
<i>J, jj</i>	Counter used in 'for' loop	1

Figure. 10: Input for the simulation functions

6.2 List of Annexes

The design of the simulation model developed through the Matlab tool. The programming code of the simulation model is divided into three parts of the annexes.

Annex A: developed one execution main file with four primary functions, aim to process the input signals, see in Annex A.

Annex B: presenting the implementation of a fictitious grid model which designed on Matlab Simulink. All the functions (annex A:) are process, to carryout the input to the fictitious grid.

Annex C: Annex C presents the overall flicker meter model on the Matlab Simulink. The input of the flicker meter is the output of the fictitious grid, described in Annex B.

6.3 Simulation Work flow for operational decision

The Matlab file (flicker calculation function.m) is calculated overall simulation results by employing simulation workflow. The workflow is differentiating depending on the selected inputs parameters. The selected (*i*) can make differences in the working flow of flicker calculation. At the beginning of running these simulations function, the users defined the number of periods and then directly measure data according to the different switching periods of every switching tries. Finally, the simulation is automatically run, and selects the internal parameters in the program without stopping the simulation. The simulation requested every time to defined the next measurement of switching the period with angle alpha (impedance angle at least two times), the simulation flow diagram shown in Fig.11.

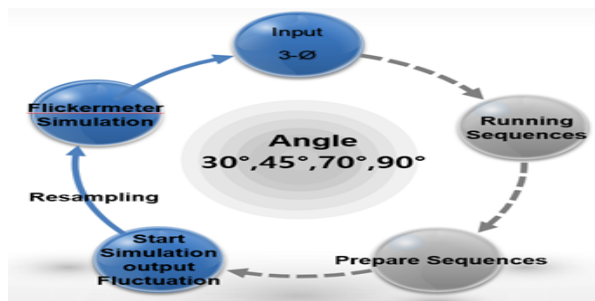


Figure. 11: Diagram of Simulation Work-flow

Table 5: Simulation: switching cycle with different periods

File name	Saved Parameter
When i = 1	
Initial values	Includes all the input entry when i =2 (save once)
Between_values	Includes 'j', 'i', 'Searchdir' (saved once)
Final_results.j_Alpha	Includes all the calculated results together
Initialvalues	Includes all the input entry when i =2 (save once)
When i = 2	
Initialvalues	Initialvalues
Includesall the input entry when i =1 (save once)	Includesall the input entry when i =1 (save once)
Between_values	Includes'j', 'i', (saved once)
General output (not related to i)	Overall Results
Simulation_results.j_Alpha	Ufic, U0,ku.psyk,f,U (3Ph-signals) & Time.1
Complete overall Results	All the values calculated by the formula including the average values.

- 1 When the cycle $i = 1$. This cycle is repeated as per $j \leq endval$ times in order to completed all the switching operation which determine by the user. After completion of loop it is done 'jj' is increased and then calculation are re-executed for another impedance angle (*Alpha*) value defined by the user till $jj \leq endval1$.
- 2 When the cycle $i = 2$. The cycle is re-done by the same procedure.

The voltage fluctuation calculated by fictitious grid, and flicker meter calculates the short and long flicker. All the file executed by program save the necessary required results internally. The different saving parameters are shown in table.5.

Measurement and Assessment

7 Measurement and Assessment

This section describes a correlative analysis of the flicker measurement and assessment concerning continuous and switching operations according to the IEC 61400-21 standard. The design of simulation model for the flicker measurement and assessment during continuous and switching operations depicted in Fig.3 and Fig.4. The outcomes of flicker measurement depend on the various dynamics of simulation results. The goal of the chapter folds into three directions of flicker measurement, 1) to test the validated design of a simulation model of flicker measurement, 2) to assure the implementation of flicker measurement model based on continuous and switching operations procedure according to the IEC 61400-21 standard, 3) to compare the results with the IEC updated standard. The overall effects evaluated by performing three tests of the flicker measurements and assessments in the grid-connected wind turbine.

1. Test to validate the results of flicker measurement and assessment.
2. Performance test of the Fictitious grid.
3. Accuracy test of the flicker meter.

1. Test to validate the results of flicker measurement and assessment.

The voltage and current are extracting in the form of time-series values $um(t)$ and $im(t)$, and the flicker coefficient is the output of the 'Normalization' block see in Fig.3. The parameter of flicker coefficient c_{ψ_k} determine the verification of the flicker measurement results according to the IEC 61400-21 standard. The flicker coefficient can be verified using a sinusoidal modulated signal based on predetermined values of the flicker

Table 6: The verification test using nominal values of the wind turbine

Nominal values of the wind turbine		
Symbol	Value	Units
Sn	3	MVA
Un	12	KV
In	144	Am

coefficient c_{ψ_k} . The measurement tests are using the parameters of the wind turbine for simulation, as shown in Table.6.

The input side current im_t is same in all the tests. However, a sinusoidal signal varying with the sinusoidal fluctuations which are characterized by the current changes $\Delta I/I$, and the amplitude modulation frequency f_m . The three phase input current equations 11-13 are written as follows:

$$im_t = \sqrt{2} \times I_n \times (1 + \Delta \frac{I}{I} \times \frac{1}{100} \times \sin(2\pi f_m t)) \times \sin(2\pi f_g t) \quad (11)$$

$$im_t = \sqrt{2} \times I_n \times (1 + \Delta \frac{I}{I} \times \frac{1}{100} \times \sin(2\pi f_m t)) \times \sin(2\pi f_g t) - (120\pi/180) \quad (12)$$

$$im_t = \sqrt{2} \times I_n \times (1 + \Delta \frac{I}{I} \times \frac{1}{100} \times \sin(2\pi f_m t)) \times \sin(2\pi f_g t) + (120\pi/180) \quad (13)$$

Where f_g is the nominal grid frequency around 50Hz. The input voltage signal um_t based on the same frequency and phase angle described in the equations 11-13. Similarly, the three phase modulated input voltage equations are as follows:

$$um_t = \sqrt{\frac{2}{3}} \times U_n \times (1 + 3 \times \frac{1}{100} \times \frac{1}{2} \times \sin(2\pi f_m t)) \times \sin(2\pi f_g t) \quad (14)$$

$$um_t = \sqrt{\frac{2}{3}} \times U_n \times (1 + 3 \times \frac{1}{100} \times \frac{1}{2} \times \sin(2\pi f_m t)) \times \sin(2\pi f_g t) - (120.\pi/180) \quad (15)$$

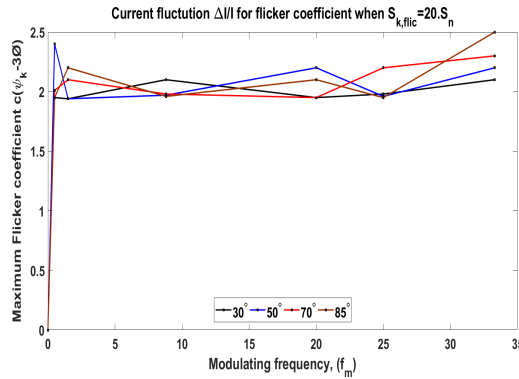
$$um_t = \sqrt{\frac{2}{3}} \times U_n \times (1 + 3 \times \frac{1}{100} \times \frac{1}{2} \times \sin(2\pi f_m t)) \times \sin(2\pi f_g t) + (120.\pi/180) \quad (16)$$

Table 7: flicker coefficient = $2,00 \pm 5$ when $S_{k,flc} = 20 \cdot S_n$

fm(Hz)	Current fluctuation $\Delta I/I$ for 50 Hz			
	$\psi_k 30^\circ$	$\psi_k 50^\circ$	$\psi_k 70^\circ$	$\psi_k 85^\circ$
0.5	8.031	10.401	17.860	49.537
1.5	3.618	4.684	8.029	21.924
8.8	0.833	1.064	1.712	3.192
20	2.294	2.773	3.748	4.763
25	3.335	3.901	4.892	5.686
33.3	6.648	7.330	8.289	8.881

Where the network impedance angle ψ_k are describing in the Table.7. The measurement consists on the short circuit apparent power $S_{k,flc} = 20 \times S_n$ of the fictitious grid. The IEC-61400-21-1 standard is giving the assurance that the observed flicker coefficient c_{ψ_k} values should be $2 \pm$ within the tolerance of ± 5 . These desired values validates the designed simulation model. Thus, the designed model of flicker measurement should be validated by the simulation results according to the IEC-61400-21-1 standard.

The measurement of flicker coefficient c_{ψ_k} during switching and continuous operation see in Fig.12, and Fig.13. The obtained results validated that the variation $2 \pm$ within the tolerance of $5 \pm \%$ maximum range in between $1.96 - t_o - 2.4$ and the average range approximate $1.90 - t_o - 2.0$. In case of without voltage fluctuation, the obtained results should validated the desired values of the IEC-61400-21-1 standard.

**Figure. 12:** Maximum flicker coefficient c_{ψ_k}

The current changes $\Delta I/I$ as per the angle ψ_k and the amplitude modulation frequency $f_m = 8.8 \text{ Hz}$ is fixed. In the switching operation, the emission of short circuit ratio (SCR) at the WT converters side, therefore SCR gradually increases and fixed the short-circuit apparent power at the

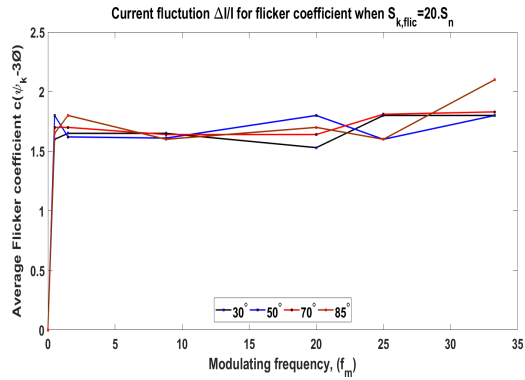


Figure. 13: Average flicker coefficient c_{ψ_k}

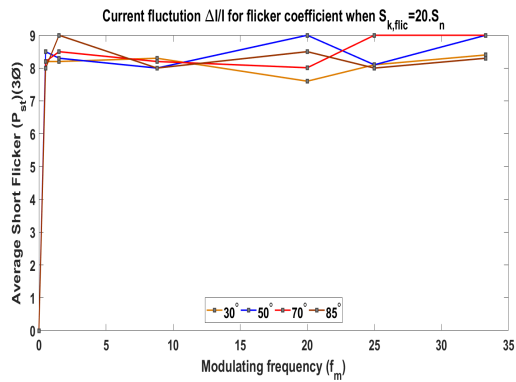


Figure. 14: Average short flicker P_{st}

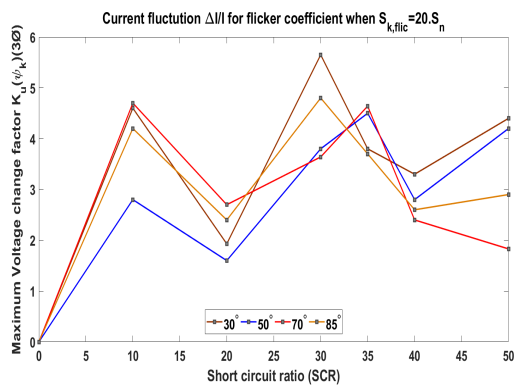


Figure. 15: Voltage changes factors Ku_{ψ_k}

Table 8: Specification of test for distorted voltage with multiple zero crossings

Harmonic order	3	5	7	9	11	13	17	19	23	25	29	31
U - % of U_n	5	6	5	1.5	3.5	3.0	2.0	1.76	1.41	1.27	1.06	0.97

fictitious grid $S_{k,flic} = 20 \times S_n$. According to the IEC standard [6], the range of short-circuit apparent power $S_{k,flic} = 20 - 50 \times S_n$ extracts from the fictitious as per the IEC standard [6].

Similarly, the three-phase average short flicker P_{st} , and average short flicker P_{st} and voltage changing factors Ku_{ψ_k} during switching and continuous operation as shown in Fig.14, and Fig.15. The short flicker P_{st} measurements is approximately average range in between 7.8 – to – 8.8 during continuous operation at $time = 10minute$, where The current changes $\Delta I/I$ as per the angle ψ_k and the amplitude modulation frequency f_m gradually increases. The voltage change factor during switching and continuous operation are changes versus SCR emission from the WT. While the short-circuit apparent power $S_{k,flic} = 20 \times S_n$ from the fictitious grid is fixed.

2. Performance test of the Fictitious grid.

In this section, two type of tests are performed by simulation, 1) to validates the simulation results, and 2) to check the overall performance of the fictitious grid. The input current signal $im_{(t)}$ and all the parameters are same as above including the grid frequency and SCR from wind turbine switching. The testing results validated by observing the flicker coefficient c_{ψ_k} , and it should be around 2.0 within a tolerance of $+/- 5\%$. The fictitious grid performance test based on distorted $um_{(t)}$ voltage with multiple zero crossings [6]. Aim to verify the procedure for generating the ideal voltage source $u_o(t)$ of the fictitious grid based on a distorted input voltage signal $um_{(t)}$. Further, the distorted input voltage signal $um_{(t)}$ measured by multiple zero crossings. The distorted voltage is known as fluctuated voltage $um_{(t)}$ which composed of the fundamental voltage and levels of harmonics are as written in the Table.8.

In the simulation process, all the harmonics have a 180° phase shift within the 50Hz fundamental. In other words, all have a negative going zero crossing in the signal while the fundamental has a positive going zero crossing. As discussed above the voltage fluctuation is sinusoidally modulated at 8.8Hz with a relative amplitude of 0.25%. The voltage

three-phase signal Um_t can be written as follows:

$$Um_t = \sqrt{\frac{2}{3}} \times U_n \times (1 + 0.25 \times \frac{1}{100} \times \frac{1}{2} \times \sin(2\pi 8.8.t)) \times \sin(2\pi f_g t) + (U_v \times \frac{1}{100} \times \sqrt{\frac{2}{3}} \times U_n \times \sin(2\pi 8.8 f n t + \pi)) \quad (17)$$

$$Um_t = \sqrt{\frac{2}{3}} \times U_n \times (1 + 0.25 \times \frac{1}{100} \times \frac{1}{2} \times \sin(2\pi 8.8 t)) \times \sin(2\pi f_g t) - (\sin(2\pi/180)) + (U_v \times \frac{1}{100} \times \sqrt{\frac{2}{3}} \times U_n \times \sin(2\pi 8.8 f n t + \pi)) \quad (18)$$

$$Um_t = \sqrt{\frac{2}{3}} \times U_n \times (1 + 0.25 \times \frac{1}{100} \times \frac{1}{2} \times \sin(2\pi 8.8 t)) \times \sin(2\pi f_g t) + (\sin(2\pi/180)) + (U_v \times \frac{1}{100} \times \sqrt{\frac{2}{3}} \times U_n \times \sin(2.\pi 8.8 f n t + \pi)) \quad (19)$$

These three phase voltage equations 17-19 consists on voltage fluctuated $um(t)$ with the inter-harmonic frequencies. In this case, the modulating frequency f_v is increased in steps of 0.5Hz and reaching the maximum modulating frequency up to 30Hz. According to the standard IEC-61400-21-1, the obtained flicker coefficient c_{ψ_k} should be $2 \pm$ with a tolerance of $5 \pm \%$.

The simulation results of the flicker coefficient c_{ψ_k} verses harmonics order during switching and continuous operations presented in Fig.16, and Fig.17.

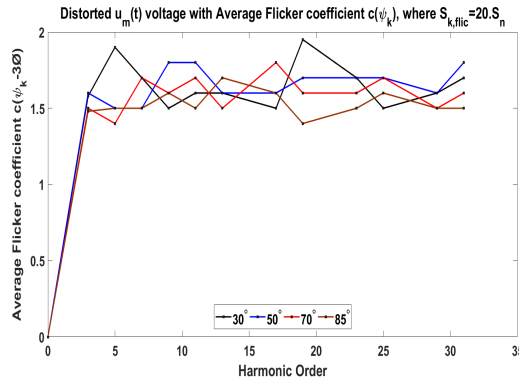


Figure. 16: Average flicker coefficient c_{ψ_k}

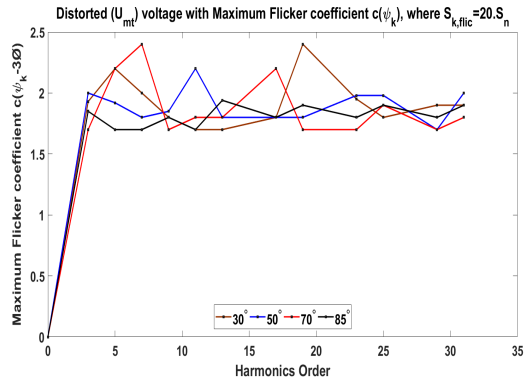


Figure. 17: Maximum flicker coefficient c_{ψ_k}

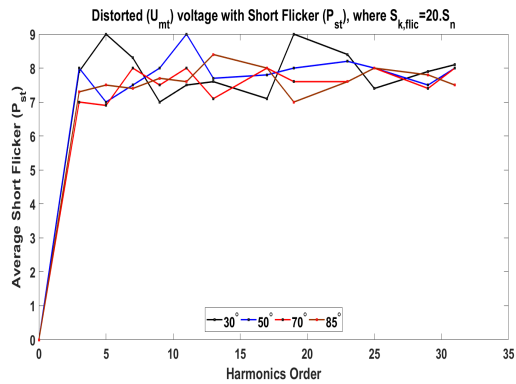


Figure. 18: Average short flicker P_{st} verses harmonics

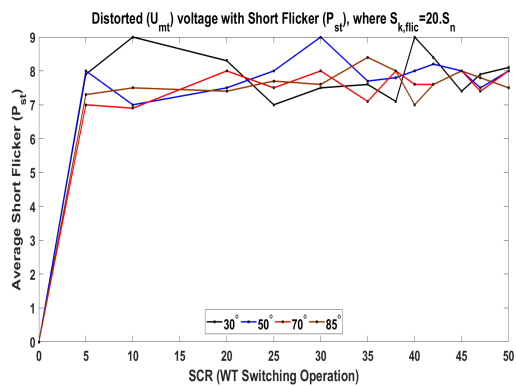


Figure. 19: Average short flicker P_{st} verses SCR

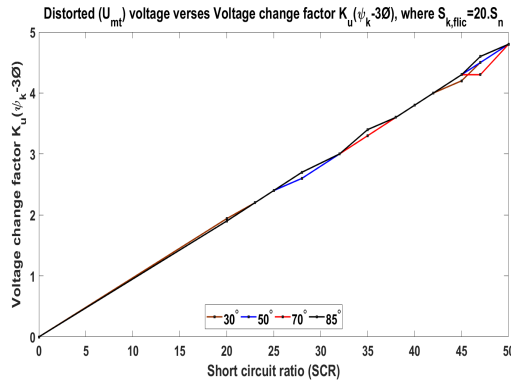


Figure. 20: Voltage changes factors Ku_{ψ_k} versus SCR

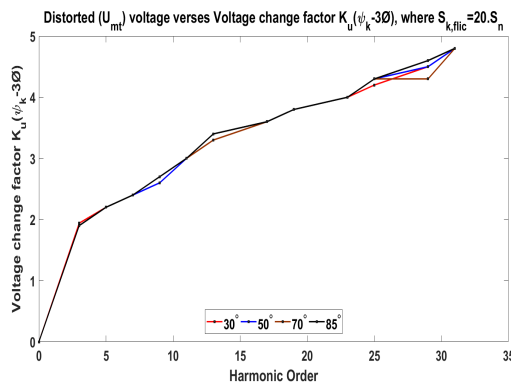


Figure. 21: Voltage changes factors Ku_{ψ_k} versus Harmonics

The flicker coefficient c_{ψ_k} achieved the prescribed values, defined in the standard IEC-61400-21-1 such as the flicker coefficient c_{ψ_k} ranges within 2.00 – 2.5, however the deviation in the level of tolerance around $5 \pm \%$ due to the inter-harmonics and SCR emission from the switching of the wind turbine.

Average short flicker P_{st} during switching and continuous operation is depicted in Fig.18, and Fig.19. The flicker performance evaluated by the measurement of average short flicker P_{st} during switching and continuous operation. The obtained results is approximate values between $P_{st} = 07 - 09$. These result analysis with harmonics and SCR values. Harmonics is the main cause of switching operation in wind turbine.

The voltage change factors and impedance angle ψ_k involved in the measurement operation of the wind turbine. The voltage change factors Ku_{ψ_k} is activated inversely proportional to the short circuit power $S_{k,flic}$ of the fictitious grid during switching and continuous operation. Thus, voltage

Table 9: The voltage fluctuation for flicker classifier

230 V/50 Hz	IEC 61000-4-15 Sinusoidal	IEC 61000-4-15 Rectangular	IEC 61000-4-15 Rectangular	
$freq : Hz$	$\Delta U/U\%$	$\Delta U/U\%$	$r(min^{-1})$	$\Delta U/U\%$
0.5	2.235	0.509	1	2.715
1.5	1.067	n.a	2	2.191
3.5	n.a	0.342	7	1.450
8.8	0.250	0.196	39	0.894
18	n.a	0.446	110	0.722
20	0.704	n.a	1620	0.407
21.5	n.a	0.592	4000	2.343
25	1.037	0.764		
28	n.a	0.915		
30.5	n.a	0.847		
33 1/3	2.128	1.671		

change factor and impedance angle ψ_k are an essential part of the measurement of flicker for a wind turbine. Therefore, the performance of the fictitious grid is estimated by the voltage change factors Ku_{ψ_k} . The voltage change factor almost directly proportional to harmonics and switching operation (SCR) in wind turbine. In case of fixed the short circuit power $S_{k,flic}$ of the fictitious grid, the voltage change factors Ku_{ψ_k} directly proportional to the SCR and harmonics, as shown in Fig.20, and Fig.21.

The results indicate, the three-phase voltage input $um_{(t)}$ reduces the level of inter-harmonic frequencies by appropriate filtering techniques. The results would be obtained effectively with minimum voltage fluctuation at the PCC.

3. Results of Accuracy Verification for IEC flicker meter

The IEC 61000-4-15 flicker meter is checked P_{inst} values from input-to-output total response characteristics. The verification test for accuracy is performed through sinusoidal and rectangular voltage changes. as described in Table.??.

The IEC 61000-4-15 standard has specified the desired requirement for the verification of accuracy i.e. $P_{st} = 1 : 00, \pm 5\%$ and $P_{inst} = 1 : 00, \pm 8\%$. In case, the flicker meter achieved the desired applicable requirement as per IEC standard. So the accuracy of the flicker meter is considered 100%. Since it is challenging to enhance the accuracy in the measurement for flicker meter according to the desired requirement of IEC standard. The squeezing point of this paper: to present the verified results with accuracy deviation in flicker meter. The verification results based on the assessment of the accuracy deviations in between *applicable desired requirement from IEC 61000-4-15 standard with the obtained results.*

The accuracy verification testing through sinusoidal and rectangular voltage

changes using voltage fluctuation waveform as given in equation 20.

$$U_t = 1 + \frac{\Delta U}{U} \times \text{signum}[\sin(2\pi f_v t)] \times \sin(2\pi f_m t) \quad (20)$$

where $\frac{\Delta U}{U}$ is voltage fluctuation, f_v is flicker frequency, and f_m is system fundamental frequency [7]. The simulation model designed in the matlab by using digital flicker meter in the power-system tools. The measurement procedure follows the accuracy and precision level in terms of flicker parameters i.e. P_{inst} , P_{st} , and voltage change in both sinusoidal and rectangular. The simulation results compared with the IEC 61000-4-15 standard, aim to observed the deviation between IEC standard and the outcomes results.

In the first test, to validated the simulation model by estimating the P_{st} with sinusoidal and rectangular voltage changes according to the Table.9 where modulating frequency is fixed. The objective of this test to analyzed the behavior of the P_{st} with voltage fluctuation in the flicker meter, are as shown in Fig.22.

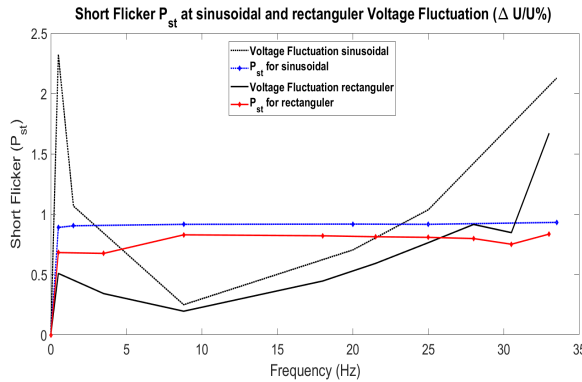


Figure. 22: P_{st} with sinusoidal and rectangular voltage fluctuation

In Fig.22,the level of P_{st} is not effecting due to sinusoidal voltage change, the main reason is cascade filters in the block 3 which rejects the unwanted fluctuation. In case of rectangular voltage change, level of P_{st} is varying with the change in rectangular voltage. The main cause is phase change which is directly impact on the results of P_{inst} and P_{st} values. Thus, the rectangular modulation useful to avoid the effects of inter-harmonics. However, the amplitude increases with voltage changes in the existing flicker meter.

In the second test performed to assess the performance of flicker meter with sinusoidal voltage change, is shown in Fig.23. The goal of the test to observed the values of P_{inst} and P_{st} by increasing voltage fluctuation in the input signals. The simulation settings for performing the continuously change the values of voltage fluctuation as per the above table Table.???. The

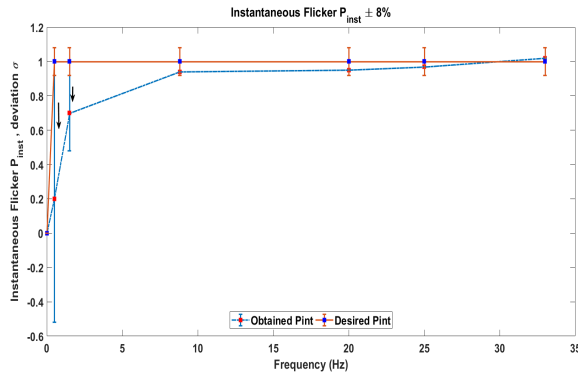


Figure 23: Sinusoidal voltage Change: P_{inst} deviation with IEC 61000-4-15

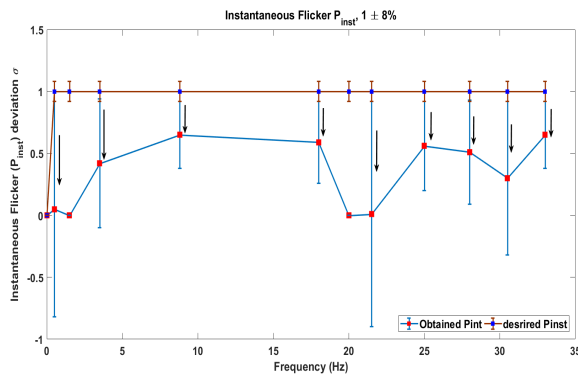


Figure 24: Rectangular voltage Change: P_{inst} deviation with IEC 61000-4-15

results presented the accuracy of the flicker meter. The main conclusion, the performance of FM is impact through change in voltage fluctuation with flicker frequency (modulated frequency). The P_{inst} is estimated by sinusoidal voltage change and compares with desired requirement of IEC 61000-4-15 standard. The wind turbine manufacture is normally estimate P_{inst} test to analyze the voltage fluctuation. The IEC standard applicable P_{inst} requirement is 1 : 00 with a tolerance of $\pm 8\%$. The measurement time is 10mint with each phase jump less than 0.5ms, and the flicker meter ignored the initial 5 – second measurement to avoids the phase jump. The input of the sinusoidal voltage without inter-harmonics is meets the desired requirement of IEC standard as in Fig.23. However, the inter-harmonics wave is the limitation to meets the desired requirement of the IEC standard. In realistic conditions, that the inter-harmonics present in the input of sinusoidal voltage [34]. Therefore, the rectangular modulation techniques is used to overcome the effects of inter-harmonics.

The third test perform to assess rectangular voltage change with proportional effect on the P_{inst} values which indicates the performance of the flicker meter. The performance of Rectangular voltage change measurement is better than sinusoidal voltage change measurement (mean the values under the tolerance range) as shown in Fig.24. In case of inter-harmonics its reaches under the desired requirement of IEC standard. Therefore, standard determine the measurement procedure by employing rectangular voltage fluctuation.

The updated version of IEC standard allowing the range of P_{st} within 2.00. However, the P_{st} range depends on the flicker coefficient c_{ψ_k} and the results of the flicker meter completely diverse in case of continuous and switching operations while performing with a grid connected wind turbine or/ with the fictitious grid [32].

Performance verification of FM by adding Harmonics To observe the values of P_{inst} and P_{st} values by increasing voltage fluctuation and including harmonics parameters in the input signals. In this case P_{inst} should be requirement is 1 : 00 with a tolerance of $\pm 8\%$ and P_{st} values within 2.00. The harmonics addition as per the above Table.8. The input waveform of the performance verification test during continuous and switching operation as given in the above equation 21.

$$Um_t = \sqrt{\frac{2}{3}} \times U_n \times (1 + 0.25 \times \frac{1}{100} \times \frac{1}{2} \times \sin(2\pi 8.8.t)) \times \sin(2\pi f_g t) + \sum U_v \times \frac{1}{100} \times \sqrt{\frac{2}{3}} \times U_n \times \sin(2\pi 8.8 f n t + \pi) \quad (21)$$

Where f_g is the nominal grid frequency 50Hz.

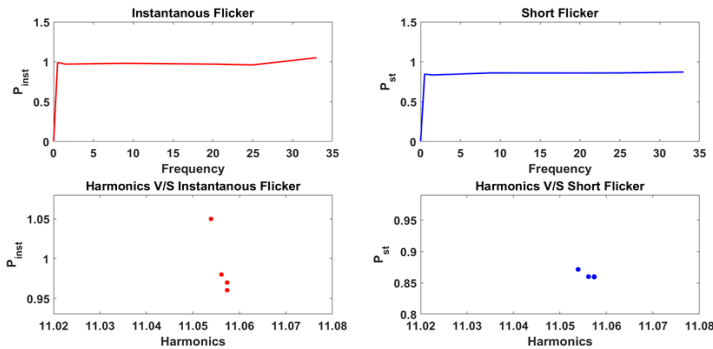


Figure. 25: P_{inst} and P_{st} : voltage fluctuation is fixed, increasing the addition of harmonics IEC 61000-21-1

In Fig.25, presenting the observation that the performance of flicker meter is only affecting by voltage changes and inter-harmonics. Further, the harmonics in signals is not affecting the performance of flicker meter. As discussed above, the inter-harmonics is declining the accuracy of flicker meter. Note. the harmonics is only impact the performance of fictitious grid.

Conclusion and Future Work

8 Conclusion and Future Work

The project hypothesis presented at the beginning of the section 1. The scope of the project and overall background history of the project discussed in the state-of-the-art 2. Further, the system model elaborates the flicker measurement process of the grid-connected wind turbine in chapter3. The IEC framework of flicker measurement describes in the chapter 4. Finally, explain the simulation model and evaluated the measurement and assessment results in 7.

In this thesis, the measurement of power quality of a grid-connected wind turbine has been investigated. Specifically focused the power quality measurement challenges concerning flicker and harmonics measurement through IEC standard.

There are following finding and conclusions of the project (Part 1):

1. The study and analysis of the overall project including the literature review of all the IEC standard discussed in the Table.1.
2. During study and analysis, found that flicker measurement process is depending on the continuous and switching operations. Moreover, the performance of the fictitious grid and flicker meter play a vital role in the accuracy of flicker measurement and assessment.
3. The project research problems were formulated through an intensive review of the state-of-the-art. The conclusion, before starting the design model for simulation, it is essential, to draw the idea into the Systems model of the flicker measurement with continuous and switching operations, and it should be according to the updated version of the IEC standard.

4. Based on the system model, to defined the framework of the flicker measurement process according to the updated standard. At this stage, found that there is plenty of space for research in the area of flicker measurement systems. Further, the overall flicker measurement systems need to improve by using robust techniques and methods. However, it is difficult to focus at one point, due to the time limitation in the research project.
5. Now at the architecture model with measurement parameters was available to develop the simulation model for flicker measurement and assessment.
6. The flicker measurement simulation model designed by using Matlab and Simulink tool. First, tests based on the interlink parts of the simulation model like fictitious grid and flicker meter, and assured that all the components are working according to the standard IEC 61000-4-21-1.
7. Now at this stage, the designed simulation model was available for the flicker measurement and assessment according to the standard IEC 61000-4-21-1.
8. There are three tests performed for the flicker measurement and assessment. 1) check to validate the results of flicker measurement and evaluation, 2) Performance test of the Fictitious grid, and 3) accuracy test of the flicker meter.
9. In test 1, simulation results are analyzed by validating the flicker measurement by the flicker coefficient c_{ψ_k} , and found that the values of flicker coefficient c_{ψ_k} approximate reach the desired values ($2 \pm$ within the tolerance of ± 5) of the standard IEC standard 61000-4-21-1.
10. In test 2, this test divided into two parts of the simulation, 1) test to validates the simulation results, and 2) test to check the overall performance of the fictitious grid.

The finding of the test 2 as follows.

- The voltage change factors Ku_{ψ_k} is inversely proportional to the short circuit power $S_{k,flic}$ of the fictitious grid during switching and continuous operation.

- The voltage change factor and impedance angle ψ_k are essential parameters of the measurement of flicker. Therefore, the performance of the fictitious grid is estimated by the voltage change factors Ku_{ψ_k} .

- The voltage change factor almost directly proportional to harmonics and switching operation (SCR) in wind turbine. In case of fixed the short circuit power $S_{k,flic}$ of the fictitious grid, the voltage change factors Ku_{ψ_k} directly proportional to the SCR and harmonics.

- In case of zero voltage fluctuation, the simulation model validated

with desired values of IEC standard. Further, harmonics and SCR ratio affects the performance of the fictitious grid.

11. Test 3 is related to the performance verification of flicker meter by adding the harmonics. The overall conclusion found that the flicker meters is only effecting by the voltage fluctuation and inter-harmonics of the flick meter itself. The harmonics signal is not affecting the performance of the flicker meter. As discussed above, the harmonics signal is only affecting the performance of the fictitious grid during continuous and switching operation.

8.1 Scientific Contribution

- * The flicker measurement model designed according to the IEC standard 61000-4-21-1.
- * Execute the simulation to find the performance of the flicker measurement model. All the simulation results verified by the IEC standard.
- * The project produces the two research articles. The first article has been accepted and now in publishing phase, and the second article is work in progress.

Validation of Flicker Measurement in Grid-connected Wind Turbine

Noman Khan*, Usman Farooq†, Pooya Davari‡, Xiongfei Wang§ and Lars Helle§

Department of Energy Technology and Vestas Wind Systems,
Aalborg University, Denmark

Email: *nghan15@student.aau.dk, †ufarooq16@student.aau.dk, ‡pda@et.aau.dk, §xwa@et.aau.dk, §lah@vestas.com

Abstract—Wind energy is the growing source of electricity and the most significant contributor to power generation worldwide. However, as the wind speed variate, it results in power fluctuations, and converters adversely affect the power quality of grid-connected wind turbines. The power quality measurement procedure is defined in the standard IEC-61400-21. The updated standard IEC-61400-21-1 provides a uniform methodology, which will ensure the accuracy of the testing and assessment, i.e., voltage quality (emissions of flicker and harmonics). The power fluctuation of the wind turbine produces variations in the illumination intensity of the light source. Such a variation produced by voltage fluctuation is known as a flicker. The flicker emission produced by the turbine due to rapid changes in wind speed results in fluctuating power, which can lead to voltage fluctuations at the point-of-common-coupling (PCC). The IEC-61000-4-15 standard describes the measurement specification of the flicker meter. The accuracy of the measuring methods is an essential part of the assessment of power quality in the grid-connected wind turbine. Therefore, the paper deals with the verification test of the measurement procedure for the flicker, and the results are demonstrated through the simulation according to the measurement and assessment standard IEC-61400-21-1.

Index Terms—Power quality, voltage fluctuation, flicker and harmonics measurements.

I. INTRODUCTION

As a matter of fact, the development of renewable energy sources has a positive impact on the environment [4]. However, the power quality issues affect distributed generation due to the infrequent nature of renewable energy resources like the speed of wind in the wind energy sector [5]. Wind energy can achieve top rank in electricity production if the industry can conquer the rising challenges of power quality [2], see in Fig.1. The International Electro-technical Commission (IEC) standard specifies the procedures for the measurement and assessment of power quality disturbances such as flicker and harmonics emission by grid-connected wind turbine (WT) [14]. Thus, power-quality does not depend only on the ratio of voltage fluctuation in the power production as other factors also contribute to it, i.e., distortion in voltage and current, transient, harmonics and flicker [17]. In wind power systems, the voltage fluctuations are measured by flicker meter to estimate the flicker severity [11]. Flicker produced during the

The authors are with the *R&D* group of power electronics under Prof.Frede Blaabjerg in the Department of Energy Technology at Aalborg University (AAU), and highly grateful for the collaboration of Vestas wind systems, Denmark.

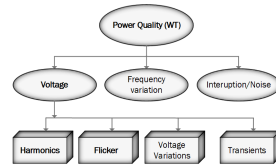


Fig. 1: Power quality challenges in wind turbine

start-up, at cut-in wind speed, switching between generators and during running operation. It is known as continuous and switching operations of the grid-connected wind turbine (WT) [14]. Moreover, the grid resistance-reactance (X/R)-ratio is an essential factor of flicker and harmonics emission [19]. The flicker emission can be limited by controlling the short-circuit-ratio (SCR) and rating of the wind turbine. There is a trade-off between flicker and operational parameters of WT. Therefore, flicker measurement is a critical challenge and requires special procedure for analysis and assessment [8]. An accurate flicker measurement allows to achieve the maximum optimized level of the power production in WT [13].

The manufacturers of WT and the IEC maintenance team have been taking actions for the standardization of power quality challenges [6] [1] and are currently working on the validation of measurement procedure. The prime objectives are to align the dynamic simulation model with the upcoming standards of wind energy generation [3], design the robust measurement procedure [9], and specify the consistency in the results and enhancing the accuracy in the results. The IEC 61400-21 standard specifies the flicker measurement and assessment procedure and defines the simulation design of a fictitious grid during continuous and switching operations. The standard of IEC-61000-4-15 [9] specifies a measuring method by simulating the process of physiological visual (lampeyebrian chain) perception [11] [16]. The flicker meter measures the short and long flicker severity independently or while integrated with a fictitious grid. The measurement accuracy declines in the digital implementation procedure of the fictitious grid due to various factors, e.g., phase lock loop (PLL) that are not precisely encircled in the IEC 61400-21 standard [17].

Considering all the factors and information stated before, this paper focuses on the flicker measurement and assessment procedure and demonstrates the measurement results according to the recently updated standard IEC 61400-21-1 [8]. The flicker assessment and measurement model is designed in Matlab (Simulink). The overall results validation is being performed by two simulation tests which include: 1) the validation of flicker measurement as per the requirement of the IEC 61400-21-1 standard, and 2) performance validation of the fictitious grid. The present study and analysis specially provide the benefits of the industry of WT manufacturers concerned with power quality and power production. The arrangement of the paper is as follows:

Section II summarizes the model architecture of flicker measurement, assessment model, and determines the main functional parameters of measurement procedure according to the IEC 61400-21-1 standard. Section III presents the comprehensively validated measurement procedure during switching and continuous operations. This section describes a correlative analysis of the flicker emission, assessment, and simulation results including flicker coefficient c_{ψ_k} , voltage changes factors Ku_{ψ_k} , and short flicker P_{st} . Finally, conclusion is presented in Section IV.

II. FLICKER MEASUREMENT MODEL IN GRID-CONNECTED WT

The architecture model of measurement and assessment procedure for flicker uses a model designed by standard IEC-61400-21-1 [17]. The flicker emission specifies that flicker is caused by grid-connected WT [18]. Therefore, the IEC-61400-21-1 standard focused on two sections, i.e., measurement procedure and further characterizing by two situations: continuous operation and switching operations [13].

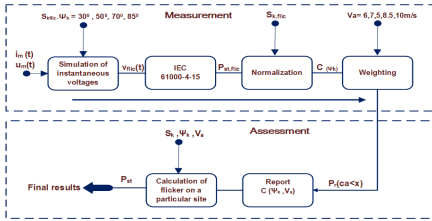


Fig. 2: Measurement and assessment procedures for flicker during continuous operation of the WT according to the IEC 61400-21-1

The normal operation of the turbine excluding start-up and shutdown time of the transaction is known as the continuous operation of the WT, and the continuous operation measurement model is shown in Fig.2. Flicker produced during continuous operation causes power fluctuation due to variation in wind speed in the WT.

There are various types of switching operational characteristics, such as a) WT start-up at cut-in wind speed, b) WT

start-up at rated wind speed or higher wind speed, and c) The switching between generators or a generator with multiple winding. The switching operations determine the support of flicker step factor and voltage change factor. Further, the parameters are described by numbers of switching (N_{10m} and N_{120m}) based on manufacturers' information. The step factor Kf_{ψ_k} and voltage change factor Ku_{ψ_k} can be regulated by the control system of the WT. The diagram of flicker measurement procedure during switching operation is shown in Fig.3.

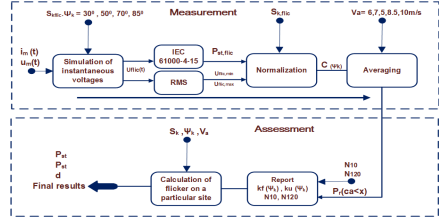


Fig. 3: Measurement and assessment procedures for flicker during switching operations of the WT in accordance with IEC 61400-21-1

A. Framework of Measurement and Assessment

As per the standard of IEC-61400-21-1, the flicker measurement procedure consists of first four blocks, and assessment is executed by the last two blocks. The assessment blocks recall the overall estimation of the blocks including the parameters of continuous and switching operations.

The estimation of the preliminary stage concerns the power quality for standardization of WT. This estimation is based on power signal and flicker evaluation, which is demonstrated in the previous IEC standards. In this context, the IEC working group of the technical committee has examined the results and compared the method based on current i_s and voltage signals u_s . Finally, IEC 61400-21-1 introduced that flicker evaluation depends on the current i_{mt} and voltage u_{mt} time-series measured at the PCC terminals nearby WT. However, the literature survey addressed that the flicker is not caused only by the WT itself [18]. In short, the voltage fluctuations also ingress from the grid side at the PCC terminal where flicker is measured [19]. Thus, the voltage fluctuations imposed on the WT depend on the grid conditions [20]. Therefore, the measurement model developed in the upgraded standard IEC 61400-21-1 allows the independent measurement of the voltage fluctuations. The model is known as a fictitious grid that enables the analysis of voltage fluctuations caused exclusively by the WT.

The fictitious grid estimates the voltage fluctuation from the input side, and precise estimated values of voltage fluctuations are delivered to the flicker meter. The flicker severity is measured by flicker Meter (FM) and the measuring procedure is determined in the IEC-61000-4-15 standard [3]. The flicker measurement procedure as per standard IEC 61400-21-1 provides the estimation to obtain various parameters

namely: voltage changes, flicker step factor, flicker coefficient, and voltage change factors during continuous and switching operations.

1) *Implementation of Fictitious Grid:* The initial stage of the voltage and current processing procedure determines the fictitious voltage $U_{flic(t)}$ and characterizes the causes of the voltage fluctuations which leads to the PCC [15]. The standardized fictitious-grid is shown in Fig.4. The fictitious

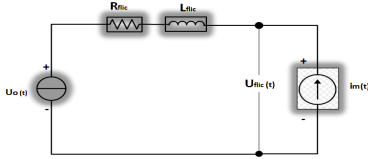


Fig. 4: Fictitious grid used for flicker assessment in Grid-connected WT

grid performed by an ideal voltage source (phase-to-neutral) integrated with instantaneous value $u_o(t)$ and impedance of the grid is represented by two electrical components such as R_{flic} in series with an inductor L_{flic} . Moreover, the WT, which described the instantaneous values of the line current source, $i_m(t)$ is also represented by the current generator of the WT. The fictitious grid's output is fluctuated voltage integrated with the instantaneous values $U_{flic(t)}$, as follows [11].

$$U_{flic(t)} = u_o(t) + R_{flic} \times i_m(t) + L_{flic} \times \frac{di_m(t)}{dt} \quad (1)$$

In equation number: 1, the critical signal is ideal voltage source $u_o(t)$ and it requires assurance for the sufficient performance of the signal $u_o(t)$. Therefore, the voltage source $u_o(t)$ must fulfill two conditions. First, flicker should be zero in the ideal voltage source $u_o(t)$. Second, the electrical angle of the $u_o(t)$ should be the same as the fundamental component of the input voltage, which means that the phase angle must be correct and in between $U_{flic(t)}$ and current source $i_m(t)$, these parameters provide $|U_{flic(t)} - u_o(t)| \ll |u_o(t)|$. Thus, $u_o(t)$ is the same as the fundamental voltage U_{flic} . Therefore, the execution properties of the $u_o(t)$ is represented by [17] as follows:

$$u_o(t) = \sqrt{\frac{2}{3}} \times U_n \times \sin(\alpha(t)) \quad (2)$$

Where U_n is the r.m.s values of the nominal voltage in the grid-connected WT, and the electrical angle ($\alpha(t)$) of the pure fundamental component, the ($\alpha(t)$) can be define as follows:

$$\alpha(t) = 2\pi \times \int_t^0 f_{dt} + \alpha(o) \quad (3)$$

where the $f(t)$ is varying frequency over the time; t is the starting time-series, and $\alpha(o)$ is the angle at time $t = 0$. Furthermore, R_{flic} and L_{flic} should be selected to drive

the appropriate network impedance phase angle ψ_k to be determined in the equation below:

$$\tan(\psi_k) = \frac{2\pi \times f_g \times L_{flic}}{R_{flic}} = \frac{X_{flic}}{R_{flic}} \quad (4)$$

where f_g is the nominal grid frequency (50 or 60 Hz), and the three-phase short-circuit apparent power of the fictitious grid is defined by the equation as follows:

$$S_{k,flic} = \frac{U_n^2}{\sqrt{R_{flic}^2 + X_{flic}^2}} \quad (5)$$

The flicker meter IEC 61000-4-15 evaluates the flicker severity P_{st} and instantaneous flicker P_{inst} . For the measurement of P_{st} and P_{inst} , the flicker meter used the short-circuit ratio $\frac{S_{k,flic}}{S_n}$ (SCR) between the range of 20 and 50. The accuracy of the flicker meter depends on the P_{st} , which should be better than 5%, this ratio is recommended by IEC 61400-21-1.

The flicker meter standard IEC-61000-4-15 defines voltage fluctuation processing procedure with the four quantifying steps: 1) the voltage change factors in percent, 2) the modulated frequency of the voltage change, 3) characteristics of the physical light-source, and 4) the procedure of the human brain recognition of the voltage fluctuation [17]. Thus, the flicker measurement procedure through the flicker meter is an efficient way of observing the voltage fluctuation [11]. The measurement procedure of the flicker meter is verified by an incandescent lamp with voltage fluctuation [9]. The fundamental phenomenon of flicker measurement is designed based on the physiological and psychological involved in the measurement of perception [7]. The literature survey analysis indicated that the procedure in IEC 61000-4-15 does not efficiently estimate the minimum voltage fluctuations, which means very low accuracy [12]. This paper does not precisely focus on the dynamics of the flicker meter. However, the flicker meter plays an important role in the verification tests of the flicker measurement.

B. Continuous Operations

The detail about the procedure of the flicker measurement and assessment during continuous operation is shown in Fig.2. The continuous operation of WT produces the flicker emission (99th or 95th percentile) coefficient ψ_k . The C_{ψ_k, V_a} is provided (95th percentile) for the grid-connected network impedance phase angles ($\psi_k = 30, 50, 70$ and 85) at different wind speed distribution ranges $V_a = 6, 7, 5, 8.5, 10m/s$. The range of wind speed is set according to the Rayleigh distribution [10], the probability distribution fits the annual wind speed distribution as $F_v = 1 - \exp(-\frac{\pi}{4}(\frac{v}{v_a})^2)$. The WT flicker coefficient is measured during continued operation as follows:

$$C_{\psi_k, V_a} = P_{It} \times \frac{S_k}{S_n} \quad (6)$$

The flicker coefficient is C_{ψ_k, V_n} , where the flicker coefficient depends on the grid impedance angle ψ_k and wind speed V_n and S_k is the short circuit apparent power of the grid. The rated apparent power of the WT is S_n , and P_{lt} indicates a long flicker emission. Normally, the low wind speed produces low flicker coefficient [17] [18].

C. Switching Operations

The characteristic shall be stated for the switching operations where significant voltage variations are given in three points, i) start-up at cut-in wind speed in WT, ii) WT start-up reached at rated wind speed, iii) the unfavorable situation of switching between generator where WTs are connected with one or more generator (multiple winding). Normally, the measurement of switching operations is within a 10-minute period N_{10} for short-flicker measurement and 2-hours N_{120} for long-flicker measurement. The flicker step factor is a standardized measurement procedure of the flicker emission with respect to a single switching operation of a WT as follows: —

$$K_f(\psi_k) = (1/30) \times \frac{S_k}{S_n} \times P_{st,ftic} \times T_p^{0.31} \quad (7)$$

where $K_f(\psi_k)$ is the flicker step factor of the WT in terms of a single switching operation, and $T_p^{0.31}$ is the duration of the voltage variation, which is due to the switching operation, P_{st} is the flicker emission from the WT, S_n is the rated apparent power of the wind turbine and S_k is known as the short-circuit apparent power of the grid. The flicker step factor considered the network impedance phase angle (30, 50, 70 and 85). The variable-speed WTs produced low flicker step factors [13] as compared to the fixed-speed WT, which may generate the range from average (pitch controlled) to high (stall controlled). In the single switching operation of a WT, the voltage change factor $K_u(\psi_k)$ is measured by the following equation:

$$K_u(\psi_k) = \sqrt{3} \times \frac{U_{fic,max} - U_{fic,min}}{U_n} \times \frac{S_k}{S_n} \quad (8)$$

Where $K_u(\psi_k)$ is the voltage change factor of the WT according to the specified switching operation. The U_{min} and U_{max} are the minimum and maximum voltage (R.M.S phase-to-neutral). The U_n is the nominal phase-to-phase voltage, S_n is the rated apparent power of the WT, and the S_k is the short-circuit apparent power of the grid. The flicker step factor and voltage change factor should be evaluated as the average results of the around 15 values.

D. Verification test and measurement results

This section describes a correlative analysis of the flicker emission measurement and assessment concerning continuous and switching operations measurement procedure according to the standard IEC 61400-21-1. The simulation framework model is designed for the flicker measurement and assessment during continuous and switching operations as depicted in Fig.2 and Fig.3. The outcomes of flicker measurement depend

TABLE I: The verification test using values of WT

Nominal values of the WT		
Symbol	Value	Units
Sn	3	MVA
Un	12	KV
In	144	Am

on the various dynamics particularly on the analysis of estimated results and adopted measurement procedure for flicker. Therefore, flicker measurement testing includes, 1) testing of the designed simulation model for flicker measurement, 2) assuring the implementation of flicker measurement model based on continuous and switching operations procedure, and 3) comparing the estimated results with the standard IEC 61400-21-1. The paper is focused on the measurement procedure results, which were validated under the light of standardization, specified in the standard IEC 61400-21-1. These are the two fundamental tests performed by manufacturers of the WT: namely 1) The validation test of the flicker measurement, 2) The accuracy performance test of the fictitious grid.

a) *The validation test of the flicker measurement:* The WT parameters used in the testing of verification are shown in Table.I. The voltage and current lead to time-series values $um(t)$ and $im(t)$, and the flicker coefficient is the output of the 'Normalization' block as see in Fig.2. The flicker coefficient can be verified using sinusoidal modulated signal based on the predetermined values of the flicker coefficient c_{ψ_k} .

The input current $im(t)$ is same in all these tests. However, a sinusoidal signal varies with the fluctuations, which are characterized by the current changes $\Delta I/I$, and the amplitude modulation frequency f_m . The three phase input current equations 9-11 are written as follows:

$$im_t = \sqrt{2} \times I_n \times (1 + \Delta \frac{I}{I} \times \frac{1}{100} \times \sin(2\pi f_m t)) \times \sin(2\pi f_g t) \quad (9)$$

$$im_t = \sqrt{2} \times I_n \times (1 + \Delta \frac{I}{I} \times \frac{1}{100} \times \sin(2\pi f_m t)) \times \sin(2\pi f_g t) - (120\pi/180) \quad (10)$$

$$im_t = \sqrt{2} \times I_n \times (1 + \Delta \frac{I}{I} \times \frac{1}{100} \times \sin(2\pi f_m t)) \times \sin(2\pi f_g t) + (120\pi/180) \quad (11)$$

Where f_g is the nominal grid frequency around 50Hz. The input voltage signal $um(t)$ with the same frequency and phase angle described in the equations 12-14, the three phase modulated input voltage equations are as follows:

$$um_t = \sqrt{\frac{2}{3}} \times U_n \times (1 + 3 \times \frac{1}{100} \times \frac{1}{2} \times \sin(2\pi f_m t)) \times \sin(2\pi f_g t) \quad (12)$$

TABLE II: Desired values of $c_{\psi_k} = 2.00 \pm 5$ when $S_{k, fic} = 20 S_n$

fm(Hz)	Current fluctuation $\Delta I/I$ for 50 Hz			
	$\psi_k 30^\circ$	$\psi_k 50^\circ$	$\psi_k 70^\circ$	$\psi_k 85^\circ$
0.5	8.031	10.401	17.860	49.537
1.5	3.618	4.684	8.029	21.924
8.8	0.833	1.064	1.712	3.192
20	2.294	2.773	3.748	4.763
25	3.335	3.901	4.892	5.686
33.3	6.648	7.330	8.289	8.881

$$um_t = \sqrt{\frac{2}{3}} \times U_n \times \left(1 + 3 \times \frac{1}{100} \times \frac{1}{2}\right) \times \sin(2\pi f_m t) \times \sin(2\pi f_g t) - (120\pi/180) \quad (13)$$

$$um_t = \sqrt{\frac{2}{3}} \times U_n \times \left(1 + 3 \times \frac{1}{100} \times \frac{1}{2}\right) \times \sin(2\pi f_m t) \times \sin(2\pi f_g t) + (120\pi/180) \quad (14)$$

Where the network impedance angles ψ_k are described in the Table.II. In the fictitious grid simulation model, the parameters regulated by the current changes $\Delta I/I$ accordingly with the angle ψ_k and the amplitude modulation frequency f_m gradually increases. The SCR of the WT is also included in the estimation of the voltage change factor. The results showed that the voltage change factor continuously changes versus SCR emission. The short-circuit apparent power $S_{k, fic} = 20 \times S_n$ from the fictitious grid is fixed. The current changes $\Delta I/I$ as per the angle ψ_k , and the amplitude modulation frequency $f_m = 8.8Hz$ is also fixed. In the scenario of switching operation, the WT converters produce the emission of SCR. Therefore, SCR gradually increases and fixes the short-circuit apparent power at the fictitious grid $S_{k, fic} = 20 \times S_n$. According to the IEC standard [8], the fictitious grid short-circuit apparent power range is $S_{k, fic} = 20 - to - 50 \times S_n$.

The IEC-61400-21-1 standard is assured that the observed flicker coefficient c_{ψ_k} should be 2 within the tolerance of $\pm 5\%$. The simulation model produces approximate results with the applicable requirement specified in the standard IEC-61400-21-1 during switching and continuous operation. The obtained results of flicker coefficient c_{ψ_k} variation around $\pm 2\%$ with the tolerance of $\pm 5\%$ maximum range in between $1.96 - to - 2.2$ (see Fig.6), and the average range approximate $1.90 - to - 2.0$ is shown in Fig.5. The maximum flicker coefficient c_{ψ_k} is seen in Fig.6. Similarly, the three-phase average short flicker P_{st} around P_{st} is $7.8 - to - 8.8$, as shown in Fig.7.

b) *The performance test of the fictitious grid:* This section validates the simulation results of the fictitious grid. The input parameters for the simulation are current signal $im(t)$, grid frequency and SCR (switching) at WT. The IEC-61400-21-1 [8] specified that the test is performed to observed the flicker coefficient c_{ψ_k} and desired requirement around 2.0 within a tolerance of $\pm 5\%$. No doubt the performance test of a fictitious grid cannot be completed without the distorted $um(t)$ voltage with multiple

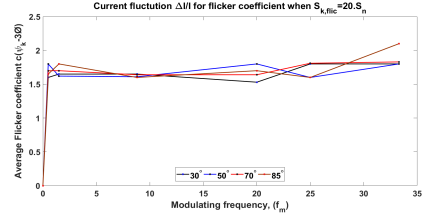


Fig. 5: Average flicker coefficient c_{ψ_k}

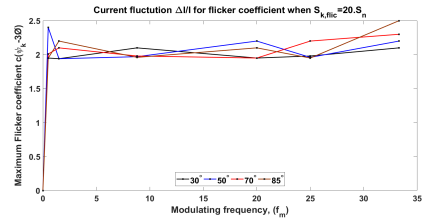


Fig. 6: Maximum flicker coefficient c_{ψ_k}

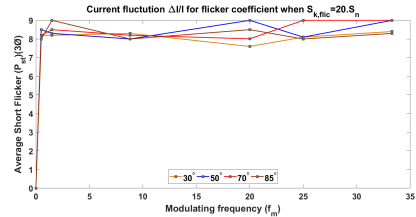


Fig. 7: Average short flicker P_{st}

zero crossings [15]. The fluctuated voltage $um(t)$ integrated with fundamental voltage and levels of harmonics are as written in the Table.III. In addition, this voltage fluctuation $um(t)$ is measured by multiple zero crossings, and the short circuit apparent power $S_{k, fic}$ is fixed in the fictitious grid. In the simulation process, all the harmonics have a 180° phase shift within the $50Hz$ fundamental. In other words, all have a negative going zero crossing in the signal while the fundamental has a positive going zero crossing. As discussed above the distorted voltage is sinusoidally modulated at $8.8Hz$ with a relative amplitude of 0.25%. The three phase voltage

TABLE III: Specification of test for distorted voltage with multiple zero crossings

Harmonic order	3	5	7	9	11	13	17	19	23	25	29	31
U - % of U_n	5	6	5	1.5	3.5	3.0	2.0	1.76	1.41	1.27	1.06	0.97

signal U_{m_t} are written as follows:

$$U_{m_t} = \sqrt{\frac{2}{3}} \times U_n \times \left(1 + 0.25 \times \frac{1}{100} \times \frac{1}{2} \times \sin(2\pi 8.8t)\right) \times \sin(2\pi f_g t) + (U_v \times \frac{1}{100} \times \sqrt{\frac{2}{3}} \times U_n \times \sin(2\pi 8.8f_n t + \pi)) \quad (15)$$

$$U_{m_t} = \sqrt{\frac{2}{3}} \times U_n \times \left(1 + 0.25 \times \frac{1}{100} \times \frac{1}{2} \times \sin(2\pi 8.8t)\right) \times \sin(2\pi f_g t) - (\sin(2\pi/180)) \quad (16)$$

$$+(U_v \times \frac{1}{100} \times \sqrt{\frac{2}{3}} \times U_n \times \sin(2\pi 8.8f_n t + \pi))$$

$$U_{m_t} = \sqrt{\frac{2}{3}} \times U_n \times \left(1 + 0.25 \times \frac{1}{100} \times \frac{1}{2} \times \sin(2\pi 8.8t)\right) \times \sin(2\pi f_g t) + (\sin(2\pi/180)) \quad (17)$$

$$+(U_v \times \frac{1}{100} \times \sqrt{\frac{2}{3}} \times U_n \times \sin(2\pi 8.8f_n t + \pi))$$

These three phase voltage equations 15-17 consists of voltage fluctuated $um(t)$ with the inter-harmonic frequencies. In this case, the modulating frequency f_n is increased with steps of $0.5Hz$ and has reached the maximum modulating frequency of up to $30Hz$. The simulation results of the average flicker coefficient c_{ψ_k} versus the harmonics order during switching and continuous operations are presented in Fig.8.

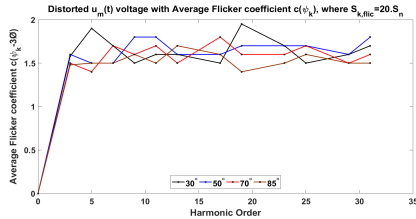


Fig. 8: Average flicker coefficient c_{ψ_k} versus harmonics order

The flicker coefficient c_{ψ_k} achieves the approximate values described in the standard IEC-61400-21-1, the obtained results within the range $1.50 - 2.05$; however the deviation in the level of tolerance is around $\pm 3\%$ due to the inter-harmonics and SCR emission from the switching operation of a WT. Further, the flicker performance estimated by average short flicker P_{st} approximate $07 - 09$. All the results, study, and

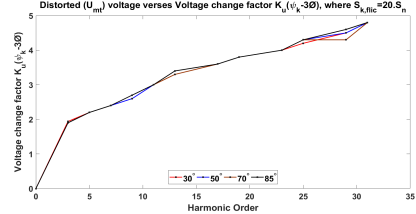


Fig. 9: Voltage changes factors Ku_{ψ_k} versus harmonics

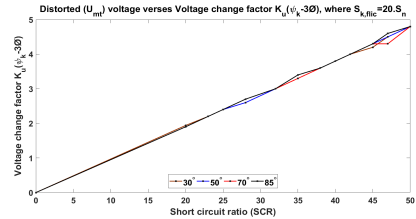


Fig. 10: Voltage changes factors Ku_{ψ_k} versus SCR

analysis ensures that the interoperability issues such as the signal detection through PLL are the critical challenges in the measurement and assessment process of the fictitious grid [18] [15]. The voltage change factors depend on the switching operation of the WT and impedance angle ψ_k also involved in the measurement procedure. In the fictitious grid during switching and continuous operation, the short circuit power $S_{k, fic}$ gradually increases with voltage change factors Ku_{ψ_k} . Therefore, it is necessary to identify that voltage change factor Ku_{ψ_k} and ψ_k strongly interlink with the flicker measurement in WT. Thus, the fictitious grid performance assesses the values of voltage change factors Ku_{ψ_k} . The values of voltage change factor is Ku_{ψ_k} , which is directly proportional to both parameters such as harmonics and switching operation (SCR) in WT as shown in Fig.9, and Fig.10. These results indicate that the three-phase voltage input $um(t)$ reduces the level of inter-harmonic frequencies by appropriate filtering techniques. The results would be obtained with minimum voltage fluctuation at the PCC. Moreover, the overall measurement procedure is effected by the performance of the fictitious grid. The measurement performance can be upgraded by implementing an efficient and robust PLL in the fictitious grid, and, on the other hand, the filtering part is also necessary to be upgraded in the flicker meter [18].

III. CONCLUSION

The study presents a procedure for determining the flicker measurement and assessment characteristics of WT. The study demonstrates the effectiveness of the digital flicker measurement during continuous and switching operations of grid-connected WTs in Section II, as per recently updated standard IEC 61400-21-1.

This paper validates the two key verification of flicker measurement tests by employing simulation model. The first test is related to the correlation analysis of the flicker emission measurement. The flicker coefficient c_{ψ_k} should be 2 within the tolerance of $\pm 5\%$ as per IEC-61400-21-1 standard, and the obtained simulation results approximately validates the applicable requirement of the standard. However the deviation in the tolerance level of flicker coefficient c_{ψ_k} around $\pm 2\%$ is in line with the tolerance of $\pm 5\%$. This deviation in the measurement is caused by the presence of inter-harmonics in the flicker meter and lack of accuracy in the PLL section of the fictitious grid.

The results from the second test demonstrates the accuracy of the fictitious grid performance. The accuracy of fictitious grid is analyzed by the average flicker coefficient c_{ψ_k} and the factors of voltage change $K_{u_{\psi_k}}$ versus harmonics and SCR. The obtained simulation results are in line with the desired values described in the standard IEC-61400-21-1. While the deviation in the level of tolerance range is around $\pm 3\%$ due to the inter-harmonics and SCR emission produced by the switching operation in the WT. The performance of fictitious grid is also affected by differential issues in the PLL. Moreover, the voltage change factors $K_{u_{\psi_k}}$ play an important role in the measurement procedure because the two factors (1) switching operation directly links with impedance angle ψ_k and (2) the short circuit power $S_{k,fluc}$. Thus, the two factors affect the measurement procedure, which are influenced by the voltage factors $K_{u_{\psi_k}}$ in the fictitious grid. To conclude, proper accuracy measurement can be assured by increasing the strength of filter operation in the Flicker meter and enhancing the signal detection performance capability of PLL in the fictitious grid.

REFERENCES

- [1] "IEEE recommended practice—adoption of IEC 61000-4-15:2010, electromagnetic compatibility (emc): Testing and measurement techniques—flicker—functional and design specifications," *IEEE 1453-2011*, pp. 1–58, Oct 2011.
- [2] B. Andresen, P. Sørensen, F. Santjer, and J. Niiranen, *Overview, status and outline of the new revision for the IEC 61400-21 Measurement and assessment of power quality characteristics of grid connected wind turbines*. Energynautics GmbH, 2013.
- [3] V. Beirovi, B. Nikoli, I. Turkovi, and I. Pavi, "The development of flicker meter according to standard iec61000-4-15 and modeling consumers which produce flickers in the power network," in *International Symposium on Power Electronics Power Electronics, Electrical Drives, Automation and Motion*, June 2012, pp. 1012–1016.
- [4] F. Blaabjerg, R. Teodorescu, M. Liserre, and A. V. Timbus, "Overview of control and grid synchronization for distributed power generation systems," *IEEE Transactions on Industrial Electronics*, vol. 53, no. 5, pp. 1398–1409, Oct 2006.
- [5] A. S. Bubshait, A. Mortezaei, M. G. Simes, and T. D. C. Busarello, "Power quality enhancement for a grid connected wind turbine energy system," *IEEE Transactions on Industry Applications*, vol. 53, no. 3, pp. 2495–2505, May 2017.
- [6] A. R. (CEO), "Sustainability powers development: Vestas wind systems," 2017, pp. 1–30.
- [7] K. Chmielowiec, "Flicker effect of different types of light sources," in *11th International Conference on Electrical Power Quality and Utilisation*, Oct 2011, pp. 1–6.
- [8] I. E. COMMISSION, "Part 21-1: Measurement and assessment of power quality characteristics of grid connected wind turbines." *IEC CDV 61400-21-1, IEC 2017*, vol. Ed. 2.0, Nov 2018.
- [9] J. Drapela, R. Langella, J. Slezinger, and A. Testa, "A tunable flicker meter to account for different lamp technologies," *IEEE Transactions on Power Delivery*, vol. 32, no. 2, pp. 872–880, April 2017.
- [10] A. E. Feijoo, J. Cidras, and J. L. G. Dornelas, "Wind speed simulation in wind farms for steady-state security assessment of electrical power systems," *IEEE Transactions on Energy Conversion*, vol. 14, no. 4, pp. 1582–1588, Dec 1999.
- [11] E. C. for Electrotechnical Standardization, "Electromagnetic compatibility (emc), part 4-15: Testing and measurement techniques flicker—functional and design specifications," *IEC: 61000-4-15*, vol. ICS 33.100.20, Feb 2010.
- [12] J. C. Gomez and M. M. Morcos, "Flicker measurement and light effect," *IEEE Power Engineering Review*, vol. 22, no. 11, pp. 11–15, Nov 2002.
- [13] J. J. Gutierrez, J. Ruiz, L. A. Leturiondo, and A. Lazkano, "Flicker measurement system for wind turbine certification," *IEEE Transactions on Instrumentation and Measurement*, vol. 57, no. 12, pp. 375–382, Dec 2008.
- [14] A. Larsson, "Flicker emission of wind turbines during continuous operation," *IEEE Transactions on Energy Conversion*, vol. 17, no. 1, pp. 114–118, Mar 2002.
- [15] A. Lazkano, I. Azkarate, J. J. Gutierrez, J. Ruiz, L. A. Leturiondo, and P. Saiz, "Measurement of the flicker characteristics of grid connected wind turbines: Instantaneous frequency versus instantaneous phase estimation methods," in *Proceedings of 14th International Conference on Harmonics and Quality of Power - ICHQP 2010*, Sept 2010, pp. 1–6.
- [16] J. Molina and L. Sainz, "Compact fluorescent lamp modeling for large-scale harmonic penetration studies," *IEEE Transactions on Power Delivery*, vol. 30, no. 3, pp. 1523–1531, June 2015.
- [17] K. Redondo and J. J. Gutierrez, "Wind turbines part 21: measurement and assessment of power quality characteristics of grid connected wind turbines," *IEC: 61400-21*, vol. Ed. 2.0, Feb 2017.
- [18] K. Redondo, J. J. Gutierrez, P. Saiz, L. A. Leturiondo, I. Azcarate, and A. Lazkano, "Accurate differentiation for improving the flicker measurement in wind turbines," *IEEE Transactions on Power Delivery*, vol. 32, no. 1, pp. 88–96, Feb 2017.
- [19] J. Sun, "Impedance-based stability criterion for grid-connected inverters," *IEEE Transactions on Power Electronics*, vol. 26, no. 11, pp. 3075–3078, Nov 2011.
- [20] C. Wei, M. Han, and W. Yan, "Voltage fluctuation and flicker assessment of a weak system integrated wind farm," in *2011 IEEE Power and Energy Society General Meeting*, July 2011, pp. 1–5.

Verification of Accuracy and Precision Evaluation of IEC Flicker Meter

1st Noman Khan
dept. of Energy Technology.
Aalborg University
Denmark
nkhan15@student.aau.dk

2nd Given Name Surname
dept. name of organization (of Aff.)
name of organization (of Aff.)
City, Country
email address

3rd Given Name Surname
dept. name of organization (of Aff.)
name of organization (of Aff.)
City, Country
email address

4th Given Name Surname
dept. name of organization (of Aff.)
name of organization (of Aff.)
City, Country
email address

5th Given Name Surname
dept. name of organization (of Aff.)
name of organization (of Aff.)
City, Country
email address

6th Given Name Surname
dept. name of organization (of Aff.)
name of organization (of Aff.)
City, Country
email address

Abstract—Flicker meter is an indispensable tool for the flicker measurement and assessment procedure of the wind turbine (WT). The flicker meter operates as a synchronized pattern defined in the IEC-61000-4-15 standard. Flicker meter is systemic apparatus that measures the sporadic behavior of voltage fluctuations. The power quality is limited due to voltage fluctuations and detectable to customers as light flicker (LF). Accuracy and precision evaluate the performance of the flicker meter. Sinusoidal and rectangular voltage changes perform the verification test of accuracy and precision. The degree of accuracy and precision can be assessed through output parameters of instantaneous flicker P_{inst} , and short flicker P_{st} of flicker meter. The main theme of this paper is to judge the performance level of the flicker meter, and the framework is divided into two parts: 1) to evaluate the flicker measurement parameters P_{inst} , and P_{st} by the simulation model, 2) to verify the accuracy and precision flicker measurement results by comparing simulation results with the desired applicable values of IEC flicker meter. The deviation between obtained simulation results and desired values of the IEC standard demonstrates the performance of the flicker meter.

Index Terms—Flicker meter, power quality, voltage fluctuation, and IEC flicker measurements.

I. INTRODUCTION

The renewable resources do not cause any adverse climate change and wind energy had the highest growth rate worldwide [1]. The technically minded wind energy manufacturer go into some of the electrotechnical issues involved in connecting a turbine to the grid. The most challenging in the list is "power quality" refers to the frequency stability, and various forms of voltage fluctuation produce (e.g., flicker or harmonic distortion) on the electrical grid. In the realistic speaking, the power companies and their customers target to achieve an alternating current with an appropriate sinusoidal shape [15]. The voltage fluctuation imposed by the wind turbine depends

on the non-linear load from the grid and trigger to produce flicker [13]. The accurate measurement and assessment of the flicker is a critical challenge due to harmonics in the input voltage signals and also because measuring instruments produce inter-harmonics during continuous operation [15]. Due to these issues, the measurement device declines the accuracy and overall performance. The IEC 61000-4-15 standard determines the specification for the flicker measurement devices. Now the question raises that 'how to examine the accuracy of the measurement and how to achieve the applicable requirements of IEC standard in the flicker measurement device'. The significant objective of the paper is to verify the degree of accuracy, precision level and indicate the performance of the measuring device according to the IEC standard.

In the last decade, many devices have been developed to measure and assess the flicker level [13]. Most of them were produced in Denmark, France, Germany, and Japan. The detection range of these devices is up to $0.5 - 33Hz$ which is approximately equal to the detection and perception range of human eye-brain $0.5 - 30Hz$ [15]. The various types of electric lamps have been used to display the flicker [2]. These lamps have their self-characteristics and operations (i.e., temperature, radiation and luminescent). Therefore, light sources have always been a debatable issue in the research [2] [16]. The history of growth is now reshaping the flicker devices with the name of flicker meter [15]. The flicker meter is the synchronized system that measures the obnoxiousness of the flicker caused by voltage changes [13]. Flicker meter is a smart instrument designed to measure impression of visual sensation induced by light and to represent it in the quantity of flicker severity [14]. In short, the flicker quantities are measured by the flicker meter (FM) [5] i.e. the short flicker severity P_{st} or long flicker severity P_t and instantaneous flicker P_{inst} flicker. This paper dealt with the voltage flicker through input waves such as sinusoidal and rectangular voltage changes. Moreover, it includes the brief description about the dynamics of mea-

The authors are with the R&D group of power electronics under Prof.Frede Blaabjerg in the Department of Energy Technology at Aalborg University (AAU), and highly grateful for the coloration of Vestas wind systems, Denmark.

surement process for the flicker meter and critically analyses the accuracy and precision parameters concerning P_{inst} and P_{st} . The most significant objective is to estimate the degree of accuracy and precision which indicates the performance of flicker meter. The accuracy and precision in terms of P_{inst} and P_{st} . If the P_{inst} and P_{st} always meets the desired requirement values of IEC 61000-4-15, even though these parameters strike different portions of the tolerances level within $\pm 8\%$, the flicker meter has a high degree of accuracy. If the P_{inst} and P_{st} under the desired values then it is considered as the high degree of precision. The ideal case, if the performance parameters P_{inst} and P_{st} are line-up or uniform with desired values of IEC standard, then it is considered to have the high degree of both accuracy and precision of flicker meter. Section II summarizes the dynamics of the flicker meter related to the frequency processing by the classic approach of rectangular modulation and discusses the functional parameters of F1-classes of the flicker meters. Section III presents the comprehensive architecture model of IEC flicker meter by describing the operational procedure of each block. Section IV is related to the correlative analysis of the performance parameters P_{inst} and P_{st} of the flicker meter and simulation results verify the degree of accuracy and precision level. The simulation results are compared with the desired values of the IEC 61000-4-15 standard. Finally, the conclusion is presented in Section V.

II. DYNAMICS OF FLICKER MEASUREMENT

The flicker meter measurement process is developed through the phenomena of the Lamp-eye-brain response, and their illuminations were rapidly changing. The architecture of flicker meter represented by the psychological processes into the perception and toleration of flicker measurement [5]. The IEC-61000-4-15 standard for flicker meter defines processing procedure of voltage fluctuation into four quantifies steps: 1) the voltage change factors, 2) the modulated frequency of the voltage change, 3) characteristics of the physical light-source, and 4) the procedure of the human brain recognition of the voltage fluctuation. Thus, the flicker meter is an efficient and robust device for the measurement of observing voltage fluctuation and flicker [5] [14], and the input signal chain and signal processing steps for flicker measurement are depicted in the Fig.1.

The design of flicker measurement model for flicker measurement performed two main operations, 1) indicates the processing impression of the visual observer, 2) instantaneous flicker P_{inst} is detect by the estimation of the magnitude characteristics of voltage fluctuation. In this scenario the frequency range of the voltage fluctuations range from $6to-10Hz$ being considered the most sensitive. The existing model designed on the sensitivity of overall flicker mostly presented in between the frequency rate $0.5 - to - 25Hz$, as the range of interest approximate $50or60Hz$ [13]. In briefly, the voltage waveform shows variation in magnitude, due to the sporadic behavior of nonlinear load, and the frequency change in the voltage envelope which refers as flicker frequency. Thus, voltage

fluctuation is scrolled in the fluctuated frequency and its magnitude is main cause of power quality degradation in the utility of wind energy [9]. The frequency processing is the main focus in this paper in terms of amplitude and phase characteristics in the signal domain. Therefore, the classic approach AM-modulation method used to measure the dynamic properties of the fluctuated voltage [10]. While the flicker meter signal chain occurrence of carrier parameter in the input voltage.

A. AM modulation of Signal Chain for Flicker meter

The assumption of the signal processing carried out in a steady state signal chain without harmonics component [9]. For example, U_{nt} is the steady state and ideal input signal, the equation 1 is written as follows.

$$U_{IN(t)} = U_m \times \text{Sin}_{wc(t)} \quad (1)$$

Where U_m is the amplitude of voltage fluctuation, f_c is the carrier wave frequency (corresponding to period of time T_c and $wc = 2\pi f_c = \frac{2\pi}{T_c}$ is the carrier frequency, and t is the time. The processing of frequency will be utilize the following input signals [9].

- 1) The carrier frequency wave is not suppressed, and the equation 2 presents the input signal of the AM modulation.

$$U_{IN(t)} = U_m \times \text{Cos}_{wc(t)} \times [1 + (\frac{\text{Delta}U}{U}) \times u_{mod}(t)] \quad (2)$$

In the equation 2, the $u_{mod}(t)$ is the modulating signal that satisfies the condition ($|u_{mod}(t)|_{max} = \frac{1}{2}$ and $\frac{\text{Delta}U}{U}$) of modulation depth:

- 2) The signal with inter-harmonics components as follows:

$$U_{IN(t)} = U_m \times \text{Cos}_{wc(t)} + U_i \text{Cos}_{(wi)} \quad (3)$$

Where interharmonics U_i is the amplitude component and $wi = 2\pi f_i$ is the interharmonics pulsation.

$$U_{fic(t)} = u_o(t) + R_{flic} \times i_m(t) + L_{flic} \times \frac{di_m(t)}{dt} \quad (4)$$

The characteristics of the input voltage fluctuation of the flicker meter consists on the above signals groups described in the equations 2-to-4. The internal signal U_{RMS} and P_{int} during initial transient component produces high peaks of the short flicker P_{st} because of the input signals $U_{IN(t)}$ process without modulation in equation 2. Therefore the existing flicker meter is not considered the first $10-5seconds$ values during measurement. The modulation depth depends on the frequent and characteristics of modulating signal directly effect on the output P_{st} of the flicker meter defined in the above equation 3. The output P_{st} is also depends on the interharmonics components presented in the equation 4. These equations specified three main classes of the flicker meter and verified with different voltage characteristics according to the IEC-flicker meter standard is described in Table.I. The IEC Flicker standard 61000-4-15 is defined the rectangular modulation. For example the rectangular voltage fluctuation

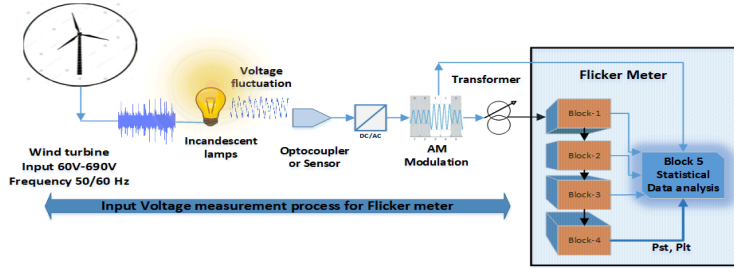


Fig. 1: Measurement procedure of the Flicker meter (IEC 61000-4-15)

at a frequency level $8.8Hz$ and an amplitude $\frac{\Delta U}{U} = 40\%$ which modulated with the frequency interest $50Hz$, rectangular modulation can be written as follows.

$$u(t) = 1 \times \sin(2\pi \times 50 \times t) \left[1 + \frac{40}{100} \times \frac{1}{2} \times \text{signum}(2\pi \times 8.8 \times t) \right] \quad (5)$$

The rectangular voltage changes performed by at a frequency of $8.8Hz$ with each period produces two distinct voltage changes, according to the increasing magnitude (one period) with decreasing magnitude (one period) around 17.6 changes per second, as shown in Fig.2.

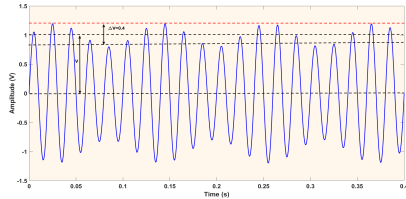


Fig. 2: Measurement of rectangular voltage changes

In IEC standard 61000-4-15 is using the correcting factor for tuning the deviation level, normally the deviation $\pm 5\%$ is suitable in tolerance specification, and correction factor is multiply with measured values of the flicker outputs P_{It} and P_{St} .

B. Classes of Flicker meters

The classification of flicker meter presented in the Table.I. These flicker meters are verified by several tests related to the voltage characteristics, modulation patterns and change in the voltage fluctuation. Normally, three classes are discussed in the measurement of flicker. Class F2: Flicker meters used for product compliance testing with constant frequency and phase [5]. Class F3: flicker meters intended for use in the power quality surveys and trouble shooting of the appliances

application where low flicker severity measurement is allowed [3].

Class F1: flicker meter used for general purposed and suitable for power quality monitoring and compliance testing, the overview of class F1 in Table. I. The calibration of voltage fluctuation according to the IEC-flicker meter depicted in Table.II [5].

This paper is verified the total response characteristics from input to output (flicker P_{inst} and P_{St}) for sinusoidal and rectangular voltage changes according to the Tables. I and II. The desired values of all the verification test points are $P_{inst,max} = 1.00$ with $\pm 8\%$ and $P_{St} = 1$ within $\pm 5\%$ including correcting factors used for tuning the level of tolerances. For class F1 Flicker meter, the voltage input circuit is accepted a wide range of nominal mains voltages and maximize the level of compatibility with the measurement of flicker meter. In general the nominal voltage between $66V - to - 690V$ for nominal frequency is $50Hz$.

III. FLICKER METER IMPLEMENTATION

The operational architecture of IEC flicker meter described by the block diagram see in Fig.3. The initial assessments are performed by block 1 and blocks 2, 3 and 4, while the final outputs accomplished by block 5. The overall operational framework is divided into two parts and each block performing one of either both assignment written as follows [15] [4].

1. The simulation response of the lamp-eye-brain diagram as per IEC-standard.
2. The results presentation by on-line statistical analysis of the signal.

a) *Block-1 (Input voltage adapter)*: The voltage adapting circuit receives the modulated signal from the input. The primary functions of the block-1 to scaling the input voltage, maintain the r.m.s level and keep the voltage fluctuation with the fundamental signal. The internal voltage level does not compromise the functioning of the rest of the instruments [4]. Thus, the adapted circuit sustained the level of internal voltage as per synchronized pattern for the further operation of the flicker meter. The flow of voltage procedure in the adapted circuit described with detail [5].

TABLE I: Classes specification for flicker meter

Test Voltage Characteristics	Intention	Vale used for test	Flicker meter classes		
Sinusoidal/Rectangular Voltage changes	Tests the response characteristic of the filters and scaling parameters	P_inst	F1	F2	F3
Rectangular voltage changes and performance testing	Tests the classifier and statistical evaluation algorithms	P_st	F1	F2	F3
Distorted voltage with multiple zero crossings	Tests the stability of the input control circuit	P_inst	F1		
Harmonics with side bands	Tests the input bandwidth	P_inst	F1		
Phase jump	Tests the stability of the input control circuit, the input bandwidth and the classifier	P_st	F1		
Frequency changes	Tests the measuring circuit (hardware)	P_inst	F1		

In short, the modulation signals created with rectangular modulation with the amplitude average 1. Further, modulated frequency voltage change is $8.8Hz$ and fundamental frequency is $50Hz$. A change in the phase relationship directly affected on the results of P_{inst} and P_{st} values. Moreover, the testing results representing the change of time function in $\Delta u/u$ amplitude modulation approximately equal to the change in the $R.M.S$ $\Delta U/U$. This block keeps the level $R.M.S$ of modulated voltage and delivers to the input of the block-2. The transformer does not modify the modulating relative fluctuation. Therefore, the half cycle $R.M.S$ values are processed by a first order low-pass (Butterworth filter) filter with a time constant of $27.3s$. However, the procedure was changed with time, and replace with the new estimations idea for RMS values processing, aim to acquire better accuracy in the estimation (without error or noise) of RMS waveform. Currently, the implementation of rectangular modulation by using zero crossing detection methods for the accurate measurement of RMS values [8]. Thus, the output of flicker meter depends on the depth of modulation (rate-of-change) in signal as compare to the fundamental signal which applied to the input of adaptive circuit (block-1). This block also carrying a calibration generator.

b) Block-2 (Squaring Multiplier): The main purpose of this block is to recover the voltage change fluctuation by squaring the output of the block-1 see Fig.3. The squaring the input voltage scaled to the reference level. The testing detail available [5] according to the IEC-61000-4-15 on the basis of simulating the behavior of a lamp. The multiplier integrated with the Butter-worth filter in block-3 and this block operated as a demodulation.

c) Block-3 (Weighting filters): The block 3 is consists of a cascade of two filters. The filter circuit consists on first low-pass filter and high pass filter (first order, $3dB$ at $0.05Hz$). The first order low-pass filter eliminates the ripple components of the output of double mains frequency. The high pass filter (HPF) can be used to eliminate the d.c. voltage component include the mains effect of HPF at the $0.05Hz$ with first order $-3dB$. The performance test include the effects of HPF filter with the $0.05Hz$ corner frequency. The second filter is a weighting filter and it is used to simulates the response of the human visual systems of the voltage change or fluctuation. The block 3 is draw the borderline

of perceptibility curve for the sinusoidal voltage fluctuation. For the analyzation of the correct weighting of non-sinusoidal and arbitrary voltage fluctuations, the appropriate choice is the complex transfer function of the block 3 and 4. Further, the correct performance model has also been checked with periodic rectangular signals as well as with transient signals [7]. Thus, the overall performance of the model has checked with periodic rectangular signals test with transient signals [5] [6].

d) Block-4 (Squaring and smoothing): The block 4 is performed two main function 1) squaring of the weighting flicker signal so as to simulate the behavior of non-linear eye-brain response of perception, 2) averaging the signal to simulate the storage effect in the brain. The squaring operator have an input and output operating ranges which accommodate the specific measurement ranges of the flicker meter. This block is composed of a squaring multiplier and a first order low-pass filter with a time constant $300ms$. The block execution on the basis of the human flicker perception such as eye and brain mutual combination. The voltage fluctuations applied to the reference flicker objective by simulated the combine non-linear response of blocks 2, 3 and 4. The output of this block represents the instantaneous flicker sensation P_{inst} and estimates the flicker severity P_{st} in the systems.

e) Block-5 (Statistical Classifier): Flicker meter statistical analysis measurement for short term (10 min) and long term (2 hours). In case of power quality evaluation, the flicker meter should indicated the P_{inst} and assess that the values under the range of flicker classifier. An observation of short-term flicker period $T_{short} = 10mint$ evaluation is designated P_{inst} statics from the level classifier in block 5 of the flicker meter, the following formula [5] is used 6.

$$P_{st} = \sqrt{0.031P_{0.1}, 0.0525P_{1s}, 0.065P_{3s}, 0.028P_{10s}, 0.08P_{50s}} \quad (6)$$

Where the percentiles values $P_{0.1} - to - P_{50s}$ and the flicker level increases from $0.1 - to - 10(mint)$, this period represented the 50% time of the observation period.

The block 5 is performed an on-line analysis of the flicker level, the block acquired all the concern parameters which is required to assess the overall flicker severity level. Thus, the purpose of this block is to derive all related flicker severity indication in terms of statistical analysis. Therefore, operation of the block 5 is performed direct calculation of the significant

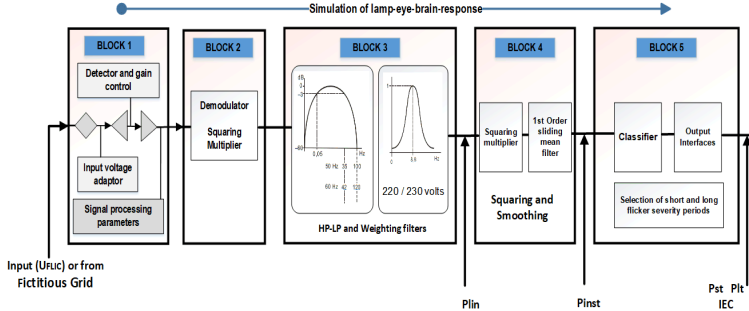


Fig. 3: Operational diagram of the IEC Flicker meter

TABLE II: The voltage fluctuation for flicker classifier

230 V/50 Hz	IEC 61000-4-15 Sinusoidal	IEC 61000-4-15 Rectangular	IEC 61000-4-15 Rectangular
freq : Hz	$\Delta U/U\%$	$\Delta U/U\%$	$r(\text{min}^{-1})$
0.5	2.235	0.509	1
1.5	1.067	n.a	2
3.5	n.a	0.342	7
8.8	0.250	0.196	39
18	n.a	0.446	110
20	0.704	n.a	1620
21.5	n.a	0.592	4000
25	1.037	0.764	
28	n.a	0.915	
30.5	n.a	0.847	
33 1/3	2.128	1.671	

parameters by sampling the instantaneous flicker signal level and further subdivided into the suitable number of classes [6]. The statistical analysis method define in the 15 numbers of classes and the flicker severity P_{st} calculation as per the performance test [5]. This block used the cumulative probability function to obtained the significant statistical values such as mean, standard deviation, flicker level being exceeded for a given percentage of time or vice-versa. The flicker meter classes are also used modulation setting for the calculation of P_{st} . The modulation setting defined in the IEC 61000-4-15 standard, the approximate range 1.788% (i.e. factor $k=2$) at the frequency vision detection range $39Hz$ with cumulative probability modulation (CPM) $0.325Hz$ and the target frequency $230V\text{olt}/50Hz$. The flicker severity estimation of P_{st} is $2 : 00$. However, the IEC standard have the accuracy concerned, and set their desire values $P_{st} = 1 : 00, \pm 5\%$ and $P_{inst} = 1 : 00, \pm 8\%$.

IV. RESULTS OF ACCURACY VERIFICATION FOR IEC FLICKER METER

The IEC 61000-4-15 flicker meter is checked P_{inst} values from input-to-output total response characteristics. The verification test for accuracy is performed through sinusoidal and rectangular voltage changes. as described in Table.II. The IEC 61000-4-15 standard has specified the desired requirement

for the verification of accuracy i.e. $P_{st} = 1 : 00, \pm 5\%$ and $P_{inst} = 1 : 00, \pm 8\%$. In case, the flicker meter achieved the desired applicable requirement as per IEC standard. So the accuracy of the flicker meter is considered 100%. Since it is challenging to enhance the accuracy in the measurement for flicker meter according to the desired requirement of IEC standard. The squeezing point of this paper: to present the verified results with accuracy deviation in flicker meter. The verification results based on the assessment of the accuracy deviations in between *applicable desired requirement from IEC 61000-4-15 standard with the obtained results.*

The accuracy verification testing through sinusoidal and rectangular voltage changes using voltage fluctuation waveform as given in equation 7.

$$U_t = 1 + \frac{\Delta U}{U} \times \text{signum}[\sin(2\pi f_v t)] \times \sin(2\pi f_m t) \quad (7)$$

where $\frac{\Delta U}{U}$ is voltage fluctuation, f_v is flicker frequency, and f_m is system fundamental frequency [5]. The simulation model designed in the matlab by using digital flicker meter in the power-system tools. The measurement procedure follows the accuracy and precision level in terms of flicker parameters i.e. P_{inst} , P_{st} , and voltage change in both sinusoidal and rectangular. The simulation results compared with the IEC 61000-4-15 standard, aim to observed the deviation between IEC standard and the outcomes results.

In the first test, to validated the simulation model by estimating the P_{st} with sinusoidal and rectangular voltage changes according to the Table.II where modulating frequency is fixed. The objective of this test to analyzed the behavior of the P_{st} with voltage fluctuation in the flicker meter, are as shown in Fig.4.

In Fig.4, the level of P_{st} is not effecting due to sinusoidal voltage change, the main reason is cascade filters in the block 3 which rejects the unwanted fluctuation. In case of rectangular voltage change, level of P_{st} is varying with the change in rectangular voltage. The main cause is phase change which is

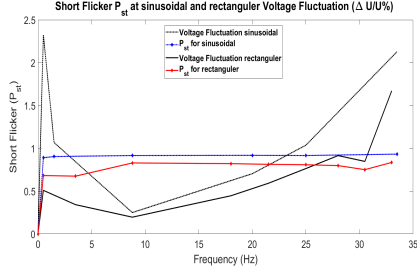


Fig. 4: P_{st} with sinusoidal and rectangular voltage fluctuation

directly impact on the results of P_{inst} and P_{st} values. Thus, the rectangular modulation useful to avoid the effects of inter-harmonics. However, the amplitude increases with voltage changes in the existing flicker meter.

In the second test performed to assess the performance of flicker meter with sinusoidal voltage change. The P_{inst} is estimated by sinusoidal voltage change and compares with desired requirement of IEC 61000-4-15 standard. The wind turbine manufacture is normally estimate P_{inst} test to analyze the voltage fluctuation.

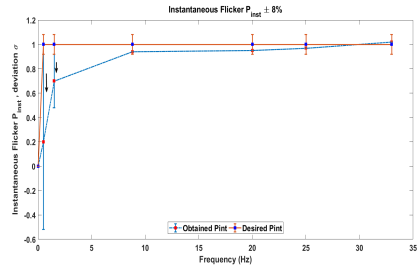


Fig. 5: Sinusoidal voltage Change: P_{inst} deviation with IEC 61000-4-15

The IEC standard applicable P_{inst} requirement is 1 : 00 with a tolerance of $\pm 8\%$. The measurement time is 10mint with each phase jump less than 0.5ms, and the flicker meter ignored the initial 5 – second measurement to avoids the phase jump. The input of the sinusoidal voltage without inter-harmonics is meets the desired requirement of IEC standard as in Fig.5. However, the inter-harmonics wave is the limitation to meets desired requirement of the IEC standard. In realistic conditions, that the inter-harmonics present in the input of sinusoidal voltage [12]. Therefore, the rectangular modulation techniques is used to overcome the effects of inter-harmonics. The third test perform to assess rectangular voltage change with proportional effect on the P_{inst} values which indicates the performance of the flicker meter. The performance of

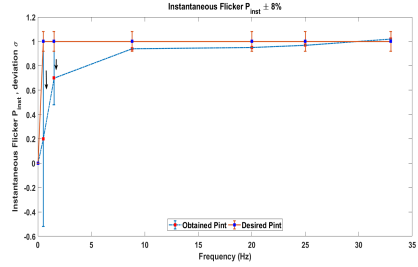


Fig. 6: Sinusoidal voltage Change: P_{inst} deviation with IEC 61000-4-15

Rectangular voltage change measurement is better than sinusoidal voltage change measurement (mean the values under the tolerance range) as shown in Fig.6. In case of inter-harmonics its reaches under the desired requirement of IEC standard. Therefore, standard determine the measurement procedure by employing rectangular voltage fluctuation.

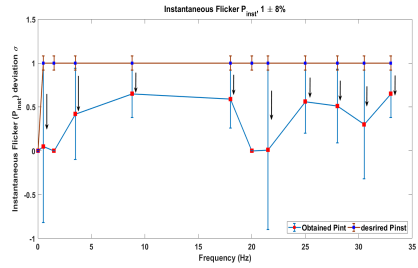


Fig. 7: Rectangular voltage Change: P_{inst} deviation with IEC 61000-4-15

The updated version of IEC standard allowing the range of P_{st} within 2.00. However, the P_{st} range depends on the flicker coefficient C_{ψ_k} and the results of the flicker meter completely diverse in case of continuous and switching operations while performing with a grid connected wind turbine or/ with the fictitious grid [11].

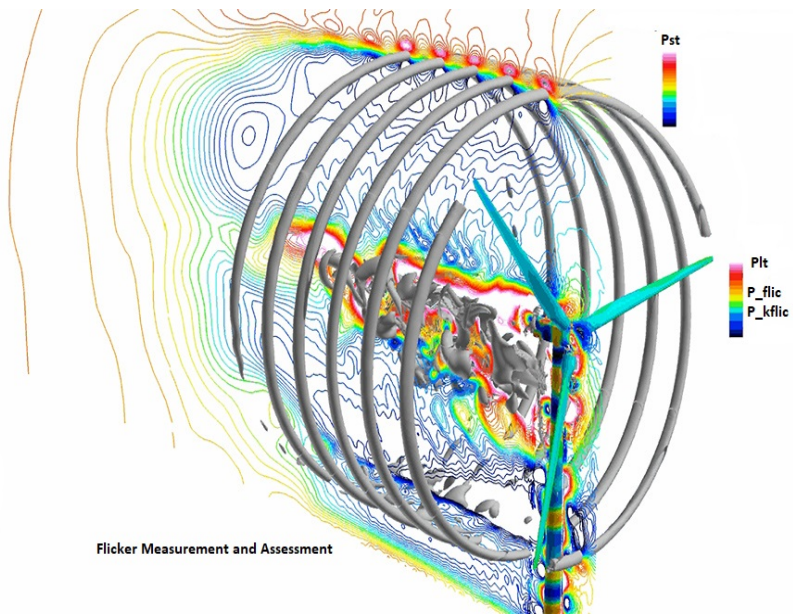
V. CONCLUSION

The study presents a procedure of the flicker meter measurement according to the IEC 61000-4-15 standard.

REFERENCES

- [1] F. Blaabjerg, R. Teodorescu, M. Liserre, and A. V. Timbus, "Overview of control and grid synchronization for distributed power generation systems," *IEEE Transactions on Industrial Electronics*, vol. 53, no. 5, pp. 1398–1409, Oct 2006.
- [2] K. Chmielowiec, "Flicker effect of different types of light sources," in *11th International Conference on Electrical Power Quality and Utilisation*, Oct 2011, pp. 1–6.

Matlab Simulation Model for Flicker Measurement



Annex A: (Signal Processing)

1. Simulation Execution code

%% This only an example file the results obtained from this file does not give a real feeling of the expected output of the Flicker_Calculation_function
This m.file in only used to generate a set of measured data and try to show how this measured data can be used in the Flicker function in order to calculate the flicker values according to the IEC 61400-21.
This m.file calls two other m.files which are:
1- IEC_Analysis_Function_Matlab_2007: which will calculate the amount of power in the generated three phase voltages and currents according to the IEC 61400-21 norm
2- Flicer_Calculation_function: which in its turn will also call another
These two m.files further call two m.file
1 - The first called m.file is used to run the following Module Flickermeter6140021_new_GL_Final_3ph.mdl which will simulate the effect of the Fictitious grid described by the IEC 61400-21
2 - The second called m.file is taken from Matlab file exchange service in order to calculate the long and short flicker values according to the IEC 61400-21 & IEC 61400-15

```
clear global
clc
F_Sample = 1000;%Hz
t = 0:(1/F_Sample):10;%Time in S
fn = 50;%Hz
U1 = 400 * sin(2*fn*pi*t);%Sine wave 1
U2 = 400 * sin((2*fn*pi*t) - (120*pi/180));%Sine wave 2
U3= 400 * sin((2*fn*pi*t) + (120*pi/180));%Sine wave 3
I1 = 5000 * sin(2*fn*pi*t);%Sine wave 1
I2 = 5000 * sin((2*fn*pi*t) - (120*pi/180));%Sine wave 2
I3 = 5000 * sin((2*fn*pi*t) + (120*pi/180));%Sine wave 3
[ua1rms,ub1rms,uc1rms,la1rms,lb1rms,lc1rms,P1pos,Q1pos,U1pos,Iact1pos,Ireact1pos,cosphi1pos,time] =
IEC_Analysis_Function_Matlab_2007(U1,U2,U3,I1,I2,I3,t,fn);
figure(1);
subplot(2,1,1)
plot(t,U1);hold on; plot(t,U2,'r');hold on; plot(t,U3,'g');xlim([0,0.2]);hold off;
subplot(2,1,2)
plot(t,I1);hold on; plot(t,I2,'r');hold on; plot(t,I3,'g');xlim([0,0.2]);hold off;
%i = 2;%an operation selector
%Sn = 1700;%rated apparent power in kW
%n = 20; % Short cicuit Ratio in %
%Alpha = 30;% Fictitious grid impedance phase angle in degree
%Un = 400;% Nominal Voltage Low voltage side in V
%Sk = 105;%Short cicuit apparent power in MVA
%Kp = 50;% Regulator gain for PLL in simulink
%Ki = 1400;% Regulator gain for PLL in simulink
%N10 = 2;% Number of switching operation with in 10 min
%N120 = 24;% Number of switching operation with in 2 h
i = 1;
endval = 1;
endval1 = 2;
Sn = mean(P1pos)/1000;
Sk = 105;
n = 20;
Un = 400;
Fn = 50;
Kp = 50;
Ki = 1400;
```

```

F_Sample = 1/F_Sample;
Simulation_dynamic_cut_time = 0.1;
N10 = 2;
N120 = 24;
Flicker_Caclulation_function
(endval,endval1,Sn,Sk,n,Un,Fn,i,Kp,Ki,F_Sample,Simulation_dynamic_cut_time,N10,N120,U1,U2,U3,I1,I2,I3,t)
clear
clc
load('Complete_Results_30.mat');

```

2. Simulation Function (IEC Analysis)

\$IEC_Analysis_Function_Matlab_2007

This function will calculate the positive sequence values of an electrical System (from its voltages and current measurements) like the active and reactive power using the IEC 61400-21 Norm. For simplicity the function assume that the measured three phase signals have the same sampling rate and the same length (that is why it accepts only one time signal as an input).

The function inputs are:

- 1- The measured three phase voltage and currents signals of an power system (Only the amplitude /Y-Values only/)
- 2- One of the time values of the measured signals like U1_time which indicate the x- Values where the sampling rate and offset values can be extracted.

3- f_grid: the nominal frequency of the power system under study (normally 50 Hz)

The function outputs are:

- 1- The three phase RMS values of the measured voltages calculated according to the norm.
- 2- The three phase RMS values of the measured currents calculated according to the norm.
- 3- P1 pos & Q1pos are the positive sequence Active- and Reactive power values calculated according to the IEC norm.
- 4- U1pos: is the positive sequence voltage calculated according to the IEC norm.
- 5- Iact1pos,Ireac1pos: is the positive sequence Active- and Reactive currents calculated according to the IEC norm
- 6- cosphi1pos: is the positive sequence power factor calculated according to the IEC norm.
- 7- The final output (time): is the time axie of the different output results. This function will also need the movstat.m file which will be used to calculate the "mvint" of the sin and cos signals in this function.
- 8- For more information please refer to the IEC 61400-21 Norm.

```

N = length(U1);
delta_t = (U1_time(2)-U1_time(1));
offset = U1_time(1);
duration = N*delta_t;
ramp_t = offset:delta_t:(duration)-delta_t;
sinwt = sin(2*pi*f_grid*ramp_t);
coswt = cos(2*pi*f_grid*ramp_t);
[r,c] = size(U1);
if r > 1
    Ua_sin = U1'.*sinwt;
    Ua_cos = U1'.*coswt;
    Ub_sin = U2'.*sinwt;
    Ub_cos = U2'.*coswt;
    Uc_sin = U3'.*sinwt;
    Uc_cos = U3'.*coswt;
    Ia_sin = I1'.*sinwt;
    Ia_cos = I1'.*coswt;
    Ib_sin = I2'.*sinwt;
    Ib_cos = I2'.*coswt;
    Ic_sin = I3'.*sinwt;
    Ic_cos = I3'.*coswt;
elseif c > 1
    Ua_sin = U1.*sinwt;
    Ua_cos = U1.*coswt;
    Ub_sin = U2.*sinwt;

```

```

Ub_cos = U2.*coswt;
Uc_sin = U3.*sinwt;
Uc_cos = U3.*coswt;
la_sin = I1.*sinwt;
la_cos = I1.*coswt;
lb_sin = I2.*sinwt;
lb_cos = I2.*coswt;
lc_sin = I3.*sinwt;
lc_cos = I3.*coswt;
end
fn = @int;
[Ua_sin] = mvstat_Matlab_2007(Ua_sin,U1_time,(1/f_grid),delta_t,fn);
Ua_sin = Ua_sin*2*f_grid;
[Ub_sin] = mvstat_Matlab_2007(Ub_sin,U1_time,(1/f_grid),delta_t,fn);
Ub_sin = Ub_sin*2*f_grid;
[Uc_sin] = mvstat_Matlab_2007(Uc_sin,U1_time,(1/f_grid),delta_t,fn);
Uc_sin = Uc_sin*2*f_grid;
[Ua_cos] = mvstat_Matlab_2007(Ua_cos,U1_time,(1/f_grid),delta_t,fn);
Ua_cos = Ua_cos*2*f_grid;
[Ub_cos] = mvstat_Matlab_2007(Ub_cos,U1_time,(1/f_grid),delta_t,fn);
Ub_cos = Ub_cos*2*f_grid;
[Uc_cos] = mvstat_Matlab_2007(Uc_cos,U1_time,(1/f_grid),delta_t,fn);
Uc_cos = Uc_cos*2*f_grid;
[la_sin] = mvstat_Matlab_2007(la_sin,U1_time,(1/f_grid),delta_t,fn);
la_sin = la_sin*2*f_grid;
[lb_sin] = mvstat_Matlab_2007(lb_sin,U1_time,(1/f_grid),delta_t,fn);
lb_sin = lb_sin*2*f_grid;
[lc_sin] = mvstat_Matlab_2007(lc_sin,U1_time,(1/f_grid),delta_t,fn); lc_sin = lc_sin*2*f_grid;
[la_cos] = mvstat_Matlab_2007(la_cos,U1_time,(1/f_grid),delta_t,fn);
la_cos = la_cos*2*f_grid;
[lb_cos] = mvstat_Matlab_2007(lb_cos,U1_time,(1/f_grid),delta_t,fn);
lb_cos = lb_cos*2*f_grid;
[lc_cos,time] = mvstat_Matlab_2007(lc_cos,U1_time,(1/f_grid),delta_t,fn);
lc_cos = lc_cos*2*f_grid;
%Cl. 7
Ua1rms = sqrt((Ua_sin.*Ua_sin+Ua_cos.*Ua_cos)/2);
Ub1rms = sqrt((Ub_sin.*Ub_sin+Ub_cos.*Ub_cos)/2);
Uc1rms = sqrt((Uc_sin.*Uc_sin+Uc_cos.*Uc_cos)/2);
Ia1rms = sqrt((Ia_sin.*Ia_sin+Ia_cos.*Ia_cos)/2);
Ib1rms = sqrt((Ib_sin.*Ib_sin+Ib_cos.*Ib_cos)/2);
Ic1rms = sqrt((Ic_sin.*Ic_sin+Ic_cos.*Ic_cos)/2);
%Cl. 8-11
U1pos_cos = (2*Ua_cos-Ub_cos-Uc_cos-sqrt(3)*(Uc_sin-Ub_sin))/6;
U1pos_sin = (2*Ua_sin-Ub_sin-Uc_sin-sqrt(3)*(Ub_cos-Uc_cos))/6;
I1pos_cos = (2*Ia_cos-Ib_cos-Ic_cos-sqrt(3)*(Ic_sin-Ib_sin))/6;
I1pos_sin = (2*Ia_sin-Ib_sin-Ic_sin-sqrt(3)*(Ib_cos-Ic_cos))/6;
%Cl. 12-17
P1pos = 1.5*(U1pos_cos.*I1pos_cos+U1pos_sin.*I1pos_sin);
Q1pos = 1.5*(U1pos_cos.*I1pos_sin-U1pos_sin.*I1pos_cos);
%Voltage, current and phase angle acc. C.14 to C.17
U1pos = sqrt(1.5*(power(U1pos_sin,2)+power(U1pos_cos,2)));
Iact1pos = P1pos/(sqrt(3)*U1pos);
Ireac1pos = Q1pos/(sqrt(3)*U1pos);
cosphi1pos = P1pos/sqrt(power(P1pos,2)+power(Q1pos,2));
%-----
end

```

3. Simulation Function (output and input signal processing)

```
$function [output_signal,output_time] = mvstat_Matlab_2007(Inputdata_signal,Inputdata_time>windowrange,reductionrange,fn)
```

```
%----- Introduction -----
```

This file is created to calculate the mathematical operation like 'max' on a pre-defined window range and with a pre-defined reduction range of an vector data.

This function will need the following inputs in order to calculate the wished results:

1- Inputdata_signal: A vector contain you're Y-Values that need to be filtered.

2- Inputdata_time: A vector contain your x-Values that need to be filtered (Normally is a time signal where the sampling rate can be extracted).

3- windowrange: in unit of time (s) is the range to calculate the needed mathematical function (The moving range ex.

mvmean(y,x,0.02,0.02) or mvrms(y,x,0.02,0.02))

4- reductionrange: in unit of time (s) is the scalling reference for the new data

5- fn : is used to define the wished mathematical operation (ex. @max, @min, @mean, @rms, @int)

%The relation between the>windowrange input and the reduction range input must be an integer value of 1:1.2:1..10:1. If not the reduction range would be corrected to get one of those relation. This specification give us the possibility to calculate the 'mvstat_final' without using a for-Loop which will save a whole amount of time for example:

```
fn = @mean
```

```
[output_signal,out_put_time] = mvstat_final (y,x,10,10)
```

the moving average will be calculated as a result of this function. every 10 s the mean value for the last 10 s will be calculated.

```
fn = @max
```

```
[output_signal,out_put_time] = mvstat_final (y,x,20,10)
```

The moving max will be calculated as a result of this function. Every 10 s the maximum value for the last 20 s will be calculated.

```
fn = @min
```

```
[output_signal,out_put_time] = mvstat_final (y,x,5,10)
```

the moving min will be calculated as a result of this function. Every % 10 s the minnum value for the last 5 s will be calculated.

Notice: when the input values of>windowrange and reduction range are not the same then at the beginning of the calculation the fn value of the a available data will be calculated.

Is m.file will also allow you to calculate the intrgration of your input data in a specific>windowrange. in this case the reduction range input should be defined as in the example:

```
fn = @int;
```

```
[Ua_sin,Ua_sin_time] = mvstat(Ua_sin,U1_time,(1/f_grid),delta_t,fn);
```

```
Ua_sin = Ua_sin*2*f_grid;
```

in this example the integration of your input data (in this case U1_sin) will be calculated ever one period (normally this mean 0.02 s or 1/50 or 1/f_grid in our case). And then the reduction range is in this case equal to the sampling time of the input data (delta = U1_time (2)-U1_time (1)). This work was done in order to bring FAMOS (IMC) software function into matlab.

%Author: Msc.Eng. Aubai Alkhatib Datum: 10.09.2013

```
%----- End of introduction -----
```

```
delta = Inputdata_time(2)-Inputdata_time(1);
```

```
length_window =>windowrange/delta;
```

```
length_reduction = reductionrange/delta;
```

```
time = Inputdata_time(end);
```

```
if>windowrange > reductionrange
```

```
number =>windowrange/reductionrange;
```

```
integer = floor(number);
```

```
fract = number-integer;
```

```
if fract >= 0.5
```

```
A =>windowrange/(integer+1);
```

```
else
```

```
A =>windowrange/(integer);
```

```
end
```

```
reductionrange_new = A;
```

```
integer_A = floor(A);
```

```
fract_A = A-integer_A;
```

```
[ttoo,b] = rat(A);
```

```

if b > 1
length_reduction_new = round(reductionrange_new/delta);
else
length_reduction_new = reductionrange_new/delta;
end
i = length_reduction_new;
ii = 1;
output = zeros();
while i < length(Inputdata_signal)
if i >= length_window
if fract_A == 0
switch func2str(fn)
case 'mean'
output(ii) = mean(Inputdata_signal((i-length_window)+1:i));
case 'max'
output(ii) = max(Inputdata_signal((i-length_window)+1:i));
case 'sum'
output(ii) = sum(Inputdata_signal((i-length_window)+1:i));
case 'min'
output(ii) = min(Inputdata_signal((i-length_window)+1:i));
case 'int'
output(ii) = sum(Inputdata_signal((i-length_window)+1:i))*reductionrange_new;
otherwise
output(ii) = rms(Inputdata_signal((i-length_window)+1:i));
end
else
switch func2str(fn)
case 'mean'
output(ii) = mean(Inputdata_signal((i-length_window):i));
case 'max'
output(ii) = max(Inputdata_signal((i-length_window):i));
case 'sum'
output(ii) = sum(Inputdata_signal((i-length_window):i));
case 'min'
output(ii) = min(Inputdata_signal((i-length_window):i));
case 'int'
output(ii) = sum(Inputdata_signal((i-length_window)+1:i))*reductionrange_new;
otherwise
output(ii) = rms(Inputdata_signal((i-length_window):i));
end
end
else
switch func2str(fn)
case 'mean'
output(ii) = mean(Inputdata_signal(1:i));
case 'max'
output(ii) = max(Inputdata_signal(1:i));
case 'sum'
output(ii) = sum(Inputdata_signal(1:i));
case 'int'
output(ii) = sum(Inputdata_signal(1:i))*reductionrange_new;
case 'min'
output(ii) = min(Inputdata_signal(1:i));
otherwise
output(ii) = rms(Inputdata_signal(1:i));
end
end

```

```

end
i = i + length_reduction_new;
ii = ii + 1;
end
if strcmp(func2str(fn),'int')
output_signal = output(length_window:length(output));
output_time = windowrange:reductionrange_new:(length(output)*reductionrange_new);
elseif isinteger(reductionrange_new)
output_signal = output;
output_time = 0:reductionrange_new:(length(output)*reductionrange_new)-reductionrange_new;
else
output_signal = output;
output_time = 0:(length_reduction_new*delta):(length(output)*(length_reduction_new*delta))-(length_reduction_new*delta);
end
elseif reductionrange > windowrange
Length_Output = fix(time/windowrange);
Length_Input_New = Length_Output*windowrange/delta;
delta_new = length_window;
delta_time = windowrange;
Input_resaped = reshape(Inputdata_signal(1:Length_Input_New),delta_new,Length_Input_New/delta_new);
switch func2str(fn)
case 'mean'
output_signal = mean(Input_resaped);
case 'max'
output_signal = max(Input_resaped);
case 'sum'
output_signal = sum(Input_resaped);
case 'int'
output = sum(Input_resaped)*delta_time;
case 'min'
output_signal = min(Input_resaped);
otherwise
output_signal = rms(Input_resaped);
end
if strcmp(func2str(fn),'int')
output_signal = output(length_window:length(output));
output_time = windowrange:delta_time:(Length_Output*delta_time)-delta_time;
else
output_time = 0:delta_time:(Length_Output*delta_time)-delta_time;
end
elseif windowrange == reductionrange
Length_Output = fix(time/windowrange);
Length_Input_New = Length_Output*reductionrange/delta;
delta_new = length_reduction;
delta_time = windowrange;
Input_resaped = reshape(Inputdata_signal(1:Length_Input_New),delta_new,Length_Input_New/delta_new);
switch func2str(fn)
case 'mean'
output_signal = mean(Input_resaped);
case 'max'
output_signal = max(Input_resaped);
case 'sum'
output_signal = sum(Input_resaped);
case 'int'
output = sum(Input_resaped)*delta_time;
case 'min'

```

```

output_signal = min(Input_reshaped);
otherwise
output_signal = rms(Input_reshaped);
end
if strcmp(func2str(fn),'int')
output_signal = output(length_window:length(output));
output_time = windowrange:delta_time:(Length_Output*delta_time)-delta_time;
else
output_time = 0:delta_time:(Length_Output*delta_time)-delta_time;
end
end
end
$

```

4. Simulation Function (Flicker calculation)

```

$function Flicker_Caclation_function
(endval,endval1,Sn,Sk,n,Un,Fn,i,Kp,Ki,F_Sample,Simulation_dynamic_cut_time,N10,N120,U1N_NS,U2N_NS,U3N_NS,I1_NS,I2_NS,I3_NS,time)

```

Initial Input data for calculating a complete flicker values of a measured data. endval1 is the number of calculation to be done (for different Grid phase angle)

- Sn is Apparent power in kW
- Sk is Short circuit apparent power in MW
- n is the rate between Sfic/Sn as defined by IEC norm.
- Un is Nominal Voltage where the measurement were done in V.
- Fn is Nominal Frequency of the grid were the measurement were done in Hz.
- 'i' is a selector between i = 1 Continuous operation and i = 2 and switching operation.
- Kp Proportional Gain Factor of the PLL Block.
- Ki Integral Gain Factor of the PLL Block.
- F_Sample is Sampling Frequency used in recording the measurements in S.
- Simulation_dynamic_cut_time is the estimated time needed by the PI controller when calculating the Frequency. (This simulation dynamic time need to be removed).
- N10 is Number of switching operation with in 10 min (As given in IEC norm)
- N120 is Number of switching operation with in 2 h (As given in IEC norm)
- Data name is the measured data name that should be analyzed and it should have the format .mat and need to contain the measured three phase voltages and current signals with their time axie.
- this file assume that the measured three phase voltage and current are identical and have the same:

1- Sampling rate (time intervals)

2- data length (Which is according to the IEC 10 min of measured data)

3- This function will also call the Flickermeter simulator (File ID: #24423 by Patrik Jourdan 12 Jun 2009 (Updated 11 Jan 2010))

(Heater 61000-4-15) in order to calculate the flicker values calculated by the Fictitious grid module (so called

Flickermeter6140021_new_GL_Final_3ph.mdl).

Please refer to the PDF documentation file in order to get more information on how this function works

Sfic = (n*Sn)/1000;% Fictitious Short circuit apparent power grid in MW

P_st_fic_complete_ave = 0;

P_st_complete_ave = 0;

P_it_complete_ave = 0;

if i == 2

P_st_fic_complete = zeros(1,endval);

P_st_complete = zeros(1,endval);

P_it_complete = zeros(1,endval);

kf_psyk_complete = zeros(1,endval);

ku_psyk_complete = zeros(1,endval);

kf_psyk_complete_ave = 0;

```

ku_psyk_complete_ave = 0;
save ('Initial
values','time','U1N_NS','U2N_NS','U3N_NS','I1_NS','I2_NS','I3_NS','endval','endval1','Sn','Sk','n','Sfic','Un','Fn','i','Kp','Ki','F_Sam
ple','Simulation_dynamic_cut_time','N10','N120','P_st_fic_complete','P_st_complete','P_lt_complete','kf_psyk_complete','ku_psyk
_complete','P_st_fic_complete_ave','P_st_complete_ave','P_lt_complete_ave','kf_psyk_complete_ave','ku_psyk_complete_ave')
elseif i == 1
P_st_fic_complete = zeros(1,endval);
P_st_complete = zeros(1,endval);
P_lt_complete = zeros(1,endval);
c_psyk_complete = zeros(1,endval);
c_psyk_complete_ave = 0;
save ('Initial
values','time','U1N_NS','U2N_NS','U3N_NS','I1_NS','I2_NS','I3_NS','endval','endval1','Sn','Sk','n','Sfic','Un','Fn','i','Kp','Ki','F_Sam
ple','Simulation_dynamic_cut_time','N10','N120','P_st_fic_complete','P_st_complete','P_lt_complete','c_psyk_complete','P_st_fic
_complete_ave','P_st_complete_ave','P_lt_complete_ave','c_psyk_complete_ave')
else
end
clear
load 'Initial values'
%-----End-----
-----
for jj=1:endval1
prompt4 = {'Please Enter The new phase angle Alpha in degree'};
name = 'Initial Input data';
numlines = 1;
defaultanswer4 = {'30'};
answer4 = inputdlg(prompt4,name,numlines,defaultanswer4);
Alpha = str2double(answer4{1});
if jj>1 && i == 2
save ('Initial
values','time','U1N_NS','U2N_NS','U3N_NS','I1_NS','I2_NS','I3_NS','endval','endval1','Sn','Sk','n','Sfic','Un','Fn','i','Kp','Ki','F_Sam
ple','Simulation_dynamic_cut_time','N10','N120','j','jj','Sequence_Path','Searchdir','P_st_fic_complete','P_st_complete','P_lt_comp
lete','kf_psyk_complete','ku_psyk_complete','P_st_fic_complete_ave','P_st_complete_ave','P_lt_complete_ave','kf_psyk_complet
e_ave','ku_psyk_complete_ave')
clear
load 'Initial values'
elseif jj>1 && i == 1
save ('Initial
values','time','U1N_NS','U2N_NS','U3N_NS','I1_NS','I2_NS','I3_NS','endval','endval1','Sn','Sk','n','Sfic','Un','Fn','i','Kp','Ki','F_Sam
ple','Simulation_dynamic_cut_time','N10','N120','j','jj','Alpha','P_st_fic_complete','P_st_complete','P_lt_complete','c_psyk_complet
e','P_st_fic_complete_ave','P_st_complete_ave','P_lt_complete_ave','c_psyk_complete_ave')
clear
load 'Initial values'
end
for j=1:endval
if i == 2
save ('Initial
values','time','U1N_NS','U2N_NS','U3N_NS','I1_NS','I2_NS','I3_NS','endval','endval1','Sn','Sk','n','Sfic','Un','Fn','i','Kp','Ki','F_Sam
ple','Simulation_dynamic_cut_time','N10','N120','j','jj','Alpha','P_st_fic_complete','P_st_complete','P_lt_complete','kf_psyk_comple
te','ku_psyk_complete','P_st_fic_complete_ave','P_st_complete_ave','P_lt_complete_ave','kf_psyk_complete_ave','ku_psyk_com
plete_ave')
I1_NS = [time' I1_NS'];
I2_NS = [time' I2_NS'];
I3_NS = [time' I3_NS'];
U1_NS = [time' U1N_NS'];
U2_NS = [time' U2N_NS'];

```

```

U3_NS = [time' U3N_NS'];
savenamerowdata = sprintf('Input_Data_Matlab_%d',j);
save (savenamerowdata,'I1_NS','I2_NS','I3_NS','U1_NS','U2_NS','U3_NS','j','i');
loadfile = [savenamerowdata];
load ([loadfile '.mat'])
% Input info for the Fictitious grid Module & Flickermeter
% afterword and the name of the saved result file
Tp = eval(sprintf('Simulation_Time_%d',j));
Fs = 1/F_Sample; %in Hz & must be greater than 2000 Hz
File_save_name = sprintf('Final_results_%d_%d',j,Alpha);
filesavename = File_save_name;
flicker_Calculation_complete
(j,i,n,Sk,Sn,Alpha,Un,Kp,Ki,Fn,F_Sample,Tp,Simulation_dynamic_cut_time,N10,N120,File_save_name);
loadfile_final = [File_save_name];
load ([loadfile_final '.mat'])
P_st_fic_complete(j) = P_st_fic_ave;
P_st_complete(j) = Pst_ave;
P_It_complete(j) = PIt_ave;
kf_psyk_complete(j) = kf_psyk_ave;
ku_psyk_complete(j) = ku_psyk_max_ave;
P_st_fic_complete_ave = mean(P_st_fic_complete);
P_st_complete_ave = mean(P_st_complete);
P_It_complete_ave = mean(P_It_complete);
kf_psyk_complete_ave = mean(kf_psyk_complete);
ku_psyk_complete_ave = mean(ku_psyk_complete);
complet_results = sprintf('Complete_Results_%d',Alpha);
save
(complet_results,P_st_fic_complete,'P_st_complete','P_It_complete','kf_psyk_complete','ku_psyk_complete','P_st_fic_complete_ave','P_st_complete_ave','P_It_complete_ave','kf_psyk_complete_ave','ku_psyk_complete_ave');
save ('Initial
values','time','U1N_NS','U2N_NS','U3N_NS','I1_NS','I2_NS','I3_NS','endval','endval1','Sn','Sk','n','Sfic','Un','Fn','i','Kp','Ki','F_Sam
ple','Simulation_dynamic_cut_time','N10','N120','j','jj','Alpha','P_st_fic_complete','P_st_complete','P_It_complete','kf_psyk_comple
te','ku_psyk_complete','P_st_fic_complete_ave','P_st_complete_ave','P_It_complete_ave','kf_psyk_complete_ave','ku_psyk_com
plete_ave')
clear
load 'Initial values'
elseif i == 1
save ('Initial
values','time','U1N_NS','U2N_NS','U3N_NS','I1_NS','I2_NS','I3_NS','endval','endval1','Sn','Sk','n','Sfic','Un','Fn','i','Kp','Ki','F_Sam
ple','Simulation_dynamic_cut_time','N10','N120','j','jj','Alpha','P_st_fic_complete','P_st_complete','P_It_complete','c_psyk_comple
te','P_st_fic_complete_ave','P_st_complete_ave','P_It_complete_ave','c_psyk_complete_ave')
load('Initial values.mat')
I1_Ns = [time' I1_NS'];
I2_Ns = [time' I2_NS'];
I3_Ns = [time' I3_NS'];
U1_NS = [time' U1N_NS'];
U2_NS = [time' U2N_NS'];
U3_NS = [time' U3N_NS'];
Tp = time(end);
%Fs = 1/F_Sample;
%Simulation_Time = Cut_Time;
savenamerowdata = sprintf('Input_Data_Matlab_%d',j);
save (savenamerowdata,'I1_Ns','I2_Ns','I3_Ns','U1_NS','U2_NS','U3_NS','j','i','Tp');
loadfile = [savenamerowdata];
load ([loadfile '.mat'])
% Input info for the Fictitious grid Module & Flickermeter

```

```

% afterword and the name of the saved result file
File_save_name = sprintf('Final_results_%d_%d',j,Alpha);
flicker_Calculation_complete
(j,i,n,Sk,Sn,Alpha,Un,Kp,Ki,Fn,F_Sample,Tp,Simulation_dynamic_cut_time,N10,N120,File_save_name,I1_Ns,I2_Ns,I3_Ns,U1_
NS,U2_NS,U3_NS);
loadfile_final = [File_save_name];
load ([loadfile_final '.mat'])
P_st_fic_complete(j) = P_st_fic_ave;
P_st_complete(j) = Pst_ave;
P_it_complete(j) = Plt_ave;
c_psyk_complete(j) = cpsyk_ave;
P_st_fic_complete_ave = mean(P_st_fic_complete);
P_st_complete_ave = mean(P_st_complete);
P_it_complete_ave = mean(P_it_complete);
c_psyk_complete_ave = mean(c_psyk_complete);
complet_results = sprintf('Complete_Results_%d',Alpha);
save
(complet_results,'P_st_fic_complete','P_st_complete','P_it_complete','c_psyk_complete','P_st_fic_complete_ave','P_st_complete
_ave','P_it_complete_ave','c_psyk_complete_ave');
save ('Initial
values','time','endval','U1N_NS','U2N_NS','U3N_NS','I1_NS','I2_NS','I3_NS','endval1','Sn','Sk','n','Sfic','Un','Fn','i','Kp','Ki','F_Sam
ple','Simulation_dynamic_cut_time','N10','N120','j','jj','Alpha','P_st_fic_complete','P_st_complete','P_it_complete','c_psyk_complet
e','P_st_fic_complete_ave','P_st_complete_ave','P_it_complete_ave','c_psyk_complete_ave')
clear
load 'Initial values'
else
end
button = questdlg('The next Row Data calculation is about to start do you want to finish running this M-file?', ...
'Exit Dialog','Yes','No','No');
switch button
case 'Yes',
disp('Exiting MATLAB');
%Save variables to matlab.mat
save
case 'No',
quit cancel;
end
end
button = questdlg('The next calculation for a new phase angle of the fictious grid Alpha is about to start do you want to finish
running this M-file?', ...
'Exit Dialog','Yes','No','No');
switch button
case 'Yes',
disp('Exiting MATLAB');
%Save variables to matlab.mat
save
case 'No',
quit cancel;
end
end
$

```

5. Simulation Function (Complete Flicker calculation by formulas)

```

$function flicker_Calculation_complete
(j,i,n,Sk,Sn,Alpha,Un,Kp,Ki,Fn,F_Sample,Tp,Simulation_dynamic_cut_time,N10,N120,File_save_name,I1_Ns,I2_Ns,I3_Ns,U1_
NS,U2_NS,U3_NS)
Initial Input data for the Flicker simulated fictitious grid
• Fn = 50;%noninal frequency in Hz
• F_Sample = 0.00025;%1/Hz Used in FAMOS (Delta X)
• Fs = 1/F_Sample; %in Hz & must be greater than 2000 Hz
• Simulation_dynamic_cut_time = 0.06;% In FAMOS Used
• Simulation_Time = 40;%run time of the simulation Used in Matlab simulink & FAMOS
Please state which measurement you want to analysis:
• i=1 for continuous operation
• i=2 for switching operation
• i = 2;%an operation selector
• Sn = 1700;%rated apparent power in kW
• n = 20; % Short cicuit Ratio in %
• Alpha = 30;% Fictitious grid impedance phase angle in degree
• Un = 400;% Nominal Voltage Low voltage side in V
• Sk = 105;%Short cicuit apparent power in MVA
• Kp = 50;% Regulator gain for PLL in simulink
• Ki = 1400;% Regulator gain for PLL in simulink
• N10 = 2;% Number of switching operation with in 10 min
• N120 = 24;% Number of switching operation with in 2 h
%-----end-----
%-----Loading measured data-----
• IFN = 'Input_Data_MATLAB_'; % The name of the Input Data file
• loadfile = strcat(IFN,i);
• open (loadfile);
%-----end-----
%----Starting the fictitious grid simulation-----
%options = simset('SrcWorkspace','current');
assignin('base','Alpha',eval('Alpha'));
assignin('base','Tp',eval('Tp'));
assignin('base','I1_Ns',eval('I1_Ns'));
assignin('base','I2_Ns',eval('I2_Ns'));
assignin('base','I3_Ns',eval('I3_Ns'));
assignin('base','U1_NS',eval('U1_NS'));
assignin('base','U2_NS',eval('U2_NS'));
assignin('base','U3_NS',eval('U3_NS'));
sim('Flickermeter6140021_new_GL_Final_3ph');
%-----end-----
%-----Saving Needed signals-----%
savefile = sprintf('Simulation_results_%d_%d',j,Alpha);
Time_1 = Ufic_t.time; % X-axis for Simulation Time
Ufic_t_1 = Ufic_t.signals.values(:,1); % Y-axis Ufic_1
Ufic_t_2 = Ufic_t.signals.values(:,2); % Y-axis Ufic_2
Ufic_t_3 = Ufic_t.signals.values(:,3); % Y-axis Ufic_3
U0_t_1 = U0_t_3ph.signals.values(:,1); % Y-axis U0_1
U0_t_2 = U0_t_3ph.signals.values(:,2); % Y-axis U0_2
U0_t_3 = U0_t_3ph.signals.values(:,3); % Y-axis U0_3
ku_psyk_1 = ku_psyk.signals.values(:,1); % Y-axis ku_psyk_1
ku_psyk_2 = ku_psyk.signals.values(:,3); % Y-axis ku_psyk_2
ku_psyk_3 = ku_psyk.signals.values(:,5); % Y-axis ku_psyk_3
f1 = Frequency_signal_realization.signals.values(:,1); % Y-axis f1

```

```

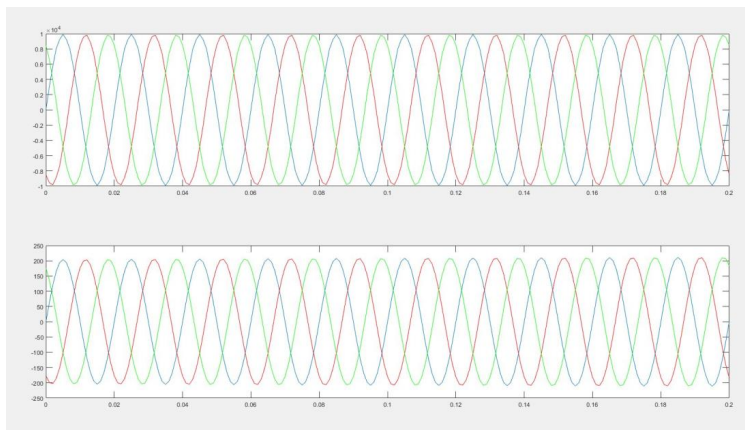
f2 = Frequency_signal_realization.signals.values(:,2);% Y-axis f2
f3 = Frequency_signal_realization.signals.values(:,3);% Y-axis f3
U1N_NS_PU = Voltage_signal_realization.signals(1,1).values(:,1);% Y-axis U1N_NS_PU
U2N_NS_PU = Voltage_signal_realization.signals(1,2).values(:,1);% Y-axis U2N_NS_PU
U3N_NS_PU = Voltage_signal_realization.signals(1,3).values(:,1);% Y-axis U3N_NS_PU
save (savefile,
'Time_1','Ufic_t_1','Ufic_t_2','Ufic_t_3','U0_t_1','U0_t_2','U0_t_3','ku_psyk_1','ku_psyk_2','ku_psyk_3','f1','f2','f3','F_Sample',
'Simulation_dynamic_cut_time','Tp');
%----- Cut now -----
Ufic_t_1 = Ufic_t_1((Simulation_dynamic_cut_time/F_Sample):end);
Ufic_t_2 = Ufic_t_2((Simulation_dynamic_cut_time/F_Sample):end);
Ufic_t_3 = Ufic_t_3((Simulation_dynamic_cut_time/F_Sample):end);
U0_t_1 = U0_t_1((Simulation_dynamic_cut_time/F_Sample):end);
U0_t_2 = U0_t_2((Simulation_dynamic_cut_time/F_Sample):end);
U0_t_3 = U0_t_3((Simulation_dynamic_cut_time/F_Sample):end);
%-----Getting Pst & S using the flickermeter-----
Fs = 1/F_Sample; %in Hz & must be greater than 2000 Hz
[P_st_fic1 S_fic1] = flicker_sim (Ufic_t_1, Fs, Fn);
[P_st_fic2 S_fic2] = flicker_sim (Ufic_t_2, Fs, Fn);
[P_st_fic3 S_fic3] = flicker_sim (Ufic_t_3, Fs, Fn);
[P_st_01 S_01] = flicker_sim (U0_t_1, Fs, Fn);
[P_st_02 S_02] = flicker_sim (U0_t_2, Fs, Fn);
[P_st_03 S_03] = flicker_sim (U0_t_3, Fs, Fn);
P_st_fic_ave = (P_st_fic1+P_st_fic2+P_st_fic3)/3;% P_st_fic average value for the 3 phases
%-----end-----
%-----Calculating c & kf & Pst & Plt according to IEC-----
Sk_fic = n*Sn;%Short circuit apparent power in KVA of the Fictitious grid
ku_psyk_max_1 = max(ku_psyk_1);
ku_psyk_max_2 = max(ku_psyk_2);
ku_psyk_max_3 = max(ku_psyk_3);
ku_psyk_max_ave = (ku_psyk_max_1+ku_psyk_max_2+ku_psyk_max_3)/3;
d_max_ave = 100*ku_psyk_max_ave*(Sn/Sk);
if (i == 1)
cpsyk_1 = P_st_fic1*(Sk_fic/Sn);
cpsyk_2 = P_st_fic2*(Sk_fic/Sn);
cpsyk_3 = P_st_fic3*(Sk_fic/Sn);
Pst_1 = cpsyk_1*(Sn/Sk);
Pst_2 = cpsyk_2*(Sn/Sk);
Pst_3 = cpsyk_3*(Sn/Sk);
Plt_1 = Pst_1;
Plt_2 = Pst_2;
Plt_3 = Pst_3;
Pst_ave = (Pst_1+Pst_2+Pst_3)/3;
Plt_ave = Pst_ave;
cpsyk_ave = (cpsyk_1+cpsyk_2+cpsyk_3)/3;
save
(File_save_name,'Pst_ave','Plt_ave','P_st_fic_ave','ku_psyk_max_ave','Ufic_t_1','cpsyk_ave','Pst_1','Pst_2','Pst_3','cpsyk_1','cps
yk_2','cpsyk_3');
elseif (i == 2)
kf_psyk_1 = (1/130)*P_st_fic1*(Sk_fic/Sn)*(Tp^0.31);
kf_psyk_2 = (1/130)*P_st_fic2*(Sk_fic/Sn)*(Tp^0.31);
kf_psyk_3 = (1/130)*P_st_fic3*(Sk_fic/Sn)*(Tp^0.31);
Pst_1 = 18*(N10^0.31)*kf_psyk_1*(Sn/(Sk*1000));
Plt_1 = 8*(N120^0.31)*kf_psyk_1*(Sn/(Sk*1000));
Pst_2 = 18*(N10^0.31)*kf_psyk_2*(Sn/(Sk*1000));
Plt_2 = 8*(N120^0.31)*kf_psyk_2*(Sn/(Sk*1000));

```

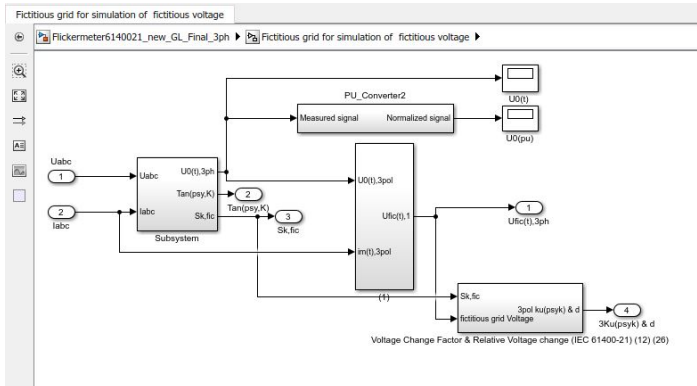
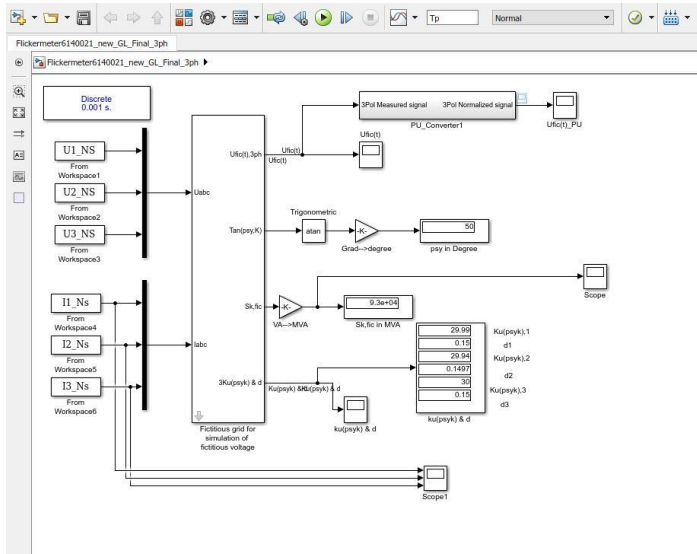
```

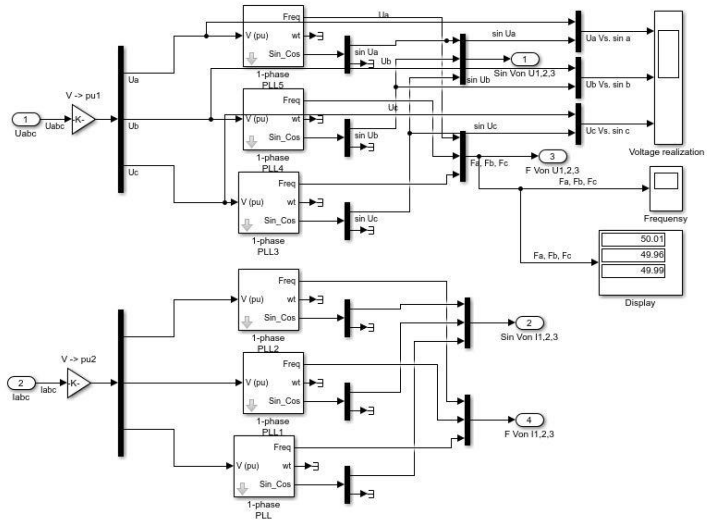
Pst_3 = 18*(N10^0.31)*kf_psyk_3*(Sn/(Sk*1000));
Plt_3 = 8*(N120^0.31)*kf_psyk_3*(Sn/(Sk*1000));
Pst_ave = (Pst_1+Pst_2+Pst_3)/3;
Plt_ave = (Plt_1+Plt_2+Plt_3)/3;
kf_psyk_ave = (kf_psyk_1+kf_psyk_2+kf_psyk_3)/3;
save
(File_save_name,'Pst_ave','Plt_ave','P_st_fic_ave','ku_psyk_max_ave','Ufic_t_1','kf_psyk_ave','Pst_1','Pst_2','Pst_3','kf_psyk_1',
'kf_psyk_2','kf_psyk_3','ku_psyk_max_1','ku_psyk_max_2','ku_psyk_max_3');
else
f1 = warndlg('Please Enter a correct value for i', 'Warning');
end
%-----end-----§

```



Annex B: Fictitious Grid Simulation Model





Reference

References

- [1] V. j. t. U. N. G. C. U. Peter C. Brun, "Advocating the potential of wind power," in *Sustainability Report*, VESTAS, pp. 1–30, 2016.
- [2] F. Blaabjerg, R. Teodorescu, M. Liserre, and A. V. Timbus, "Overview of control and grid synchronization for distributed power generation systems," *IEEE Transactions on Industrial Electronics*, vol. 53, pp. 1398–1409, Oct 2006.
- [3] A. S. Bubshait, A. Mortezaei, M. G. Simões, and T. D. C. Busarello, "Power quality enhancement for a grid connected wind turbine energy system," *IEEE Transactions on Industry Applications*, vol. 53, pp. 2495–2505, May 2017.
- [4] K. Redondo, J. J. Gutierrez, P. Saiz, L. A. Leturiondo, I. Azcarate, and A. Lazkano, "Accurate differentiation for improving the flicker measurement in wind turbines," *IEEE Transactions on Power Delivery*, vol. 32, pp. 88–96, Feb 2017.
- [5] J. Ruiz, J. J. Gutierrez, A. Lazkano, and S. R. de Gauna, "A review of flicker severity assessment by the iec flickermeter," *IEEE Transactions on Instrumentation and Measurement*, vol. 59, pp. 2037–2047, Aug 2010.
- [6] I. E. COMMISSION, "Part 21-1: Measurement and assessment of power quality characteristics of grid connected wind turbines..," *IEC CDV 61400-21-1*, IEC 2017, vol. Ed. 2.0, Nov 2018.
- [7] E. C. for Electrotechnical Standardization, "Electromagnetic compatibility (emc), part 4-15: Testing and measurement techniques flickermeter- functional and design specifications," *IEC: 61000-4-15*, vol. ICS 33.100.20, Feb 2010.
- [8] K. Chmielowiec, "Flicker effect of different types of light sources," in *11th International Conference on Electrical Power Quality and Utilisation*, pp. 1–6, Oct 2011.

- [9] M. K. Walker, "Electric utility flicker limitations," *IEEE Transactions on Industry Applications*, vol. IA-15, pp. 644–655, Nov 1979.
- [10] A. Larsson, "Flicker emission of wind turbines during continuous operation," *IEEE Transactions on Energy Conversion*, vol. 17, pp. 114–118, Mar 2002.
- [11] J. C. Gomez and M. M. Morcos, "Flicker measurement and light effect," *IEEE Power Engineering Review*, vol. 22, pp. 11–15, Nov 2002.
- [12] J. Ruiz, J. J. Gutierrez, A. Lazkano, and S. R. de Gauna, "A review of flicker severity assessment by the iec flickermeter," *IEEE Transactions on Instrumentation and Measurement*, vol. 59, pp. 2037–2047, Aug 2010.
- [13] J. Molina and L. Sainz, "Compact fluorescent lamp modeling for large-scale harmonic penetration studies," *IEEE Transactions on Power Delivery*, vol. 30, pp. 1523–1531, June 2015.
- [14] T. Keppler, N. R. Watson, J. Arrillaga, and S. Chen, "Theoretical assessment of light flicker caused by sub- and interharmonic frequencies," *IEEE Transactions on Power Delivery*, vol. 18, pp. 329–333, Jan 2003.
- [15] T. Kim, E. J. Powers, W. M. Grady, and A. Arapostathis, "Detection of flicker caused by interharmonics," *IEEE Transactions on Instrumentation and Measurement*, vol. 58, pp. 152–160, Jan 2009.
- [16] J. Slezinger and J. Drapela, "An alternative flickermeter evaluating high-frequency interharmonic voltages," in *2012 IEEE International Workshop on Applied Measurements for Power Systems (AMPS) Proceedings*, pp. 1–6, 2012.
- [17] A. Zargari, P. Moallem, and A. Kiyoumarsi, "Studying and improvement of operation of iec flickermeter," in *Iranian Conference on Electrical Engineering*, pp. 925–931, May 2010.
- [18] A. Hooshyar and E. F. El-Saadany, "Development of a flickermeter to measure non-incandescent lamps flicker," *IEEE Transactions on Power Delivery*, vol. 28, pp. 2103–2115, Oct 2013.
- [19] J. Drapela and J. Slezinger, "Design and utilization of a light flickermeter," in *2012 IEEE International Workshop on Applied Measurements for Power Systems (AMPS) Proceedings*, pp. 1–6, Sept 2012.
- [20] L. M. Craig, M. Davidson, N. Jenkins, and A. Vaudin, "Integration of wind turbines on weak rural networks," in *International Conference on Opportunities and Advances in International Electric Power Generation (Conf. Publ. No. 419)*, pp. 164–167, Mar 1996.

- [21] P. Sorensen, J. Tande, L. Søndergaard, and J. Kledal, "Flicker emission levels from wind turbines," vol. 20, pp. 39–46, 01 1996.
- [22] Z. Saad-Saoud and N. Jenkins, "Models for predicting flicker induced by large wind turbines," *IEEE Transactions on Energy Conversion*, vol. 14, pp. 743–748, Sep 1999.
- [23] T. Thiringer, T. Petru, and S. Lundberg, "Flicker contribution from wind turbine installations," *IEEE Transactions on Energy Conversion*, vol. 19, pp. 157–163, March 2004.
- [24] P. Jorgensen, J. O. Tande, A. Vikkelso, P. Norgand, J. S. Christensen, P. Sorensen, J. D. Kledal, and L. Søndergaard, "Power quality and grid connection of wind turbines," in *14th International Conference and Exhibition on Electricity Distribution. Part 1. Contributions (IEE Conf. Publ. No. 438)*, vol. 1, pp. 6/1–6/6 vol.2, June 1997.
- [25] K. Redondo, J. J. Gutierrez, P. Saiz, L. A. Leturiondo, I. Azcarate, and A. Lazkano, "Wind turbines part 21: measurement and assessment of power quality characteristics of grid connected wind turbines.," *IEC: 61400-21*, vol. Ed. 2.0, Feb 2017.
- [26] G. G. K. R. S. F. e. a. Sorensen, Poul, "European wind turbine testing procedure developments. task 2: Power quality. risø national laboratory," vol. 01, pp. 12–200, 01 2001.
- [27] J. J. Gutierrez, J. Ruiz, L. A. Leturiondo, and A. Lazkano, "Flicker measurement system for wind turbine certification," *IEEE Transactions on Instrumentation and Measurement*, vol. 57, pp. 375–382, Dec 2008.
- [28] J. Sun, "Impedance-based stability criterion for grid-connected inverters," *IEEE Transactions on Power Electronics*, vol. 26, pp. 3075–3078, Nov 2011.
- [29] C. Wei, M. Han, and W. Yan, "Voltage fluctuation and flicker assessment of a weak system integrated wind farm," in *2011 IEEE Power and Energy Society General Meeting*, pp. 1–5, July 2011.
- [30] J. Drapela and J. Slezinger, "Design and utilization of a light flickermeter," in *2012 IEEE International Workshop on Applied Measurements for Power Systems (AMPS) Proceedings*, pp. 1–6, Sept 2012.
- [31] A. Lazkano, I. Azkarate, J. J. Gutierrez, J. Ruiz, L. A. Leturiondo, and P. Saiz, "Measurement of the flicker characteristics of grid connected wind turbines: Instantaneous frequency versus instantaneous phase estimation methods," in *Proceedings of 14th International Conference on Harmonics and Quality of Power - ICHQP 2010*, pp. 1–6, Sept 2010.

- [32] N. Khan and L. H. et al; "Validation of flicker measurement in grid-connected wind turbin," *APPEEC, IEEE Conference 2018*, pp. 1523–1531, July 2018.
- [33] N. Khan and L. H. et al; "Verification of accuracy and precision evaluation of iec flicker meter," *IEEE Conference 2018*, pp. 153–151, Oct: 2018.
- [34] T. Keppler, N. R. Watson, J. Arrillaga, and S. Chen, "Theoretical assessment of light flicker caused by sub- and interharmonic frequencies," *IEEE Transactions on Power Delivery*, vol. 18, pp. 329–333, Jan 2003.
- [35] K. Chmielowiec, "Flicker effect of different types of light sources," in *11th International Conference on Electrical Power Quality and Utilisation*, pp. 1–6, Oct 2011.
- [36] D. Geiger, M. Arechavaleta, M. Halpin, and M. Tremblay, "Evaluating alternatives to voltage fluctuation and flicker measurements based on iec standard 61000-4-15," in *2016 10th International Conference on Compatibility, Power Electronics and Power Engineering (CPE-POWERENG)*, pp. 53–57, June 2016.
- [37] A. E. Feijoo, J. Cidras, and J. L. G. Dornelas, "Wind speed simulation in wind farms for steady-state security assessment of electrical power systems," *IEEE Transactions on Energy Conversion*, vol. 14, pp. 1582–1588, Dec 1999.

Part 2

Model of the Harmonics Measurement and Assessment



HARMONICS Measurement
The Green Way to Sustained Energy Savings

Contents

Declaration of Authorship	i
Abstract	iii
Acknowledgements	iv
List of Figures	vii
List of Tables	viii
Abbreviations	ix
Physical Constants	x
Symbols	xi
1 f	1
2 State of the art	2
2.0.1 Harmonic and their Impact on the wind turbine	3
2.1 Fast Fourier Transform (FFT)	5
2.1.1 Frequency Resolution	6
2.1.2 Review of the frequency detection methods	7
2.1.3 Spectral leakage and windowing	7
3 Harmonic Measurement Model	9
3.1 Measurement in Standard	10
3.1.1 Structure	10
3.1.2 Resampling	11
3.1.3 Grouping	12
3.1.4 Sub-grouping Harmonics	12
3.1.5 Sub-grouping inter-Harmonics	13
3.1.6 Total Harmonic Distortion	14
4 Harmonic measurement of the wind turbine	15
4.0.1 Equipment Accuracy fro Hamronic Measurment	16

4.0.2	Harmonic function of active power	16
4.0.3	Anemometer	16
4.0.4	Anti-aliasing filter	17
5	Simulation of the harmonic model	19
5.1	Case 1	21
5.1.1	Case A: 0.2s Window without Grouping	21
5.1.2	Case B: 0.2s Window with Grouping	22
5.1.3	Case C :10 cycle without grouping	22
5.1.4	Case D: IEC method	23
5.2	Case 2	24
5.2.0.1	Conclusion	25
5.3	Aggregation	26
6	Model Validation	28
6.0.1	Prevailing angle	28
6.0.2	Statistical validation of Harmonic Magnitude	30
7	Conclusion	32
7.1	Future Work	33
.1	Annexes E	34
.2	Annexes D	36
	Bibliography	43

List of Figures

2.1	Wind Farm [1]	2
2.2	Frequency Resolution	6
3.1	Reference Model IEC method	11
3.2	IEC grouping of spectral components for harmonics and for Inter-harmonics	13
4.1	Components of Harmonic measurement System	15
4.2	Wind speed function of active power	17
4.3	Anti-aliasing filter	17
5.1	Input Signal	19
5.2	Harmonic level comparison between 10 cycles and Fixed Window (0.2s)	25
5.3	Harmonic level comparison between IEC Standard and fixed window (0.2s)	25
5.4	Aggregation vs 10 cycle	26
5.5	Aggregation vs four different frequency	27
5.6	Zoom in version of Fig 1.11	27
6.1	10 cycle	29
6.2	Fixed window	29
6.3	Normal Distribution of 10 cycle	30
6.4	Normal Distribution of one minute aggregation samples	31
1	Harmonic Meter Model GUI	34

List of Tables

2.1	Series of IEC standards related to Harmonic	5
3.1	Computation Time	12
4.1	Description of requirements for measurement equipment	16
5.1	Harmonic Order	20
5.2	RMS value of Harmonic levels	20
5.3	Harmonic levels without Grouping	21
5.4	Harmonic levels with Grouping	22
5.5	Harmonic levels with 10 cycle without grouping	23
5.6	Harmonic levels with IEC method	24

Chapter 2

State of the art

Wind Turbine technology is growing exponentially in the global market and their level of penetration into the grid also increasing. In the past, wind turbine integration didn't impact the power system grid. However, currently due to the large number of the wind farm 2.1 installations, there has been an increase in the level of power quality issues in the grid [2].



FIGURE 2.1: Wind Farm [1]

Furthermore, due to the improvement in power electronic the advanced wind technology uses power electronic, as an interface between turbine and grid which transfer electric power at the correct frequency and magnitude. Moreover, control active and reactive power of the turbine for the grid emphasizes on the power electronic inclusion as per power quality relevance. [3]

. The intermittent property of the wind turbine due to variation in the wind speed may cause instability into the power system which ultimately transfer in efficient electric power to the dwelling which is intolerable for the (distribution system operators) DSP

and (transmission system operators) TSO. Also, integration arise more problem to the power system, for example:

- . Power system operation planning
- . Environment

but the most important is power quality related to harmonics as it is relevant to the grid integration requirement (voltage, frequency, and distortion under the acceptable limit) [4]. The installation of the wind Farm is prohibited when they emit harmonic more than the allowed limits recommended by the International Electrotechnical Commission(IEC) standard. Moreover, the concern related to wind turbine power quality is increasing globally and their impact on the grid. The analyzing tool and procedure play a vital role in the measurement and assessment of power quality to analyse harmonic levels.

Ideally, the electric power system operates with sinusoidal voltage and current with system frequency (50 or 60 Hz, 50 Hz is used throughout this thesis). However, in reality, the signal deviates from the ideal signal due to the different parameter. One of those difference is called harmonic distortion: a phenomenon that a signal varies from the ideal signal and can be decomposed into the different signal at different frequency rather than grid or fundamental frequency.[5][6][7]. Additionally, distribution or transmission operators set to power quality limits into the grid which compels wind turbine manufacturers to concentrate on the design in order to eliminate harmonics and improve power quality [8][9].

In the power system, the cause of harmonics is non-linear loads. The non-linear load is a device which draws sinusoidal voltage but the current is distorted from the source. Example of non-linear loads is an arc furnace, speed drives, medical equipment, electrical motors, transformer, and other power electronic which affect the grid [10]. The usage of this devices has become common and the necessity of harmonics analysis is more desired.

The effect of harmonic currents and voltages on the grid is tremendous as they increase the losses and over-heating of a transformer, power cables and other electrical components. They also cause the tripping of relays during unplanned cases and inaccurate measurement values of voltage and current [11].

2.0.1 Harmonic and their Impact on the wind turbine

The wind turbine is divided into four category type1, type2, type3 and type 4. The wind turbine with an induction generator is connected directly to the grid and cause

less harmonic distortion during continuous operation. Normally type1 and type2 fall in this category and little emphasis on the harmonic analysis is done and according to IEC 61400-21, it is not obliged to measure the harmonic of direct couple fixed speed wind turbine [12]. However, for type3 and type4 wind turbine, it is necessary to analyse harmonic measurement as they contain back to back power converter which injects harmonic into the grid with reasonable magnitude. The measurement of harmonic in practical life is a complex task as after integration at the point of common coupling chances of resonance harmonic occurrence is high also background harmonics of the grid are present which make it difficult to differentiate between wind turbine harmonics and grid harmonics. However, it is preferable to measure an event of less background harmonic distortion and exclude the measurement during high background harmonic analysis [12]. Harmonic emission and propagation are considered as a power quality issues for up-to-date variable speed wind turbine and more concern need to be taken. The standard 61400-21 include the measurement produce of the harmonics analysis of grid-connected wind turbine. The main impact of the harmonic indices within the wind farm is following

- . Losses in the generation and transmission within a wind farm
- . Increasing the magnitude of harmonic due to parallel and series resonance
- . Decrease life span of the electrical component due to thermal stress
- . Incorrect behaviour of protection scheme

Therefore,It is important to analyze the harmonic phenomena of the wind turbine in order to investigate their effect on the power system and improve the performance of the wind turbine or farm[13].The International Electrotechnical Commission (IEC) developed and released the IEC-standards 61400-21, 61000-4-7 and latest updated 61400-21-1 as part of the IEC 61000 series for testing and assessing power quality characteristics of grid-connected wind energy technology in an accurate and precise way. [1]. The detail of standard series is given in table 2.1

IEC Standard	Description
61000-3-6	It explain the type to be used for harmonic measurement such as voltage and current transducer.
61000-4-7	It give the characteristic about the harmonic measurement tool but does not give detail about frequency detection method.
61400-21	It explains the measurement procedure of harmonic from the grid connected wind turbine.
61400-21-1	It includes the procedure to measure phase angle of harmonics and validation of the model.

TABLE 2.1: Series of IEC standards related to Harmonic

2.1 Fast Fourier Transform (FFT)

To measure the harmonics levels with accuracy and precision different methods had been developed with the passage of time which consist of parametric technique developed on the Prony method [14] and non-parametric technique with windowing, FFT and interpolation of the spectrum data obtained [15] [16]. The most common and widely used for spectral analysis and calculation of different harmonic component is based on the algorithm called Fast Fourier transform (FFT) and also recommended in IEC 61000-4-7. It compute the discrete Fourier transform with high computational efficiency than other algorithm to obtain (phase angle, harmonic levels and THD etc) information of the interested signal[17].

The discrete fourier transform take the sequence of N complex number of time samples $x_n = x_0, \dots, x_{N-1}$ and transforms into another sequence of complex numbers frequency domian X_n [18].

$$X_n = \frac{1}{N} \sum_{n=1}^{N-1} x_n e^{-j2\pi \frac{K}{N} n} \quad (2.1)$$

where the vector u_k form an orthogonal basis over the set of N-dimensional complex vectors

$$u_k = [e^{-j2\pi \frac{K}{N} n}]^T \quad (2.2)$$

FFT method contain conditions to be follow in order to perform accurate results such as periodic signal, number of samples in the discrete data should be 2^n where n=10,11. Etc. However, their exist some limitation like frequency resolution and spectral leakage. The input signal to be analyze is divided into two category stationary and non-stationary signal. The processing of FFT tool is better on stationary signal and performed for the harmonic analysis of the grid connected wind turbine. The indices (mean, variance, probability density function) of the stationary signal are time invariant, also establishing the grid fundamental frequency near to its nominal value is a prerequisite of having

balance between generation and consumption. In reality, it is difficult to fulfill this condition which cause variation in the frequency of the voltage and current consequently effecting the power quality also violating the stationary assumption and create uncertainty in the harmonic analysis tool.

Non-stationary time series signal can be approximate close to stationary by windowing the time series into section so called block of data and signal characteristic are analyze on this window. Afterward the window is moved to new block and the calculation are repeated for a new window. The mean, variance, harmonics magnitude, phase angle, probability density function of the signal, become dependent of time and location of the window. Basically, This technique is used in harmonic analysis and also adopted by IEC standards [19].

2.1.1 Frequency Resolution

The signal to be processed for harmonic analysis usually transform from the time domain to the frequency domain by using Discrete Fourier Transform (DFT) tool. The efficiency of the result can be improved by applying Fast Fourier Transform (FFT) algorithm as it is computationally fast [206]. Basically, the frequency resolution is the distance between two spectral line [20] as shown in 2.2 and is defined in 2.3

$$\text{FrequencyResolution} = \Delta f = \frac{f_s}{N} = \frac{1}{T_{ow}} \quad (2.3)$$

Where f_s is sampling frequency, N is the number of samples within the observation window, T_{ow} is the time within the observation window . Because of the limitation of

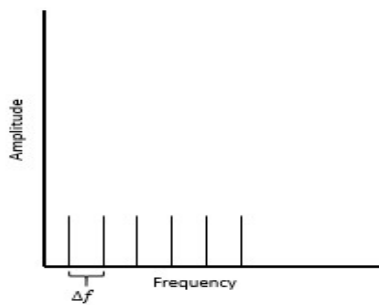


FIGURE 2.2: Frequency Resolution

the resolution, the spectrum cannot be accurately expressed if the harmonic frequency does not lie on the spectral line or not the integer multiple of frequency resolution. This may cause dummy harmonic component to appear in the harmonic spectrum which is

known as picket-fence effects. However, it can be solved by increasing the resolution or by adding the zero padding and also interpolation [21]

2.1.2 Review of the frequency detection methods

Power System frequency detection plays vital role in the measurement of the harmonic levels, as in case of precise synchronization of detecting periodic cycles there is no truncation error and amplitude of the spectrum bin is accurate, otherwise non-periodic cycles cause spectral leakage in the frequency domain due to discontinuity at the end of the window which will alter the harmonic levels and vary the overall results. In addition to that, fast and reliable frequency detection is prerequisite for better power control, load shedding, load re-connection and power system protection.

There are different types of method to detect the frequency of the power system. In, [22], [23] phase locked loop (PLL) is used to detect the fundamental frequency of the single phase in the presence of stationary and disturbance. The PLL is developed on software that is based on a time-domain coordinate transformation and Hilbert transformation technique. In [24], zero crossing detection is used for fundamental power system frequency detection, [25] used multi-stage filter to remove harmonic, noise, commutation notches without altering the phase of the signal and detect the frequency by using zero crossing. In [210] the frequency is estimated by applying the hanning window on the original signal before using FFT and then different formula is imposed based on the left and right sample value near to the highest amplitude spectrum in frequency domain. In reference [26] least square method and singular value decomposition (SVD) is used but it is disadvantage in real application because of higher computational load.

2.1.3 Spectral leakage and windowing

In practical application, the FFT tool process finite observation interval of data, these phenomena is known as windowing. This process cause errors or spectral leakages in the frequency domain specifically in event of un-synchronization and presence of inter-harmonic which are not multiple of fundamental frequency. Therefore, the detection of fundamental power system frequency is vital. Basically, in leakage cross talk occur between different frequencies or energy of spectral bins distribute among the other bins causing error in real magnitude of harmonics.

In order to reduce the phenomena of leakage related with finite observation intervals windowing function is used before applying FFT tool. Windowing is the weighting function that are multiply with the finite intervals signal in time domain to reduce the loss

of continuity at the end of the windowing. There exist different types of window functions like hanning window, hamming window, rectangular window, Blackman window and flattop win window etc giving different results in the frequency domain so choosing window has great effect on the performance of the measurement of harmonic analysis. An in-dept detail of the window function is presented in [26]. The most commonly used window for harmonic analysis is rectangular and hanning window also the IEC standard 61000-4-7 proposed to use rectangular and hanning window for the measurement of the harmonic analysis. It is preferable to use rectangular in case of synchronization otherwise hanning window is used in situation of un-synchronization, in simulation section it is demonstrated the difference in error of using windowing types during synchronization and un-synchronization. The rectangular window is the easiest function to implement, it is defined in 2.4

$$W_{rec}(n) = \begin{cases} 1 & 0 \leq n \leq N \\ 0 & elsewhere \end{cases} \quad (2.4)$$

Where W_{rec} is rectangular window, $n = 0, 1, 2, \dots, N-1$ and N = number of samples within observation interval.

In frequency domain the main lobe width of rectangular window is three bins. The first side-lobe is 13 dB less than the main lobe with falloff at 20 dB per decade. It gives the best frequency resolution with lowest main lobe width and more detail is given in [27]. While hanning function is define by 2.5

$$W_{han}(n) = 0.5 \left(1 - \cos \left(2\pi \frac{n}{N} \right) \right), \quad 0 \leq n \leq N \quad (2.5)$$

It is of the cosine-squared type with gain of 0.5 and main lobe approximately double than the rectangular window. In frequency domain the first sidelobe is 32 dB less than the main lobe peak with falloff at 60 dB per decade.[28].

A time domain signal $S(L)$ windowed is represent by 2.6

$$S_w(L) = S(L) \times W(L) \quad (2.6)$$

$W(L)$ is window coefficients and $L = 0, 1, \dots, N-1$

Chapter 3

Harmonic Measurement Model

The focus of this chapter is to developed the meter model which is based on the procedure given in the IEC standard 61000-4-7. The detail is in section 3.1. However, it is not explained in the standard about the tool to perform the specific task. The following points are

- 1- It is not mentioned that which frequency detection method is select in order to obtain 10 cycles of the signal.
- 2- No detail about the resampling of the signal to achieve power of 2 samples within the observation interval.
- 3- No explanation on the use of low pass anti aliasing filter.
- 4- No detail about the validation of the model as well as frequency detection method to capture the 10 cycles of the signal.

Later the updated standard was released IEC 64100-21-1 in which phase angle and prevailing angle ratio(PAR) is included. The purpose of the PAR is to validate the model precision and accuracy. However, one indication of validation is not enough and statistics tool i-e standard deviation, probability density is used to validate the model frequency component magnitude.

3.1 Measurement in Standard

The IEC standard uses the specific notation 3.1 of the Fourier series to derive different indices [29] regarding, total harmonic distortion, harmonics, and inter-harmonics.

$$f(t) = c_0 + \sum_{\rho=1}^{\infty} c_{\rho} \sin\left(\frac{\rho}{N} w_f t + \varphi_{\rho}\right) \quad (3.1)$$

where c_0 is the dc component of the signal. c_{ρ} is the amplitude of the component with frequency $f_{\rho} = \frac{\rho}{N} f_0$, N is the number of fundamental period within the window length. ρ is the order of the spectral line in the frequency domain, w_f is the angular frequency of the fundamental and φ_{ρ} is the phase angle of the spectral line ρ .

3.1.1 Structure

The step by step procedure to calculate the harmonic is following

- 1- Analog signal which has to be analyzed is sampled.
- 2- By applying frequency detection, 10 cycles of the signal is captured and stored.
- 3- The 10 cycles of the signal is resampled (detail in section 3.1.2) to obtain the power of 2. samples.
- 5- Fast Fourier tool (FFT) is applied to the 10 cycles window of the signal to transform from the time domain into the frequency domain.
- 6- Grouping which is explained in section 3.1.3 is applied in the frequency domain to obtain different frequency component.

In most of the literature, for the analysis of harmonic 0.2s window is used. As it is assumed that within this observation the signal is periodic and stationary assumption is satisfied. Basically, for 50 Hz fundamental frequency the length of the simple window is 0.2s, ideally for 50 Hz frequency 10 cycles lies within 200ms window length $10/50=0.2$ s, however in reality the frequency of the grid varies deviating from the ideally window length 0.2 i.e. the frequency of the grid can vary with tolerance of 0.5 % of 50 Hz. In case of 49.5 Hz, the 10 cycles would fall within $10/49.5=0.202$ s window length Therefore, the more accurate term is used in the IEC standard is 10 cycles for 50 Hz 12 cycles for 60 Hz [29]. The rectangular window as mention earlier is applied when the measurement window is synchronized. However, in case of loss of synchronization Hanning window is applied. The IEC standard requires that 10 cycles agree with an integer number of

samples within 0.03 %. In order to synchronize the measurement window with the fundamental frequency of the power system grid zero crossing frequency detection methods is adopted which is explain in state of the art section. The reason for using zero crossing is to capture the exact 10 cycles and compare the model with different methods to analyze the accuracy, precision and performance. The reference diagram or structure is illustrated in figure 3.1.

. When DFT is performed on the signal, the time series signal is transformed into fre-

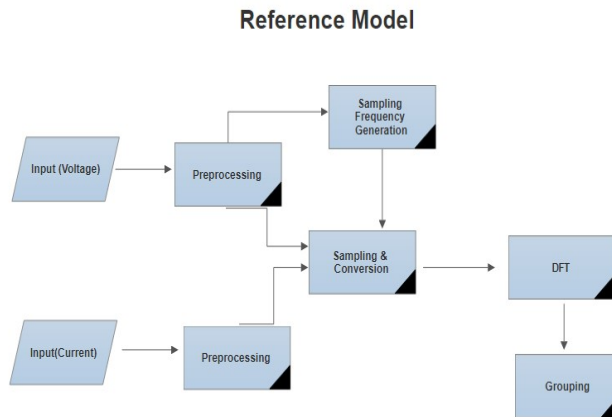


FIGURE 3.1: Reference Model IEC method

quency spectrum with frequency resolution depending on the length of the signal within the window. Usually after the resampling the length is interpolated to give 5 Hz of frequency resolution.

3.1.2 Resampling

After detecting the frequency and capturing 10 cycles it is necessary to resample the signal in order to achieve integer number of samples in the measurement window. The sampling rate 5.120 Ks/s/ch is used, which mean that one second contains 5120 samples and 10 cycles consist of 1024 samples if the fundamental frequency is 50 Hz. However, in practical life, the power system frequency is varying and the limits of tolerance in the standards are between 49.5-50.5 Hz. The block of data having 10 cycles with the fundamental frequency between 49.5-50.5 Hz excluding 50 Hz contain samples which are not power of 2. t. For example, after capturing of 10 cycles with the frequency of 50.5 Hz with a sampling rate of 5.120 ks/s/ch, it contains $\frac{10}{50.5} \times 5120 = 1013$ samples

which are not power of 2 and violate the stationary condition of FFT. Basically, during interpolation new samples between the present samples is calculated. Different interpolation methods can be used to resample the signal with 1024 samples in 10 cycles which are shown in the table 3.1 with computation time. In each of the cases, the presented time is

Order	Interpolation method	Computation time[ms]
1	Linear	110
2	Coerce	70
3	Cubic Spline	130
4	Hermitian Spline	430
5	FIR filter	290

TABLE 3.1: Computation Time

measured for resampling of 10 cycles of measured data. Different interpolation has a crucial effect on the levels of harmonic and hence can give dissimilar results. The simplest interpolation gives inappropriate results in a situation like a complex and noisy signal. However, for processing of a large amount of data it is unreasonable to use Hermitian Spline and FIR filter due to high computation time. The recommended interpolation is cubic spline as it contains reasonable computation time and gives good result in case of complex or noisy signal.

3.1.3 Grouping

In reality the frequency and magnitude of the signal from the power system are fluctuating producing spectral leakage or energy dispersion of harmonics spreading across the adjacent spectral line. The standard gives different grouping methods to ensure precise magnitude and assessment of the indices (voltage, current).

3.1.4 Sub-grouping Harmonics

To calculate the magnitude of harmonics more accurately, the frequency bin is grouped according to 3.2 or figure 3.2.

$$M_{sg,h}^2 = \sum_{n=-1}^1 M_{c,(N \times h + n)}^2 \quad (3.2)$$

M_c is the RMS value of the indices (voltage, current), $M_{sg,h}$ is the resultant R.M.S value of the harmonic sub-group, N is the number of fundamental period and h is the harmonic number. The term (Nh)+n specify the order of the spectral number of particular

harmonic.

3.1.5 Sub-grouping inter-Harmonics

For inter-harmonic analysis, the output of the DFT is grouped in such a way that the spectral components in adjacent to between each harmonic line as illustrated in 3.3 and figure 3.2 represent this grouping method.

$$M_{isg,h}^2 = \sum_{n=2}^{N-2} M_{c,(N \times h + n)}^2 \quad (3.3)$$

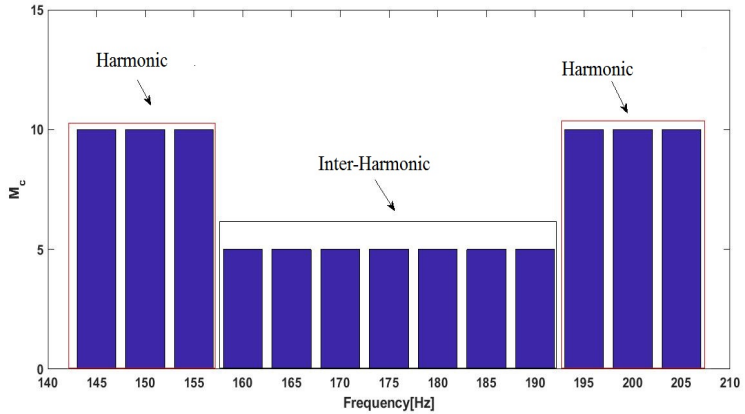


FIGURE 3.2: IEC grouping of spectral components for harmonics and for Inter-harmonics

After the grouping, different frequency components magnitude can be measure and analyze for assessment. However, the equation 3.2 and 3.3 is used for the calculation of harmonic and inter-harmonic up to 40 order. For measurement of frequency greater than 40 harmonic order equation 3.4 is valid.

$$M_{B,b} = \sqrt{\sum_{f=b-95Hz}^{b+100Hz} M_{c,f}^2} \quad (3.4)$$

where $M_{c,f}$ is the Root mean square value of the spectral component at the frequency f , for example the $M_{c,3200}$ is the RMS value of spectral component at 3200 Hz and $M_{B,b}$ is the output of each band.

3.1.6 Total Harmonic Distortion

The total harmonic distortion is an vital parameter that represent the level of harmonic distortion (voltage and current) in the waveform. It is defined as of the ratio of the r.m.s. value of the harmonic sub-groups $M_{sg,h}$ to the r.m.s. value of the sub-group associated with the fundamental $M_{sg,1}$ and represent by eq 3.5.

$$THDS_M = \sqrt{\sum_{h=h_{min}}^{h_{max}} \left(\frac{M_{sg,h}}{M_{sg,1}}\right)^2} \quad \text{where } h_{min} \geq 2 \quad (3.5)$$

where M_{sg} can be voltage (V) or Current (I), h is order of harmonic, h_{min} is the lowest number of harmonic that is 2 and h_{max} is highest number of harmonic. Usually, the maximum order of harmonic 40 is considered, since higher order of frequency have small impact on the stability of the power system. Theoretically, the lower is the value of THD, smaller is the level of harmonic distortion in the output signal. For the assessment of power quality related to harmonic levels, there is limitation of THD is recommended in the IEC standard 61000-2-3 at the point of coupling (PCC) of the distribution system. The PCC is the point where the connection between non-linear devices and the power system occur [30].

Chapter 4

Harmonic measurement of the wind turbine

The procedure to calculate the harmonic plays a vital role in the accuracy and precision of the indices harmonic level. Error in the first stage can have a huge impact on the other stages of the procedure which eventually alter the end result, therefore, every step should be analysed and developed with optimization and error free. The model of the digital data acquisition system with the component is given in figure 4.1 which is according to the IEC standard 64100-21. .

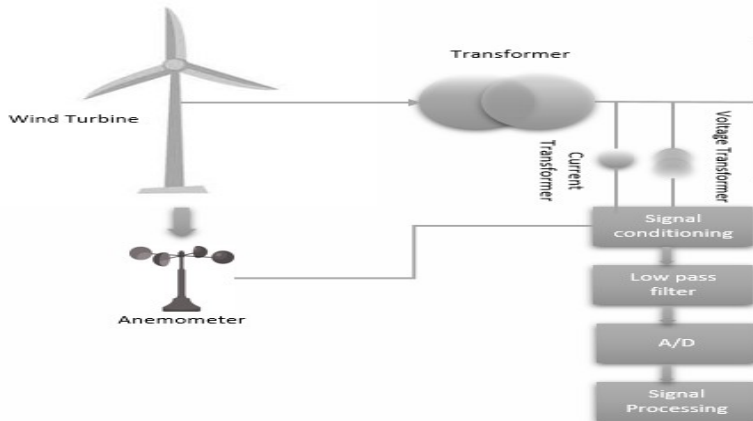


FIGURE 4.1: Components of Harmonic measurement System

4.0.1 Equipment Accuracy fro Hamronic Measurment

The required class of equipment for the measurement of harmonic signal is shown in table 4.1. The description about the indices(voltage and current) is given in the IEC standard 61000-3-6 [31].

Equipment	Required Accuracy
Voltage transducers	Class 1.0
Current Transducers	Class 1.0
Filter + A/D converter + Data acquisition	1 % of full scale
Frequency	10 mHz

TABLE 4.1: Description of requirements for measurement equipment

4.0.2 Harmonic function of active power

The standard IEC 61000-4-7 [29] concern regarding (voltage or current) harmonic assessment and power quality for low frequencies up to 40 times of the fundamental power system frequency (2Khz) approximately. However, in the first edition of IEC 64100-21 the voltage harmonic level at the common point of coupling (PCC) is a function of the Wind turbine harmonic current level and also of grid impedance and phase angle, therefore, the large capacity of low harmonic current emission wind turbine can be integrated at PCC [32]. According to the updated standard IEC 64100-21, the concern current frequencies are up to 50 times the grid frequency which is calculated according to the equation 3.2 3.3 and the emission level of harmonic are given for different values of power production. [12]. The values of the individual current harmonic component and the total harmonic current distortion shall be given in tables in percentage of I_n and data should be arranged in active power bins for different power production levels:10, 20, , 100 (%)of nominal power (P_n) of the wind turbine; therefore 11 active power bins are obtained[12].

4.0.3 Anemometer

The anemometer is used to measure the wind speed from which active power of the wind turbine is calculated by having the knowledge of the active power vs wind speed graph is given in the data sheet by the manufacturer example is seen in 4.2. The minimum sampling of wind speed signal is 1 Hz and the error related to the position of it should be less than 1%. It is obtained to analyze the power quality at the different active power of the turbine with 10 min data average. .

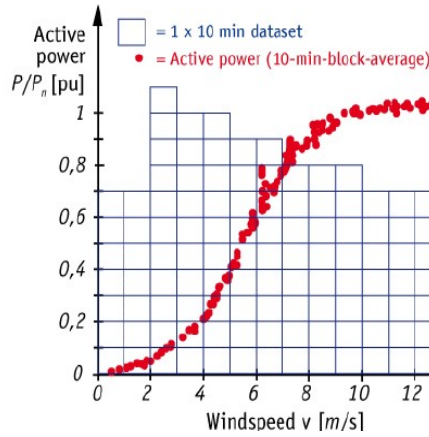


FIGURE 4.2: Wind speed function of active power [33]

4.0.4 Anti-aliasing filter

To obtain accurate result during the A/D conversion it is necessary to remove unwanted frequency components from the analogue signal. According to WhittakerNyquistKotelnikovShannon theorem, the sample signal can be recreated from its sample on the condition that it is sample with twice the highest frequency present in the process signal, this minimum frequency is called the Nyquist frequency, meaning the analog signal $x(t)$ is sampled at frequency of $f_s = 1/T_s > 2f$, the discrete signal is expressed as $x[n]=x(nT_s)$, where n for all integer, then the sample signal is fully recreated [19].

The anti-aliasing filter is a low pass filter which is a normal part of a digital measurement device that is implemented before analogue to digital conversion (see 4.3) to remove high-frequency components appear at the low-frequency region. . The initial step to

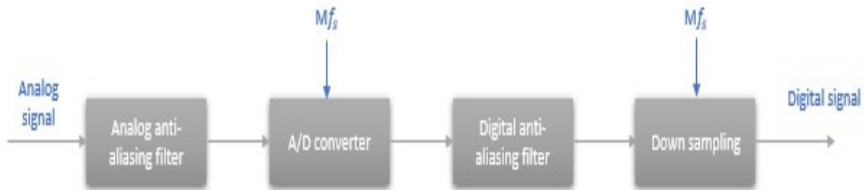


FIGURE 4.3: Anti-aliasing filter

measure harmonics indices (voltage, current) level is to remove unwanted high-frequency components. When an analogue signal is sampled with a sampling frequency of f_s , the

sampling frequency should be two times the highest frequency component that is present in the digital signal.

$$f_s = 2f_n \quad (4.1)$$

otherwise higher frequency components will appear in the lower frequency region of the digital signal due to aliasing phenomena. The problem with aliasing is that it is unable to detect at the output of the analogue to digital conversion and also utter the harmonic magnitude spectrum level. To prevent the high-frequency component from affecting the measured spectrum, an anti-aliasing filter is used.

One of the drawbacks of applying a high order filter is the introduction of time delay and phase error. A decreasing phase error is not an issue by itself, but more concern is the difference in time delay for various frequency. Most common low pass filter are Butterworth, Chebyshev, inverse Chebyshev, and elliptic functions. Chebyshev filter contains gradual transient from passband region to stop band region and can be used for application which can tolerate ripples in the passband. An elliptic filter also known as Cauer filters are more complex compared to the design of other filters and contain ripples in both pass band and stop band, Unfortunately, both will utter the magnitude response and are undesirable for harmonic measurements and their detail can be found in [100]. Among them, Butterworth also known as maximally flat magnitude is normally used because it gives a maximum flat response (horizon) at $w=0$ and $w=\infty$ with linear phase response and performs close to the ideal filter. These characteristics are very vital in case of harmonic measurement where each frequency within the passband has to be filtered in the same manner, the only issue is large roll off from pass band to stop band which can be solved by using high sampling frequency [34].

The Nth-order Butterworth filter is describe in equation 4.2

$$|H(w)|^2 = \frac{1}{1 + (\frac{w}{w_c})^{2N}} \quad (4.2)$$

where the falloff of w_c is -3db.

After the signal is processed through the filter it is feed into the signal processing block to calculate the different indices of the signal. The working of the signal processing is described in chapter 3.

Chapter 5

Simulation of the harmonic model

The design of the simulation model is developed in the MATLAB coding and its user-friendly tool is made in Graphic User Interface (GUI) of MATLAB. The description about GUI is elaborated in annexes E.

Four methods are analyzed and compare to find out which one gives more promising results. For simulation and validation of the model the signal used is from IEC standard 64100-21-1. The signal contains the flavour of the original signal from the wind turbine. The resemble signal is represented in 5.1 and the waveform is shown in fig5.1.

$$u_m(t) = \sqrt{\frac{2}{3}} \times u_n \times \sin(2\pi f_g t) \times \left(1 + 0.25 \times \frac{1}{100} \times \sin(2\pi f_f t) \times \frac{1}{2}\right) + \left\{ \sum_v u_v \times \frac{1}{100} \times \sqrt{\frac{2}{3}} \times u_n \times \sin(2\pi v f_g t + \pi) \right\} \quad (5.1)$$

where $u_n = 12$ KV nominal wind turbine voltage value, v is the harmonic order, $f_f = 8.8$ Hz is the fluctuated frequency, u_v % of u_n . f_g is grid frequency.

. The distorted voltage $u_m(t)$ consists of the fundamental voltage and the harmonic levels

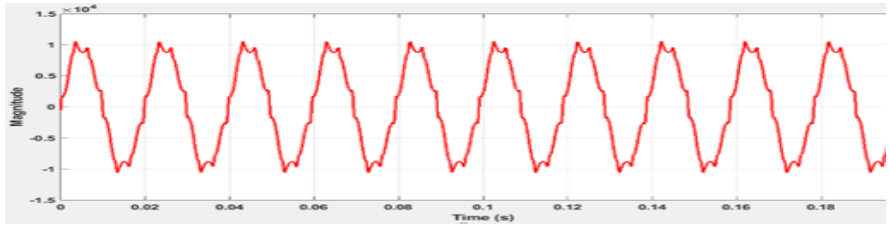


FIGURE 5.1: Input Signal

which is shown in the table 5.1. All harmonics have a 180 phase shift with respect to the 50Hz/60Hz fundamental i.e. have a negative going zero crossing when the fundamental

has a positive going zero crossing.

Harmonic Order v	u_v % of u_n
3	5
5	6
7	5
9	1.5
11	3.5
13	3
17	2
19	1.76
23	1.41
25	1.27
29	1.06
31	0.97

TABLE 5.1: Harmonic Order

For simplicity to understand the methods accuracy and difference they show as compared to the original value of harmonic magnitude the table 5.2 represent the harmonic levels in Root Mean Square (RMS).

Harmonic Order v	u_v % of u_n	Magnitude of u_v	$\sqrt{\frac{2}{3}} \times u_v $
1	100	1200	9798
3	5	600V	489.9V
5	6	720	587.88V
7	5	600	489.9V
9	1.5	180V	146.97V
11	3.5	420V	342.93V
13	3	360V	293.94V
17	2	240V	195.96V
19	1.76	211.2V	172.448V
23	1.41	169.2V	138.158V
25	1.27	152.4V	124.43V
29	1.06	127.2V	103.58V
31	0.97	116.4V	95.04V
THD			11.06 %

TABLE 5.2: RMS value of Harmonic levels

5.1 Case 1

5.1.1 Case A: 0.2s Window without Grouping

The reason for taking the 0.2s time interval is within this limit the signal is approximately periodic and validate the stationary assumption. The equation 5.1 is used as a voltage input signal, it is simulated for 10 cycles and within this period the grid frequency is 50.1Hz. The signal is re-sampled to obtain 1024 samples in order to have frequencies spectral line of the FFT tool projected by one complex vector in the orthogonal basis and not to spread over the whole basis.

When the signal is transformed into the discrete spectrum or frequency domain, the frequency resolution is 5 Hz meaning, the first spectral line represents the dc offset value while, the second spectral line show 5 Hz, the third represent 10 Hz, the fourth represents 15 Hz and so on . Similarly the 11th spectral line represents first harmonic, 21st represent 2nd, 31st third harmonics etc. The result is shown in table 5.3. The process

Harmonic Order v	u_v % of u_n	Magnitude of u_v (V)	$\sqrt{\frac{2}{3}} \times u_v $ (V)	Without Grouping (V)	Error%
1	100	1200	9798	9760	0.38
3	5	600V	489.9V	501.09	0.119
5	6	720	587.88V	578.84	0.0904
7	5	600	489.9V	476.84	0.13
9	1.5	180V	146.97V	139.70	0.0727
11	3.5	420V	342.93V	316.184	0.267
13	3	360V	293.94V	257.77	0.3617
17	2	240V	195.96V	159.37	0.4
19	1.76	211.2V	172.448V	129.4	0.43
23	1.41	169.2V	138.158V	92.54	0.45
25	1.27	152.4V	124.43V	74.031	0.5
29	1.06	127.2V	103.58V	52.3	0.52
31	0.97	116.4V	95.04V	40.4	0.54
THD			10.54 %		

TABLE 5.3: Harmonic levels without Grouping

provide inappropriate results for harmonic magnitude. The error between two values is due to aperiodic, non-cyclic signal within the interval observation. It causes few frequency component to spanned along the whole spectral region. However, the error is significant for high harmonic because the low harmonic are more dominant and there leakage influence on high frequency is significant.

5.1.2 Case B: 0.2s Window with Grouping

In this scenario, the grouping method of IEC standard 61000-4-7 is used for measurement of given signal in which the time series signal is transformed into discrete frequency domain where the spectral line is added according to equation (5.53). However, the signal is not synchronized. The result is shown in table 5.4. The results are improved

Harmonic Order v	u_v % of u_n	Magnitude of u_v (V)	$\sqrt{\frac{2}{3}} \times u_v $ (V)	Grouping (V)	Error%
1	100	1200	9798	9795	0.03
3	5	600V	489.9V	503.1	0.132
5	6	720	587.88V	584	0.003
7	5	600	489.9V	486	0.034
9	1.5	180V	146.97V	144.5	0.0245
11	3.5	420V	342.93V	333	0.09
13	3	360V	293.94V	279.65	0.1429
17	2	240V	195.96V	184.33	0.116
19	1.76	211.2V	172.448V	159.4	0.13
23	1.41	169.2V	138.158V	127.377	0.10
25	1.27	152.4V	124.43V	114.286	0.12
29	1.06	127.2V	103.58V	96.53	0.0705
31	0.97	116.4V	95.04V	89	0.0532
THD			10.98 %		

TABLE 5.4: Harmonic levels with Grouping

as compared to without grouping method. The error is small and the grouping method is effective in case of spectral leakage.

5.1.3 Case C :10 cycle without grouping

In this case, the signal within the observation is 10 cycle or periodic. Spline interpolation is applied in order to achieve 1024 samples. The result is shown in table 5.5 when the signal is transformed from time domain into frequency domain.

Harmonic Order v	u_v % of u_n	Magnitude of u_v (V)	$\sqrt{\frac{2}{3}} \times u_v $ (V)	IEC method (V)	Error%
1	100	1200	9798	9797	0.01
3	5	600V	489.9V	490.1	0.002
5	6	720	587.88V	587.86	0.0002
7	5	600	489.9V	489.93	0.0003
9	1.5	180V	146.97V	146.56	0.0041
11	3.5	420V	342.93V	342.82	0.0011
13	3	360V	293.94V	293.64	0.003
17	2	240V	195.96V	195.51	0.0045
19	1.76	211.2V	172.448V	171.71	0.0073
23	1.41	169.2V	138.158V	136.904	0.0125
25	1.27	152.4V	124.43V	122.67	0.0176
29	1.06	127.2V	103.58V	100.919	0.02661
31	0.97	116.4V	95.04V	91.15	0.0389
THD			11.04 %		

TABLE 5.5: Harmonic levels with 10 cycle without grouping

The spectral leakage of the signal is very small as compared to fixed window (0.2s) methods which are due to periodic cycles within the observation interval.

5.1.4 Case D: IEC method

In this case, the IEC standard method is used which is explained in chapter2, the signal within the observation is 10 cycle or periodic. Spline interpolation is applied in order to achieve 1024 samples. The result is shown in table 5.6 when the signal is transformed from time domain into frequency domain.

Harmonic Order v	u_v % of u_n	Magnitude of u_v (V)	$\sqrt{\frac{2}{3}} \times u_v $ (V)	IEC method (V)	Error%
1	100	1200	9798	9797	0.01
3	5	600V	489.9V	490.195	0.002
5	6	720	587.88V	587.86	0.0002
7	5	600	489.9V	489.93	0.0003
9	1.5	180V	146.97V	146.97	0.00
11	3.5	420V	342.93V	342.828	0.0010
13	3	360V	293.94V	293.650	0.0029
17	2	240V	195.96V	195.5227	0.004
19	1.76	211.2V	172.448V	171.726	0.00722
23	1.41	169.2V	138.158V	136.917	0.0124
25	1.27	152.4V	124.43V	122.699	0.0173
29	1.06	127.2V	103.58V	100.93	0.0265
31	0.97	116.4V	95.04V	91.174	0.0386
THD			11.05 %		

TABLE 5.6: Harmonic levels with IEC method

The result of the IEC method is close to the real value of harmonic and is appropriate for harmonic measurement. The error is small as compared to other methods.

5.2 Case 2

All the cases are same as mention previous, the difference is fundamental frequency and error in harmonic levels. The graph 5.2 show the comparison between 10 cycle without grouping and fixed window 0.2s without grouping. As it can be seen that 10 cycle give appropriate result because of the periodic signal within the observation interval. While, the graph 5.3 represent comparison between IEC standard and fixed window (0.2s) with grouping. The vale of standard is more close to real value.

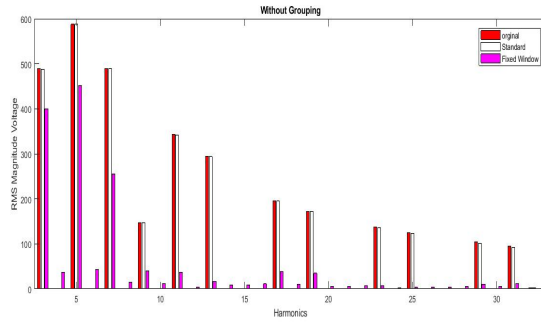


FIGURE 5.2: Harmonic level comparison between 10 cycles and Fixed Window (0.2s)

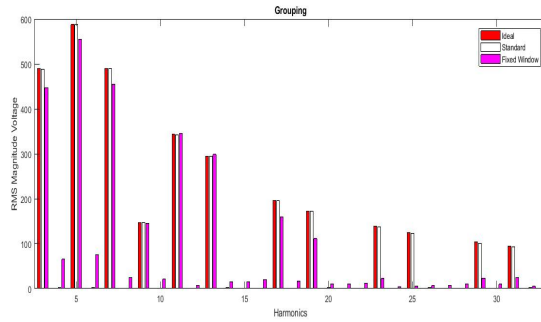


FIGURE 5.3: Harmonic level comparison between IEC Standard and fixed window (0.2s)

5.2.0.1 Conclusion

The IEC standard method gives the best result in both cases and the fixed window (0.2s) without grouping give significant deviation. In both cases, the magnitude of harmonic levels changes when the fundamental frequency varies and in real power system the frequency changes from 49.5 Hz to 50.5 Hz. In order to measure the harmonic and assess it aggregation is used.

5.3 Aggregation

As the magnitude of the spectral component are changing between discrete Fourier time (DFT) windows, aggregation is needed. The harmonic magnitude aggregation considered in the standard is aggregated arithmetic average according to c_h

$$c_h = \frac{1}{n} \sum_{i=1}^n |c_{h,i}| \quad (5.2)$$

where n is the number of aggregated DFT windows, $c_{h,i}$ the complex value of the h -th harmonic from the estimated spectrum from 10-cycle window and c_h is the aggregated h -th harmonic magnitude.

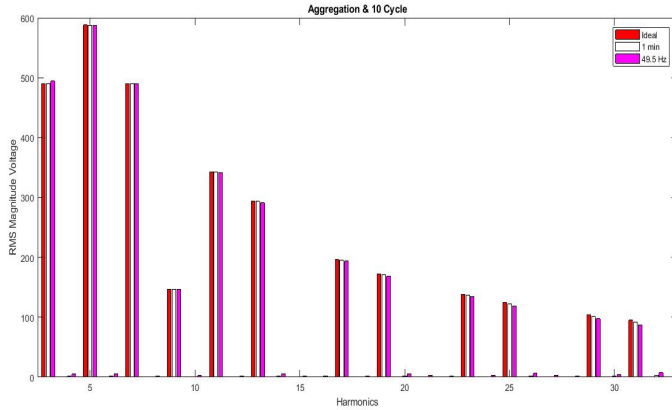


FIGURE 5.4: Aggregation vs 10 cycle

In the fig 5.4 magnitude of 10 cycles with fundamental frequency 49.5 Hz and one minute of aggregation while 5.5 represents four different fundamental frequency and one-minute aggregation value which show that aggregation value show more promising result. The one-minute interval contains the variable frequency from 49.5 to 50.5 Hz. Different frequencies show the divergent magnitude of harmonic and it's inaccurate to rely on one 10 cycle value. .

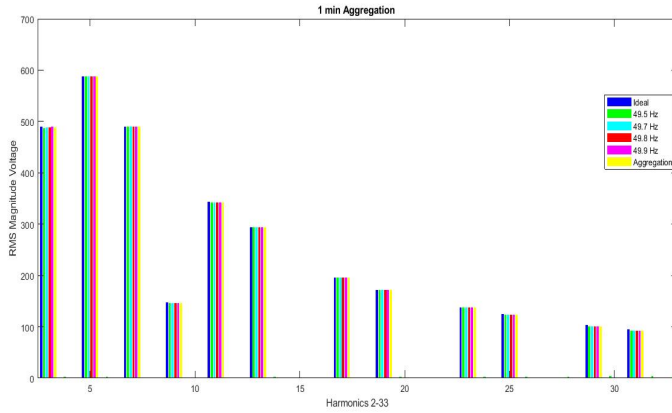


FIGURE 5.5: Aggregation vs four different frequency

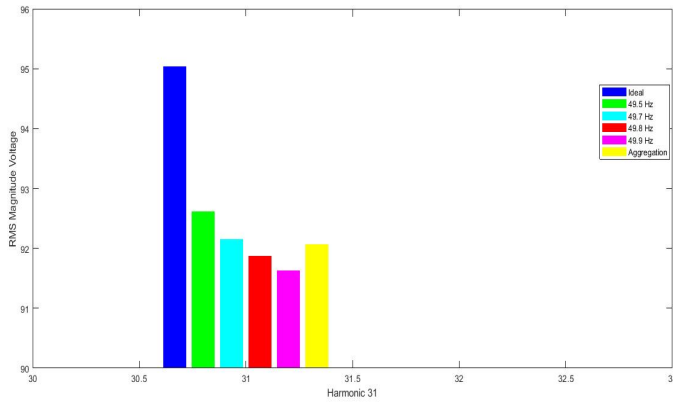


FIGURE 5.6: Zoom in version of Fig 1.11

Chapter 6

Model Validation

The new IEC standard 61400-21-1 give the method to validate the model.

6.0.1 Prevailing angle

The application of prevailing angle are following

- . To evaluate the measurement uncertainty in the model
- . The distribution of harmonic angles obtained directly from DFT can give an overview of the measurement system accuracy
- . The prevailing angle ratio expressed in equation 6.1

$$PAR = \frac{|\sum_{i=1}^n C_{h,i}|}{\sum_{i=1}^n |C_{h,i}|} = \frac{|\sum_{i=1}^n (a_{h,i} + b_{h,i})|}{\sum_{i=1}^n |(a_{h,i} + b_{h,i})|} \quad (6.1)$$

- . If the prevailing angle ratio is close to unity it means that there is no significant variation of the harmonic angle during the analysed interval. If the value is much lower than 1 it means that the angle variation can be caused either by uncertainties, significant changes in the analysed system or lack of analysed harmonic phase lock to the fundamental frequency

The graph 6.1 and 6.2 shows the prevailing angle of two methods fixed window and 10 cycles. As it can be seen that 10 cycles give PAR close to unity while the other one less than 0.5 percent which shows the un-synchronization . Also the angle of 10 cycle is gather around one point while the dispersion for the other.

.
.

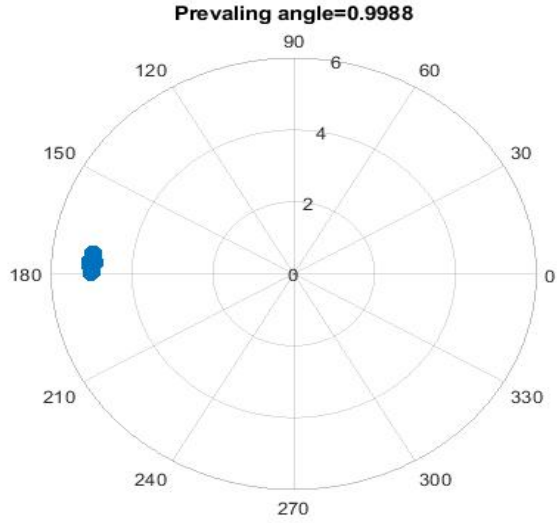


FIGURE 6.1: 10 cycle

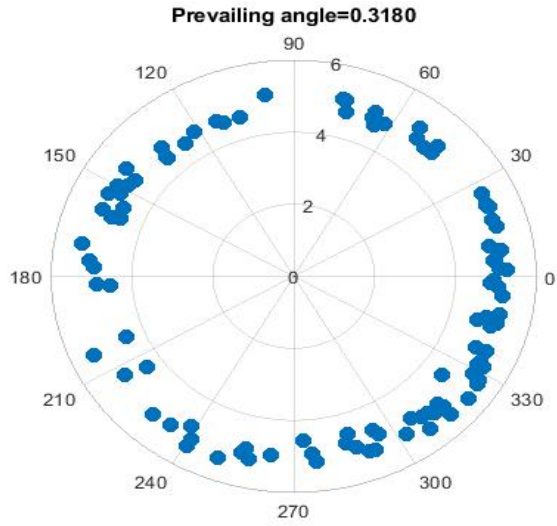


FIGURE 6.2: Fixed window

6.0.2 Statistical validation of Harmonic Magnitude

In order to validate the magnitude of the harmonic measurement, standard deviation is used which check the precision of the measurement. It is useful way to characterize the reliability of the measurements. The formula of the standard deviation is given in equation 6.2

$$s = \sqrt{\frac{1}{N-1} \sum_{i=1}^N (x_i - x_n)^2} \quad (6.2)$$

where

$$x_n = \frac{1}{N} \sum_{i=1}^N x_i \quad (6.3)$$

Also probability distribution of analysed harmonics magnitude can be broadly used in comparison of the same frequency components from different block of data sets.. Additionally description of harmonics from its probability distribution perspective provides better overview about harmonic phenomena and power quality. It is expressed in equation 6.4

$$f(x) = \frac{1}{\sqrt{2\pi}\sigma} e^{-\frac{(x-\mu)^2}{2\sigma^2}}, -\infty < x < \infty \quad (6.4)$$

The graph 6.3 shows the normal distribution of seventh order harmonic without aggregation which means that one sample represents the magnitude of 7th harmonic where the simulation time is 18 minute that contains 5400 samples and within that interval, the frequency is varying from 49.5 to 50.5 Hz. Its mean value is 489.723 V with standard deviation 0.52 and variance of 0.280. . While the graph 6.4 show the normal distri-

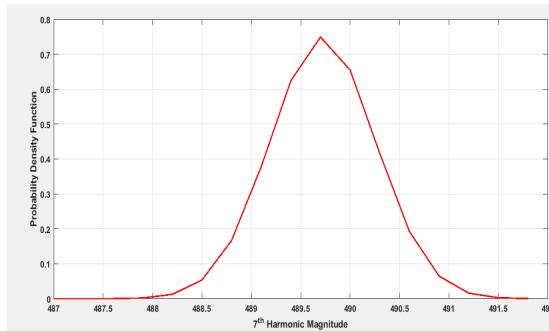


FIGURE 6.3: Normal Distribution of 10 cycle

bution of one minute aggregated data. The standard deviation is 0.102 with variance of 0.01. As small standard deviation means that the value is close to expected value and more precise is the result. Therefore, it is better to aggregate the data for harmonic measurement and assessment.

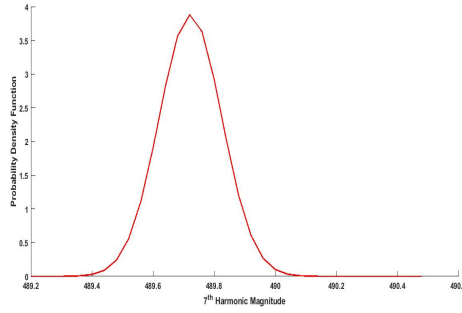


FIGURE 6.4: Normal Distribution of one minute aggregation samples

Chapter 7

Conclusion

- 1- The performance of the harmonic model give more accurate result by capturing the 10 cycles of the signal.
- 2- The fluctuation in frequency and voltage amplitude of the signal causes spectral leakage within the observation interval. Grouping should be done according to equation 3.3,3.2 and 3.4 to improves the performance of the harmonic model..
- 3- As the magnitude and phase angle of the spectrum varies between FFT window, aggregation is applied to improve the performance of the model.
- 4- PAR is used to validate the model and check the performance of capturing 10 cycles. In case, the phase angle of the same frequency component at different time interval is gathered around and show PAR close to unity, the model performance is good. While the scattered phase angle and low PAR represent the poor performance of harmonic model.
- 5- Also, the standard deviation is used for validation and precision of the model, a large standard deviation of harmonic measurement of same frequency component at different time represent that the model performance is poor and small standard deviation indicates good performance.
- 6- The performance of the model improves by resampling the signal to achieve the power of 2 samples within the 10 cycles of observation interval.

7.1 Future Work

- 1- Analyze the system in the presence of inter-harmonic frequency.
- 2- The effect of spectral leakage on the frequencies higher than 2500 Hz.
- 3- Analyze the behaviour of Voltage Source Converter characteristic and un-characteristic harmonic.
- 4- Effect of the power system parallel and series resonant harmonic on the measurement of harmonic.
- 5- Measure the harmonic of a wind turbine at different power production to analyze and assess the emission of harmonic.
- 6- The effect of the window on inter-harmonics.
- 7- Compare the result of FFT and wavelet transform. To analyze the measurement and assessment of the harmonic.

.1 Annexes E

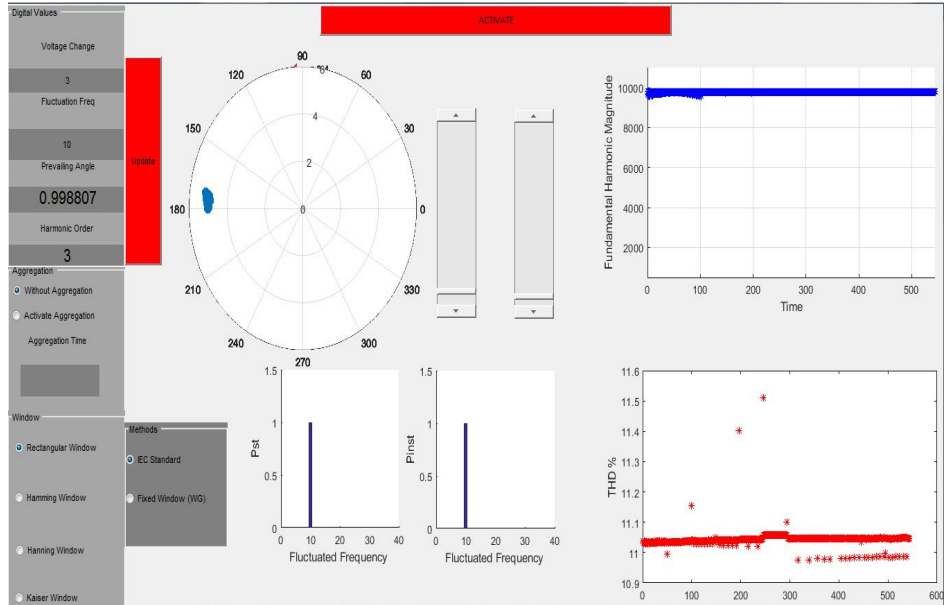


FIGURE 1: Harmonic Meter Model GUI

The model gives harmonic levels, phase angles, prevailing ratio, THD, fundamental harmonic magnitude and flicker measurement of the signal. For an understanding of the model, the signal given in the IEC standard 614000-21-1 is used and voltage change fluctuated frequency is entered manually which is according to standard 61400-4-15 to analyze its effect on the flicker meter and harmonic model. The time period for simulation is one minute and frequency is vary from 49.5 to 50.5 Hz. The working process of the model is following

- . The digital panel shows the indices of voltage change, fluctuated frequency which is entered manually. It also displays harmonic order and prevailing ratio. By observing the PAR, one can sure the synchronization to achieve 10 cycles as close to unity mean good frequency detection and less than 0.5 represent the loss of synchronization
- . The polar axis graph shows the result of phase angles direction and harmonic magnitude.

-
- . Two sliders along with polar graph are shown, the first one controls the order of harmonic order and other to flickers.
 - . By changing the first slider, the harmonic order is changed along with its phase angle and the result is shown in the polar axis.
 - . The order of harmonic is display in the digital panel.
 - . The bottom graph shows the THD in the measured signal.
 - . The top graph shows the magnitude of the fundamental signal.
 - . The window panel allows the option to select different window on the signal before FFT processing.
 - . Aggregation panel gives the possibility to adjust the mean of number of 10 cycle according to user demand. By default, it is 1 sec.

.2 Annexes D

```

%% Defining Polar Axis
ax = polaraxes;
ax.RAxis.Color = 'r';
ax.RAxis.Location = 90;
ax.Position = [0 0.45 0.63 .45];
%% Initating Slider
numSteps = 40;
set(handles.slider1, 'Min', 1);
set(handles.slider1, 'Max', 40);
set(handles.slider1, 'Value');
set(handles.slider1, 'SliderStep', [1/(numSteps-1) , 1/(numSteps-1) ]);
% save the current/last slider value
handles.lastSliderVal = get(handles.slider1, 'Value');
S = get(handles.slider1, 'Value');
S = floor(S)

fs=5120; \\
Ts=1/fs; \\
yy=1; \\
a1=1; \\
kk=0; \\
n=0; \\
gainfactor=1; \\
LengthofTimeperiod(sec)=10; \\
MOvementofslider=S; \\
for f=49.5:0.1:50.5 \\
Flux=sqrt(2/3)*12000; \\
TT=kk:Ts:kk+pg; \\
Timeperiod{yy}=TT; \\
k1{yy}=(5/100*sqrt(2/3)*12000*sin(2*pi*3*f*TT+pi))+ \\
(6/100*sqrt(2/3)*12000*sin(2*pi*5*f*TT+pi))+ \\
(5/100*sqrt(2/3)*12000*sin(2*pi*7*f*TT)); \\
k2{yy}=(1.5/100*sqrt(2/3)*12000*sin(2*pi*9*f*TT))+ \\
(3.5/100*sqrt(2/3)*12000*sin(2*pi*11*f*TT))+ \\
(3/100*sqrt(2/3)*12000*sin(2*pi*13*f*TT)); \\

```



```

jj{1}=zeros(1,1024);
v{1}=zeros(1,1024);
Fk{n+2}=(jj{n+2}(end))-(jj{n+1}(end));
resamplelength{n+2}=1024/Fk{n+2};
pp{n+2}=jj{n+2}(end);
xx{n+2}= jj{n+2}(1):1/Fpizaa{n+2}:jj{n+2}(end);
kp{n+2}=-xx{n+2}(end)+pp{n+2};
    bb{n+2}= jj{n+2}(1):1/Fpizaa{n+2}:(xx{n+2}(end)+(2*kp{n+2}));
    splinel{n+2}=spline(jj{n+2},v{n+2},bb{n+2});
ff{n+2}=(fft((splinel{n+2}))/length(splinel{n+2}));

LOWPASS_ORDER = 5; % Filter order is 5
j=1+i; % w = a bw1 = butter(LOWPASS_ORDER,LOWPASS_CUTOFF/(fs/2),'low');
n=n+1; % [h,bw, a,bw,b];
p=p+1;
end
end
yy=yy+1;
kk=kk+pg;
end
for n=0:n-1
y1{n+2}= ff{n+2};
Hnn{n+2}=zeros(40,3);
ghgg{n+2}=zeros(40,3);
Hn{n+2}=zeros(40,3);
ghg{n+2}=zeros(40,3);
H{n+2}=zeros(40,1);
gh{n+2}=zeros(40,1);
Hinn{n+2}=zeros(39,7);
Hin{n+2}=zeros(39,7);
Hi{n+2}=zeros(39,1);
%% harmonics grouping
for i=10:10:400
complexfft{n+2}(i/10,:)=y1{n+2}(i+1);
magnitufft{n+2}(i/10,:)=abs(y1{n+2}(i+1));

```

```

        Hn{n+2}(i/10,:)=2*abs(y1{n+2}(i:i+2));
    end
    phaseangle{n+2}=(angle(complexfft{n+2}(1)/complexfft{n+2}(L)));
    magnitudephaseangle{n+2}=(magnitudfft{n+2}(L)/magnitudfft{n+2}(1))*100;
    prevaillinganlge{n+2}=complexfft{n+2}(L);
    magprevaillinganlge{n+2}=magnitudfft{n+2}(L);

    %%Squaring
    for i=1:1:40
        for j= 1:1:3
            Hnn{n+2}(i,j)=Hn{n+2}(i,j)*Hn{n+2}(i,j);
        end
    end
    %%summing
    for i=1:1:40
        H{n+2}(i,:)= sqrt(sum(Hnn{n+2}(i,:))*gainfactor);
    end
    % inter-harmonics grouping
    for i=20:10:400
        Hin{n+2}(i/10-1,:)=y1{n+2}(i-7:i-1);
    end
    %%Squaring
    for i=1:1:39
        for j= 1:1:7
            Hinn{n+2}(i,j)=Hin{n+2}(i,j)*Hin{n+2}(i,j);
        end
    end
    %%summation
    for i=1:1:39
        Hi{n+2}(i,:)= sum(Hinn{n+2}(i,:));
    end

    end

    %%Adding Harmonic upto 40

```

```
TH{n+2}=zeros(40,1);
for i=2:1:40
    TH{n+2}(i,:)=(H{n+2}(i)/H{n+2}(1))^2;
end
THD{n+2}=sqrt(sum(TH{n+2}));
end
THDD=cell2mat(THD)*100;

frida=cell2mat(H);
aggregation=[];
sample_size=300*1;
for frida_size=1:sample_size:length(frida)-sample_size

aggregation=[aggregation sum((frida(:,frida_size:frida_size+(sample_size-1)))))/sample_size];
aggreg_inv=aggregation';

end
er=size(aggreg_inv);
er=er(1);

for thd_size=1:1:er
for thd_add=1:1:40
aggregatedthd(thd_add,thd_size)=(aggregation(thd_add,thd_size)/aggregation(1,thd_size))^2;
end

end
aggregatedthd=sqrt(sum(aggregatedthd(2:end,:)));

phaseanglemat=cell2mat(phaseangle);
magnitudephaseanglemat1=cell2mat(magnitudephaseangle);
prevailinganlgemat=cell2mat(prevailinganlge);
magprevailinganlgemat=cell2mat(magprevailinganlge);
```

```
prevailinganglemat=cell2mat(prevailingangle);
magprevailinganglemat=cell2mat(magprevailingangle);
prevailingangle3=abs(sum(prevailinganglemat))/sum(magprevailinganglemat)
polarscatter(phaseanglemat,magnitudephaseanglemat1,75,'filled')
if a2==1

    axes(handles.axes1)
    plot(THDD,'r*')
    xlabel(handles.axes1,'Time')
    ylabel(handles.axes1,'THD %')
else
end
if a2 == 2

    axes(handles.axes1)
    plot(agrregatedthd)
else
end

set(handles.pa,'string',prevailingangle3)
set(handles.harmonic,'string',S)
axes(handles.axes8)
axis([0 length(frida) 500 11000])
hold on
grid on
axes(handles.axes8)
plot(frida(1,:), 'b*')
xlabel(handles.axes8,'Time')
ylabel(handles.axes8,'Fundamental Harmonic Magnitude')

guidata(hObject, handles);
```

Bibliography

- [1] vestas. vestas, 2018. URL https://www.vestas.com/en/media/images#!grid_0_content_2_Container.
- [2] J. Hjerrild . Kocewiak and C. L. Bak. Harmonic analysis of offshore wind farms with full converter wind turbines. Oct 2009.
- [3] Frede Blaabjerg and Zhe Chen. Power electronics for modern wind turbines. *Synthesis Lectures on Power Electronics*, 1(1):1–68, 2005.
- [4] Kai Yang. *On harmonic emission, propagation and aggregation in wind power plants*. PhD thesis, Luleå tekniska universitet, 2015.
- [5] I F II. Ieee recommended practices and requirements for harmonic control in electrical power systems. *New York, NY, USA*, 1993.
- [6] EN Standard. 50160, voltage characteristics of public distribution systems. *Henrik Markiewicz & Antoni Klajn*, 1994.
- [7] EN IEC. 61000-3-6 electromagnetic compatibility. *Limits–Assessment of emission limits for the connection of distorting installations to MV, HV and EHV power systems, Ed, 2*, 2008.
- [8] Leonard L Grigsby. *Power system stability and control*. CRC press, 2016.
- [9] Bin Wu, Yongqiang Lang, Navid Zargari, and Samir Kouro. *Power conversion and control of wind energy systems*, volume 76. John Wiley & Sons, 2011.
- [10] Barry W Kennedy. *Power quality primer*. McGraw Hill Professional, 2000.
- [11] Alexander Kusko and Marc T Thompson. *Power quality in electrical systems*, volume 23. McGraw-Hill, 2007.
- [12] Wind TurbinesPart. 21: Measurement and assessment of power quality characteristics of grid connected wind turbines. *IEC Standard*, pages 61400–21, 2008.
- [13] Gilbert M Masters. *Renewable and efficient electric power systems*. John Wiley & Sons, 2013.

-
- [14] S. M. Kay and S. L. Marple. Spectrum analysis a modern perspective. *Proceedings of the IEEE*, 69(11):1380–1419, Nov 1981. ISSN 0018-9219. doi: 10.1109/PROC.1981.12184.
- [15] H. Renders, J. Schoukens, and G. Vilain. High-accuracy spectrum analysis of sampled discrete frequency signals by analytical leakage compensation. *IEEE Transactions on Instrumentation and Measurement*, 33(4):287–292, Dec 1984. ISSN 0018-9456. doi: 10.1109/TIM.1984.4315226.
- [16] V. K. Jain, W. L. Collins, and D. C. Davis. High-accuracy analog measurements via interpolated fft. *IEEE Transactions on Instrumentation and Measurement*, 28(2):113–122, June 1979. ISSN 0018-9456. doi: 10.1109/TIM.1979.4314779.
- [17] D. Agrez. Weighted multipoint interpolated dft to improve amplitude estimation of multifrequency signal. *IEEE Transactions on Instrumentation and Measurement*, 51(2):287–292, April 2002. ISSN 0018-9456. doi: 10.1109/19.997826.
- [18] Jos Arrillaga and Neville R Watson. *Power system harmonics*. John Wiley & Sons, 2004.
- [19] Math HJ Bollen and Irene YH Gu. *Signal processing of power quality disturbances*, volume 30. John Wiley & Sons, 2006.
- [20] IEC61000 IEC. 61000-4-7: Electromagnetic compatibility (emc). *Testing and measurement techniques-General guide on harmonics and interharmonics measurements and instrumentation, for power supply systems and equipment connected thereto, CEI-IEC, Geneva*, 2002.
- [21] G. W. Chang, C. Y. Chen, and M. C. Wu. A modified algorithm for harmonics and interharmonics measurement. In *2007 IEEE Power Engineering Society General Meeting*, pages 1–5, June 2007. doi: 10.1109/PES.2007.385724.
- [22] A. Cataliotti, V. Cosentino, and S. Nuccio. A phase-locked loop for the synchronization of power quality instruments in the presence of stationary and transient disturbances. *IEEE Transactions on Instrumentation and Measurement*, 56(6):2232–2239, Dec 2007. ISSN 0018-9456. doi: 10.1109/TIM.2007.908350.
- [23] M. Aiello, A. Cataliotti, V. Cosentino, and S. Nuccio. Synchronization techniques for power quality instruments. *IEEE Transactions on Instrumentation and Measurement*, 56(5):1511–1519, Oct 2007. ISSN 0018-9456. doi: 10.1109/TIM.2007.903585.
- [24] M. M. Begovic, P. M. Djuric, S. Dunlap, and A. G. Phadke. Frequency tracking in power networks in the presence of harmonics. *IEEE Transactions on Power Delivery*, 8(2):480–486, April 1993. ISSN 0885-8977. doi: 10.1109/61.216849.

- [25] O. Vainio and S. J. Ovaska. Digital filtering for robust 50/60 hz zero crossing detectors. In *Proceedings of 1995 IEEE Instrumentation and Measurement Technology Conference - IMTC '95*, pages 62–, April 1995. doi: 10.1109/IMTC.1995.515103.
- [26] T. Lobos, T. Kozina, and H. . Koglin. Power system harmonics estimation using linear least squares method and svd. In *IMTC/99. Proceedings of the 16th IEEE Instrumentation and Measurement Technology Conference (Cat. No.99CH36309)*, volume 2, pages 789–794 vol.2, May 1999. doi: 10.1109/IMTC.1999.776975.
- [27] F. J. Harris. On the use of windows for harmonic analysis with the discrete fourier transform. *Proceedings of the IEEE*, 66(1):51–83, Jan 1978. ISSN 0018-9219. doi: 10.1109/PROC.1978.10837.
- [28] J. Barros and R. I. Diego. Effects of windowing on the measurement of harmonics and interharmonics in the iec standard framework. In *2006 IEEE Instrumentation and Measurement Technology Conference Proceedings*, pages 2294–2299, April 2006. doi: 10.1109/IMTC.2006.328581.
- [29] International Electrotechnical Commission et al. Electromagnetic compatibility (emc)part 4-7: Testing and measurement techniquesgeneral guide on harmonics and interharmonics measurements and instrumentation, for power supply systems and equipment connected thereto. Technical report, IEC 61000-4-7, Second Edition, 2002 08, 2002.
- [30] Lukasz Hubert Kocewiak, Jesper Hjerrild, and Claus Leth Bak. Harmonic analysis of offshore wind farms with full converter wind turbines. In *Proc. 7th International Workshop on Large Scale Integration of Wind Power and on Transmission Networks for Offshore Wind Farms*, pages 539–544, 2009.
- [31] International Electrotechnical Commission et al. Iec 61000-4-30. *Electromagnetic compatibility (EMC)-Part, 4*, 2003.
- [32] Hanna Emanuel, Martin Schellschmidt, Stephan Wachtel, and Stephan Adloff. Power quality measurements of wind energy converters with full-scale converter according to iec 61400-21. In *Electrical Power Quality and Utilisation, 2009. EPQU 2009. 10th International Conference on*, pages 1–7. IEEE, 2009.
- [33] Sokratis Tentzerakis, Fritz Santjer, and Marcel Bärschneider. Methodology for the evaluation of wind turbine harmonic emissions. In *12th German Wind Energy Conference (DEWEK), Bremen, Germany*, volume 19, page 20, 2015.
- [34] Edmund Lai. *Practical digital signal processing*. Elsevier, 2003.